

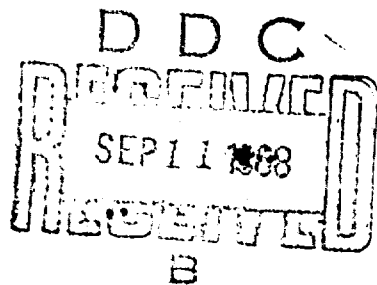
AD674369

RESEARCH PAPER P-405

EXAMPLES OF GRAPHICAL SOLUTION
OF SIX PROBLEMS IN ENGINEERING,
MECHANICS, AND OPERATIONAL ANALYSIS

Michael Watter

July 1968



INSTITUTE FOR DEFENSE ANALYSES
SCIENCE AND TECHNOLOGY DIVISION

Reproduced by the
CLEARINGHOUSE
for Federal Scientific & Technical
Information Springfield Va. 22151

IDA Log No. HQ 68-8604
Copy 83 of 150 copies

RESEARCH PAPER P-405

EXAMPLES OF GRAPHICAL SOLUTION
OF SIX PROBLEMS IN ENGINEERING,
MECHANICS, AND OPERATIONAL ANALYSIS

Michael Watter

July 1968

This document has been approved for public release and sale;
its distribution is unlimited.



INSTITUTE FOR DEFENSE ANALYSES
SCIENCE AND TECHNOLOGY DIVISION
400 Army-Navy Drive, Arlington, Virginia 22202

Contract DAHC 15 67 C 0011
ARPA Assignment 19

ACKNOWLEDGMENTS

I am indebted to the reviewers of this paper, Drs. Alfred W. Jones, Philip H. Lowry, and W. Scott Payne, for their constructive criticism of its original form and content. I am grateful for their thoughtful comments, which I have endeavored to incorporate to improve the readability and clarity of the presentation of my theme. The impetus to prepare this paper stems from many enjoyable discussions with Dr. Jones. It is he who posed to me the problem of the range of a fleet of aircraft, just as once before Dr. N. J. Fine had aroused my interest in the jeep problem. To me, an engineer, these exchanges were both challenging and inspiring.

ABSTRACT

This paper illustrates the use of graphical analyses by presenting the solution of six problems in the fields of operational analyses, mechanics, and engineering: The Jeep Problem, the Range of a Fleet of Aircraft, a Beam under Combined Compression and Transverse Load, the Problem of Car Replacements, Determination of Ballistic Trajectory Parameters, and the Two-Magnetic-Reactor Problem.

The purpose of this paper is to arouse an interest in a methodology which is further enhanced by the graphical display capability available in today's computers with all its potential problem solving flexibility. The examples treated in this paper are not the stereotyped problems forming the usual subject of textbooks on graphical methods and, in that sense, should prove of greater interest to the reader.

CONTENTS

I. Introduction	1
II. The Jeep Problem	5
III. Graphical Solution to Example Problem No. 1 (The Jeep Problem)	13
IV. The Range of a Fleet of Aircraft	21
V. Graphical Solution to Example No. 2 (The Range of a Fleet of Aircraft)	29
A. Case of Aircraft with Equal Speeds	29
B. Case of Aircraft of Different Speeds and Efficiencies	35
VI. Graphical Solution to Example No. 3 (A Beam Under Combined Compression and Transverse Load)	37
A. Precise Bending Moment	37
B. Precise Shear	40
C. Maximum Bending Moment	41
D. Deflections	41
E. Example Showing Application of the Method	43
VII. Graphical Solution to Example No. 4 (The Problem of Car Replacements)	45
VIII. Graphical Solution to Example No. 5 (Determination of Ballistic Trajectory Parameters)	51
A. Ballistic Trajectory Construction	52
B. Determination of Speeds and Times Along the Trajectory	53
C. Use of Logarithmic Scales for Determination of Speeds and Times	55
D. Times	55
E. Example	57
IX. Graphical Solution to Example No. 6 (The Two- Magnetic-Reactor Problem)	59
A. Method A: Graphical Solution	60
B. Application of the Method	67
C. Method B: Grapho-Analytical Solution	72
X. Conclusions	79
Appendix A. A New Application of the Logarithmic Polar Diagram	81

I. INTRODUCTION

Graphical solutions have not been popular in the United States; and now, with the widespread use of computers, it may seem even more a remote possibility to arouse interest in a skill not widely employed. On the other hand, the graphical input and display capability and computer processing of graphical information may yet foster the acceptance of graphical solutions and prove to be a tool to train graphical visualization.

This training is as important as the training in any other mathematical symbolism, without which the shorthand of operations and relationships would remain as hieroglyphics before discovery of the Rosetta stone. A quite natural question would be to inquire as to the reasons for previous lack of enthusiasm for graphical solutions. That may have been due to many causes: lack of training in the use of graphics; the hard-to-understand disdain of engineering students of their own language--the language of drawings; the preponderance of analytically minded mathematicians to geometers, etc. The principal cause, however, may have been unfounded fear of the lack of accuracy of graphical solutions. I say "unfounded" because more often than not the accuracy of a graphical solution is amply adequate, even without having to alibi it by mentioning the underlying assumptions, physical constants, and other factors which preclude our precise knowledge of a given physical phenomenon.

The virtue of a graphical approach is twofold: a diagram often suggests to a trained mind a solution, but in all cases contains a visual interplay of variables indicating their relative importance. In that sense alone, I feel justified in quoting Oliver Heaviside--although his statement was unrelated to graphics--that there is no

better way to prove a fact than to show it to be a fact. Here the use of the words "to show" is intended to convey an idea of a picture, a diagram; but, of course, to a trained mind a shorthand symbol is just as clear.

I have selected from my experience six problems--one as recent as this paper, some going back to my early work in aircraft engineering. Each of the six example problems selected was chosen to demonstrate an approach, to make a point, and to illustrate the solutions of practical problems encountered in practice.

The first two problems, the jeep problem and the range of a fleet of aircraft, were selected because their analytical solutions as offered in mathematical literature did not suggest that equally accurate, and in fact rigorous, solutions were possible using considerably more elementary graphical approach. The solution to both of these problems is approached by drawing diagrams showing the relationship of the fuel consumed as a function of distance, and in the jeep problem, the direction of travel. The actual solution becomes understandable by proper juxtaposition of lines and figures.

The third problem, that of a beam under combined compression and transverse load, illustrates the reaction of a mind disposed toward graphical approach. The expression of the bending moment for a beam under combined compression and transverse load had been derived long before I found it necessary to use it. Also, its use was widespread in those days because airplanes were biplanes, and in wing construction one used routed wooden spars. The critical design points were not obvious; to verify the adequacy of design, the stress analyst used his desk calculator to arrive at the bending moments and shears and physical properties of the spar cross section to verify local factor of safety. It was perhaps natural that with my preference for graphics, that type of solution suggested itself because of the trigonometric nature of the analytical expression of the bending moment. In reality, of course, these functions represent the limiting magnitude of appropriate infinite series.

The fourth problem, that of car replacements, once more offered an illustration of how by drawing a diagram showing the relationship of a number of cars, their ages, and stipulated change of their mean age after a specified period, the solution suggested itself. Of course, the problem as posed and its solution are based on the assumption of linear variation of car ages and the discarding of oldest cars to arrive at a new mean car age. The finding of the answer requires careful examination of the diagram and the ability to recognize unimportant inaccuracy in areas being balanced to find the location of the solution line.

The fifth problem, the determination of ballistic trajectory parameters, is interesting because it calls for the application of several disciplines and because it demonstrates that often the fear of a graphical solution's not being accurate enough is ill-founded. This example problem shows comparison of the results obtained graphically, analytically by the use of a desk calculator, and finally those arrived at from a computer program. It is significant that even the apogee velocity, which graphically is obtained as a difference of two relatively large numbers, differs by less than one percent from the computer answer. This is amply accurate, considering the fact that in this particular case the assumption of a trajectory in vacuum and a nonrotating earth were considered acceptable for the purpose for which the problem had to be solved. The additional interest of the solution resides in the use of logarithmic coordinates employed to save certain arithmetic calculations.

The two-magnetic-reactor problem, the sixth problem, is an illustration of a problem whose solution was entirely intuitive. I assume that unless one is inclined to think graphically one would have difficulty in sensing the steps which led one to the eventual solution. On the other hand, once there was a graphical solution its transformation to a grapho-analytical form, a simpler and more elegant form, became clear.

Appendix A contains my extension of the use of the logarithmic polar diagram of an airplane proposed and used by me as a young engineer. It is reported here because it is the original use of the logarithmic scales by Mr. Rith that started me on their use and interest in graphical solutions in some of my analytical work.

II. THE JEEP PROBLEM*

N.J. Fine, Washington, D.C.

1. Introduction. The problem in logistics with which this paper deals was proposed to the author by Gail Young and Ivan Niven, both of Purdue University, in the latter part of 1945. The original source is unknown to the author. At that time Niven had obtained a partial solution based on certain assumptions. After the first submission of this paper it was learned that L. Alaoglu had also obtained a complete solution. He mentioned that similar problems had arisen in air transport operations in the China theater. It has also been suggested that there may be applications to Arctic expeditions and interplanetary travel. This paper, however, will confine itself to the lowly jeep.

Suppose that a jeep can carry a maximum load of n gallons of gas and can travel c miles per gallon. The jeep is required to cross a desert x miles wide. Our problem is to prescribe a method for making the journey most economically and to find the least sufficient amount of gas. It is not obvious that such a method exists, and it would be more exact to speak of the greatest lower bound, until the existence of the minimum is established.

We shall assume that n and c are both unity. This involves no loss of generality; it is equivalent to taking as our unit of distance nc , the number of miles that the jeep can travel on a full load.

If $x \leq 1$, the problem is trivial. If x exceeds 1, however, gas dumps will have to be established at various points along the way. It will be convenient to take the path of the jeep along the positive x -axis, starting at x and ending at the origin. The gas dumps will then form a subdivision σ of the interval $(0, x)$:

$$\sigma: 0 < x_1 < x_2 < \cdots < x_r < x,$$

in which the x_i denote the positions of the dumps (assumed to be finite in number). If s is any non-negative number less than x , the subdivision σ induces a subdivision of $(0, s)$ by deletion of all the stations to the right of s . There will be no ambiguity if we refer to this induced subdivision by the same symbol, σ . Other subdivisions will be denoted by σ' , σ'' , and so forth. If all the stations (points of division) of σ are contained among the stations of σ' , we shall say that σ' is a refinement of σ , written $\sigma' < \sigma$.

We may now rephrase our problem. Once a subdivision is fixed, the amount of gas required is still a function of the method of establishing and employing its stations. We shall denote by $f(x, \sigma)$ the greatest lower bound of this amount for all possible methods, and by $f(x)$ the greatest lower bound of $f(x, \sigma)$ for all possible subdivisions σ . Our task is to discover the form of $f(x)$.

In §2 we introduce the standard method of establishing and using the stations of a given subdivision σ , and we prove that this method is at least as economical as any other. This enables us to determine $f(x, \sigma)$ in §3. A rather surprising application of the standard method leads to the result (§4) that if $\sigma' < \sigma$, then $f(x, \sigma') \leq f(x, \sigma)$. In §5 we determine criteria for non-improvement

Reproduced by permission of the publisher.

by refinement. These criteria lead us to the construction of an optimum σ^* and to the explicit representation of $f(x, \sigma^*) = f(x)$ (§6). In §7 we derive a simple and accurate asymptotic formula for $f(x)$. The last section is devoted to a few remarks, including a comparison of the exact solution with the result obtained by considering the stations equally spaced (one of Niven's assumptions).

2. The standard method. One very natural method of employing the stations of a given σ is to build up the stockpile of gasoline at x , by making all the trips between x and x_r before going to x_{r-1} , and to continue in this way throughout the journey. In other words, once we go beyond any station x_i we never return to the preceding one, x_{i+1} .

Suppose that, by some other method, m complete round trips are made starting at x , followed by a last, one-way trip from x to x_r . The i th one of the round trips consists of A_i , the one-way trip from x to x_r ; B_i , the round trip starting and ending at x_r ; and C_i , the return trip from x_r to x . Let g_i be the amount of gas in the jeep at the start of A_i . Since $2(x-x_r)$ is the amount used in performing trips A_i and C_i , the amount $g_i - 2(x-x_r)$ plus the residue of the preceding trips is sufficient to perform B_i . If we replace the sequence $A_1, B_1, C_1, A_2, B_2, C_2, \dots, A_m, B_m, C_m, A_{m+1}$, by $A_1, C_1, A_2, C_2, \dots, A_m, C_m, A_{m+1}$, and deposit at x_r the amount $g_i - 2(x-x_r)$ after each A_i ($i = 1, 2, \dots, m$), and $g_{m+1} - (x-x_r)$ after A_{m+1} , we shall then be in a position to perform all the B_i in exactly the same order as before. When this has been done, the final configuration will not have been altered and no more gas will have been used. The same reasoning applies to all the trips starting at x_r , and so, by induction, the standard method is established as being at least as economical as any other. Henceforth we shall assume its use.

3. Determination of $f(x, \sigma)$. Now we suppose that there is given a subdivision

$$\sigma: 0 = x_0 < x_1 < \dots < x_r < x_{r+1} = x,$$

and that $f(x_{i-1}, \sigma)$ has already been determined. Clearly $f(x_0, \sigma) = 0$, so we have the initial step in the inductive definition of $f(x_i, \sigma)$. Let k_i be the number of trips to be made from x_i to x_{i-1} . Obviously $k_i \geq 1$. No gas is to be left behind at x_i , since that would imply waste. Hence the difference between $f(x_i, \sigma)$ and $f(x_{i-1}, \sigma)$ must be accounted for by the amount used in the $2k_i - 1$ trips between the two stations. Writing $\Delta_i = x_i - x_{i-1}$, we have

$$(1) \quad f(x_i, \sigma) - f(x_{i-1}, \sigma) = (2k_i - 1)\Delta_i, \quad (i = 1, \dots, r+1).$$

We must now determine k_i . The maximum amount of gas that can be transported on each of the first $k_i - 1$ trips is $1 - 2\Delta_i$; on the last, $1 - \Delta_i$, since there is no return. The total must not be less than the amount required to proceed from x_{i-1} . Hence

$$(2) \quad k_i(1 - 2\Delta_i) + \Delta_i \geq f(x_{i-1}, \sigma).$$

From (1) it is clear that the number of trips must be as small as possible so that

$$(3) \quad (k_t - 1)(1 - 2\Delta_t) + \Delta_t < f(x_{t-1}, \sigma),$$

provided that $k_t > 1$. It is easy to see that $k_t = 1$ for $x_t \leq 1$, and that $f(x_t, \sigma) = x_t$ in this case. If $x_t > 1$, we have $k_t > 1$. In this case, (2) and (3) determine the integer k_t uniquely, and $f(x_t, \sigma)$ is then obtained from (1). We remark that if the equality

$$m(1 - 2\Delta_t) + \Delta_t = f(x_{t-1}, \sigma)$$

holds for some integer m , then $k_t = m$.

We shall now derive a useful relationship between k_t and $f(x_t, \sigma)$. If we eliminate $f(x_{t-1}, \sigma)$ between (1) and (2), we have, for all $t \geq 1$,

$$(4) \quad k_t \geq f(x_t, \sigma).$$

Similarly, (1) and (3) yield

$$(5) \quad k_t - 1 < f(x_t, \sigma),$$

provided that $k_t > 1$. But we see directly that (5) is also valid for $k_t = 1$, so (4) and (5) hold for all $t \geq 1$. If we define $\{a\}$ as the least integer not less than a , then for all $t \geq 1$ we may write

$$(6) \quad k_t = \{f(x_t, \sigma)\}.$$

Since $f(z, \sigma)$ is an increasing function of z ,

$$(7) \quad k_t \leq k_{t+1}, \quad t \geq 1.$$

Summing (1), we obtain

$$(8) \quad f(x, \sigma) = \sum_{t=1}^{n+1} (2k_t - 1)\Delta_t.$$

4. Refinements of subdivisions. Let σ' be a refinement of σ . The quantity $f(x, \sigma)$ may be thought of as the result obtained by applying a *non-standard* method to σ' , namely, passing over those stations of σ' which do not belong to σ . It follows immediately from §2 that $f(x, \sigma')$ is not greater than $f(x, \sigma)$, that is,

$$(9) \quad f(x, \sigma') \leq f(x, \sigma) \quad \text{if } \sigma' < \sigma.$$

If (x_{t-1}, x_t) is an interval of σ , with the associated parameter k_t , and if $(x_{t-1} = y_0, y_1), (y_1, y_2), \dots, (y_{p-1}, y_p = x_t)$ are intervals of σ' , with parameters $k', k'', \dots, k^{(p)}$, then

$$(10) \quad k^{(p)} = \{f(x_t, \sigma')\} \leq \{f(x_t, \sigma)\} = k_t.$$

Using (7), we obtain

$$(11) \quad k' \leq k'' \leq \dots \leq k^{(p)} \leq k_t.$$

From (8),

$$(12) \quad f(x_i, \sigma') - f(x_{i-1}, \sigma') = \sum_{i=1}^p (2k^{(i)} - 1)(y_i - y_{i-1}).$$

Equation (1) may be written in the form

$$(13) \quad f(x_i, \sigma) - f(x_{i-1}, \sigma) = \sum_{i=1}^p (2k_i - 1)(y_i - y_{i-1}).$$

Subtracting the members of (12) from those of (13), we have

$$(14) \quad f(x_i, \sigma) - f(x_i, \sigma') = f(x_{i-1}, \sigma) - f(x_{i-1}, \sigma') + 2 \sum_{i=1}^p (k_i - k^{(i)})(y_i - y_{i-1}).$$

We observe that all the differences in (14) are non-negative. From this we deduce that actual improvement by refinement takes place if and only if we can find an interval (x_{i-1}, x_i) and an integer i such that $k_i > k^{(i)}$. By (11), this is equivalent to $k_i > k'$.

5. Properties of σ^* . Our problem will be solved if we can find a subdivision σ^* for which

$$(A) \quad f(x, \sigma^*) \leq f(x, \sigma) \quad \text{for every } \sigma.$$

We can bring to bear the results of §4 by proving that any σ^* which satisfies (A) also satisfies (B) that follows, and conversely.

$$(B) \quad f(x, \sigma^*) = f(x, \sigma') \quad \text{for every } \sigma' < \sigma^*.$$

Clearly, (A) and (9) imply (B). Conversely, suppose that (B) is satisfied, and let σ be any subdivision whatsoever. We choose for σ' the common refinement of σ and σ^* . From (B), $f(x, \sigma^*) = f(x, \sigma')$; another application of (9) shows that $f(x, \sigma') \leq f(x, \sigma)$. Combining these we obtain (A).

Using the criterion established at the end of §4, we find that (B) is equivalent to

(C) *For every $t = 1, 2, \dots, r+1$, and for every y such that $x_{t-1} < y \leq x_t$,*

$$k' = \{f(y, \sigma^*)\} = k_t = \{f(x_t, \sigma^*)\}.$$

We shall now show that (C) is equivalent to (D):

(D) *For every $m = 1, 2, \dots, [f(x, \sigma^*)]$, there exists an integer s such that $f(x_s, \sigma^*) = m$.*

Suppose first that (C) fails for some t and y . Since $f(x, \sigma^*)$ is strictly increasing,

$$(15) \quad f(x_{t-1}, \sigma^*) < f(y, \sigma^*).$$

By the definitions of k' and the function $\{ \cdot \}$,

$$(16) \quad f(y, \sigma^*) \leq k'.$$

Since (C) fails, $k' < k_t$, that is,

$$(17) \quad k' \leq k_t - 1.$$

Finally, since $k_t = \{f(x_t, \sigma^*)\}$ cannot exceed $f(x_t, \sigma^*)$ by as much as unity,

$$(18) \quad k_t - 1 < f(x_t, \sigma^*).$$

Combining (15), (16), (17), and (18), we see that the integer k' lies strictly between $f(x_{t-1}, \sigma^*)$ and $f(x_t, \sigma^*)$. By monotonicity, k' cannot be equal to $f(x_s, \sigma^*)$ for any s , so (D) fails.

Conversely, if m is an integer satisfying

$$(19) \quad f(x_{t-1}, \sigma^*) < m < f(x_t, \sigma^*),$$

we can find a number y such that

$$(20) \quad f(y, \sigma^*) = m,$$

and (C) is violated. To prove this, set

$$(21) \quad y = x_{t-1} + \frac{m - f(x_{t-1}, \sigma^*)}{2m - 1},$$

and let $\Delta = y - x_{t-1}$. Clearly Δ is positive, and

$$(22) \quad m(1 - 2\Delta) + \Delta = f(x_{t-1}, \sigma^*).$$

Referring to the remark in §3, we see that m is the parameter associated with the interval (x_{t-1}, y) , and

$$(23) \quad f(y, \sigma^*) = f(x_{t-1}, \sigma^*) + (2m - 1)(y - x_{t-1}) = m,$$

which proves (20). This completes the proof that (D) is equivalent to (C), (B), and (A).

6. Construction of σ^* . It is now almost trivial to construct a σ^* satisfying (D) and therefore (A). Merely choose the stations x_i^* so that $f(x_i^*, \sigma^*) = t$. Clearly this can be done for $t = 1$. Suppose that x_1^*, \dots, x_{t-1}^* have been found. We must determine x_t^* by

$$(24) \quad k_t = \{f(x_t^*, \sigma^*)\} = t,$$

$$(25) \quad f(x_t^*, \sigma^*) - f(x_{t-1}^*, \sigma^*) = (2k_t - 1)(x_t^* - x_{t-1}^*).$$

The left member of (25) equals unity; hence

$$(26) \quad x_t^* - x_{t-1}^* = (2t - 1)^{-1}.$$

Therefore

$$(27) \quad x_t^* = 1 + \frac{1}{3} + \frac{1}{5} + \dots + \frac{1}{2t - 1}.$$

It is easy to verify that (27) leads to the required equations $k_i = f(x_i^*, \sigma^*) = t$. The subdivision σ^* so determined evidently satisfies (D). If r is the greatest integer for which x_r^* does not exceed x , we may write

$$(28) \quad f(x) = f(x, \sigma^*) = r + (2r + 1)(x - x_r^*),$$

and

$$(29) \quad 0 \leq x - x_r^* < (2r + 1)^{-1}.$$

It has now been shown that $f(x)$, which represents the number of gallons needed to take the jeep x miles, is a function which is piecewise linear over intervals of length 1, $1/3$, $1/5$, $1/7$, and so on, the slope of the graph over the n th interval being the n th odd number so that the function takes consecutive integral values at the corner points.

7. An asymptotic formula for $f(x)$. From equation (1) it is possible to get a rough idea about the order of magnitude of $f(x)$. We have approximately

$$\begin{aligned} \Delta f &= (2k - 1)\Delta x, \\ k &= f(x). \end{aligned}$$

Neglecting the -1 compared with k , we find

$$\begin{aligned} \frac{\Delta f}{f} &= 2\Delta x \\ \log f &\approx 2x + C_1, \\ f &\approx C_2 e^{2x}. \end{aligned}$$

We shall not attempt to make these heuristic methods precise, but shall proceed directly to a derivation based on the exact solution obtained in the preceding section. Let us define

$$(30) \quad S(r) = 1 + \frac{1}{2} + \frac{1}{3} + \cdots + \frac{1}{r}.$$

It is well known that for large r ,

$$(31) \quad S(r) = \log r + C + \frac{1}{2r} + O\left(\frac{1}{r^2}\right),$$

where C is Euler's constant, .577 · · · , and the $O(1/r^2)$ denotes an error term whose absolute value does not exceed a certain constant, independent of r , multiplied by $1/r^2$. This constant may vary from one equation to the next. From (27), (30), and (31), we have

$$\begin{aligned} x_r^* &= S(2r) - \frac{1}{2} S(r) = \left(\log(2r) + C + \frac{1}{4r} + O\left(\frac{1}{r^2}\right) \right) \\ (32) \quad &\quad - \left(\frac{1}{2} \log r + \frac{1}{2} C + \frac{1}{4r} + O\left(\frac{1}{r^2}\right) \right). \end{aligned}$$

Therefore,

$$x_r^* = \log(2\sqrt{r}) + \frac{1}{2}C + O\left(\frac{1}{r^2}\right).$$

Taking exponentials,

$$(33) \quad \exp\left(x_r^* - \frac{C}{2}\right) = 2\sqrt{r} \exp\left(O\left(\frac{1}{r^2}\right)\right) = 2\sqrt{r} \left(1 + O\left(\frac{1}{r^2}\right)\right).$$

Squaring, we obtain

$$(34) \quad \frac{1}{4} \exp(2x_r^* - C) = r + O\left(\frac{1}{r}\right).$$

Thus, writing $g(u) = \frac{1}{4} \exp(2u - C)$,

$$(35) \quad f(x_r^*) = r = g(x_r^*) + O\left(\frac{1}{r}\right) = g(x_r^*) + O(e^{-2x_r^*}).$$

Now for any u satisfying

$$(36) \quad x_r^* < u \leq x < x_{r+1}^*,$$

we have, by equation (28),

$$(37) \quad f'(u) = 2r + 1.$$

Also,

$$(38) \quad g'(u) = 2g(u) > 2g(x_r^*) = 2r + O\left(\frac{1}{r}\right),$$

$$(39) \quad g'(u) < 2g(x_{r+1}^*) = 2r + 2 + O\left(\frac{1}{r}\right),$$

$$(40) \quad f'(u) - g'(u) = O(1).$$

Integrating (40) between x_r^* and x , we find

$$(41) \quad \begin{aligned} f(x) - g(x) &= (f(x_r^*) - g(x_r^*)) + \int_{x_r^*}^x (f'(u) - g'(u)) du \\ &= O\left(\frac{1}{r}\right) + O(x - x_r^*) = O\left(\frac{1}{r}\right) \\ &= O(e^{-2x}). \end{aligned}$$

Therefore, for all x ,

$$(42) \quad f(x) = \frac{1}{4} \exp(2x - C) + O(e^{-2x}).$$

It will be observed that the error term is not only of lower order than the principal term, but it actually tends to zero exponentially. Also, the approximate

equation derived by such high-handed methods at the beginning of this section turns out to be much more accurate than might have been expected.

8. Remarks. Suppose we decide to use equal subdivisions of the interval $(0, x)$, N in number. We can prove that if N is chosen to vary with x so that x^2/N tends to zero, then the increase in the amount of gas required (over the exact solution) is less than 50% for large x . To counterbalance this increase, however, the number of stations required will be very much smaller. For example, if N varies as the cube of x , it will also vary as the cube of $\log r$. Hence, if we take into account the cost (in time, energy, material, and so on) of setting up the stations, it might very well happen that the equal subdivisions would be more economical. Of course, we should then have an entirely new problem.

For a fixed x and sufficiently large N , we can come as close as we please to the minimum $f(x)$ by means of N equal subdivisions. An amusing fact here is that the minimum can be *attained* if and only if x is rational.

We close with several remarks about the character of the solution σ^* we have obtained here. It is obvious that this solution is not unique, since every refinement of σ^* is also a solution. It can be shown that the converse is also true; that is, every solution is a refinement of σ^* . Furthermore, if we consider the class of subdivisions σ for which the function $f(x, \sigma)$ is *continuous*, we can prove that this class is identical with the class of all solutions. It would be of interest to see whether this criterion can be obtained directly, and whether the minimum $f(x)$ can be derived from it.

III. GRAPHICAL SOLUTION TO EXAMPLE PROBLEM NO. 1 (THE JEEP PROBLEM)

Postulates for optimum solution are:

1. The number of trips between two consecutive stations is always odd.
2. The graph of the fuel consumed during the entire trip, viewed from the terminus, is a series of straight lines having a continually increasing slope.
3. To obtain maximum efficiency, the jeep must always initiate each trip to the next dump station fully loaded.

Consistent with Dr. Fine's choice for n and c , we take $n = c = 1$. This means that if the ordinate axis is c when the abscissa axis is n , a 45 deg line gives the relationship between miles traveled and fuel consumed.

Figure 1 graphically portrays the relationship between possible fuel dump locations (c_n), fuel consumed in traveling between each pair of proximate points ($c_n F_n$, $F_n F'_n$), and fuel available after a single trip between each such pair. The word "possible" in specifying the fuel dump locations and the figure are drawn consonant with the postulates I and III and Dr. Fine's choice for n and c .

Examining Fig. 1, we can see that segments $F_n F'_n$ represent the quantity of fuel which can be deposited at the fuel dump and still leave enough fuel ($F_n F''_n$) to travel back for the next fuel load pickup. Thus, if the fuel dump is located $1/3$ of the range from start, a round trip consumes $2/3$ of the range, resulting in the deposit at the dump being $1/3$ of the range. A trip to the dump without return permits deposit of $2/3$ of the range.

Similarly, if the distance between dumps is $1/5$ range, the round trip permits deposit of $3/5$ of the range, while the last single trip makes it possible to deposit $4/5$ of the range.

The efficiency of depositing fuel, i.e., the ratio of the deposited fuel to that consumed in the round trip, increases as the distance between fuel dump points decreases.

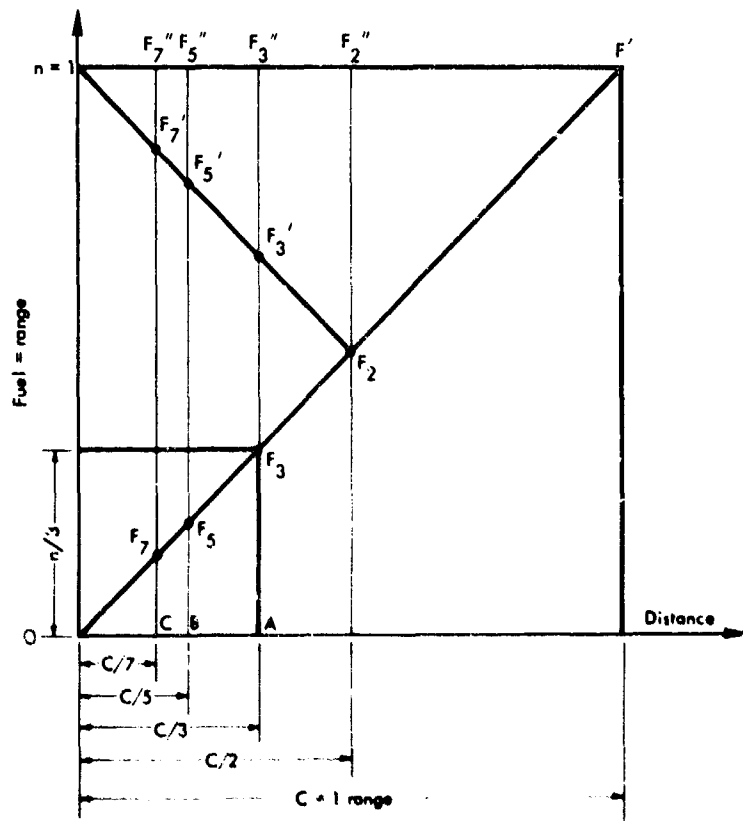


FIGURE 1.

We now proceed in Fig. 2 to construct a graphical solution of a possible relationship between fuel requirements and locations of fuel dumps for ranges exceeding that of the jeep. Consistent with postulate III, we start at the terminus and establish fuel dump previous to it as being a full jeep range away. The triangle OAF establishes the relationship between fuel consumed (the ordinate) and distance traveled (the abscissa). The location of the nearest fuel dump can be inferred from the observation that, consistent with postulates I and III, $x = 1/3$ is a logical contender for the preferred distance. The figure shows the three trips involved in the transfer and establishes the sufficiency of point F_3 as a solution.

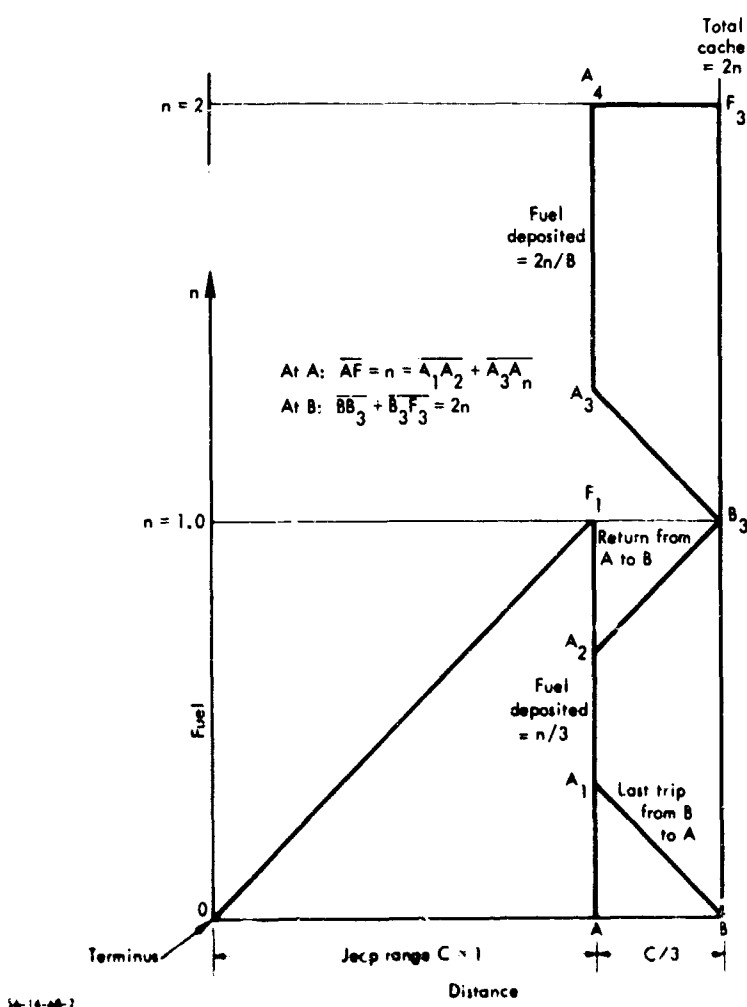


FIGURE 2.

One observes now that the next fuel dump must contain sufficient amount to permit the deposit of two full ranges* at fuel dump 1/3. This requires preferably increased efficiency of fuel transfer. Thus, it is logical to assume the new fuel dump location somewhat closer, which suggests the point 1/5 as the choice. In Fig. 3 it is readily established by drawing the appropriate 45 deg lines representing the trips between the 1/3 point and the new point that five such trips consume one jeep range while affording the deposition of two ranges at point 1/3, thus producing point F_5 . Using similar reasoning, we construct points F_7 , F_9 , etc., corresponding to progressively decreasing distance between fuel dumps.

Thus, we have arrived at a solution which is consonant with our three postulates.

Now we shall endeavor to prove that this solution represents the preferred solution.

The 1/3 range distance seems to be so logical that it is reasonable to question the introduction of the 1/5 and 1/7 fuel dumps. As a test we will eliminate fuel dump 1/5 and replace fuel dump 1/7 with a new fuel dump located, from fuel dump 1/3, a distance of another 1/3 range. Figure 4 shows that this choice of a new fuel dump penalizes by one full range--from F_7 to F'_3 --not even considering the slight loss of the distance.

*The word "range" is used here to designate the amount of fuel needed for that distance.

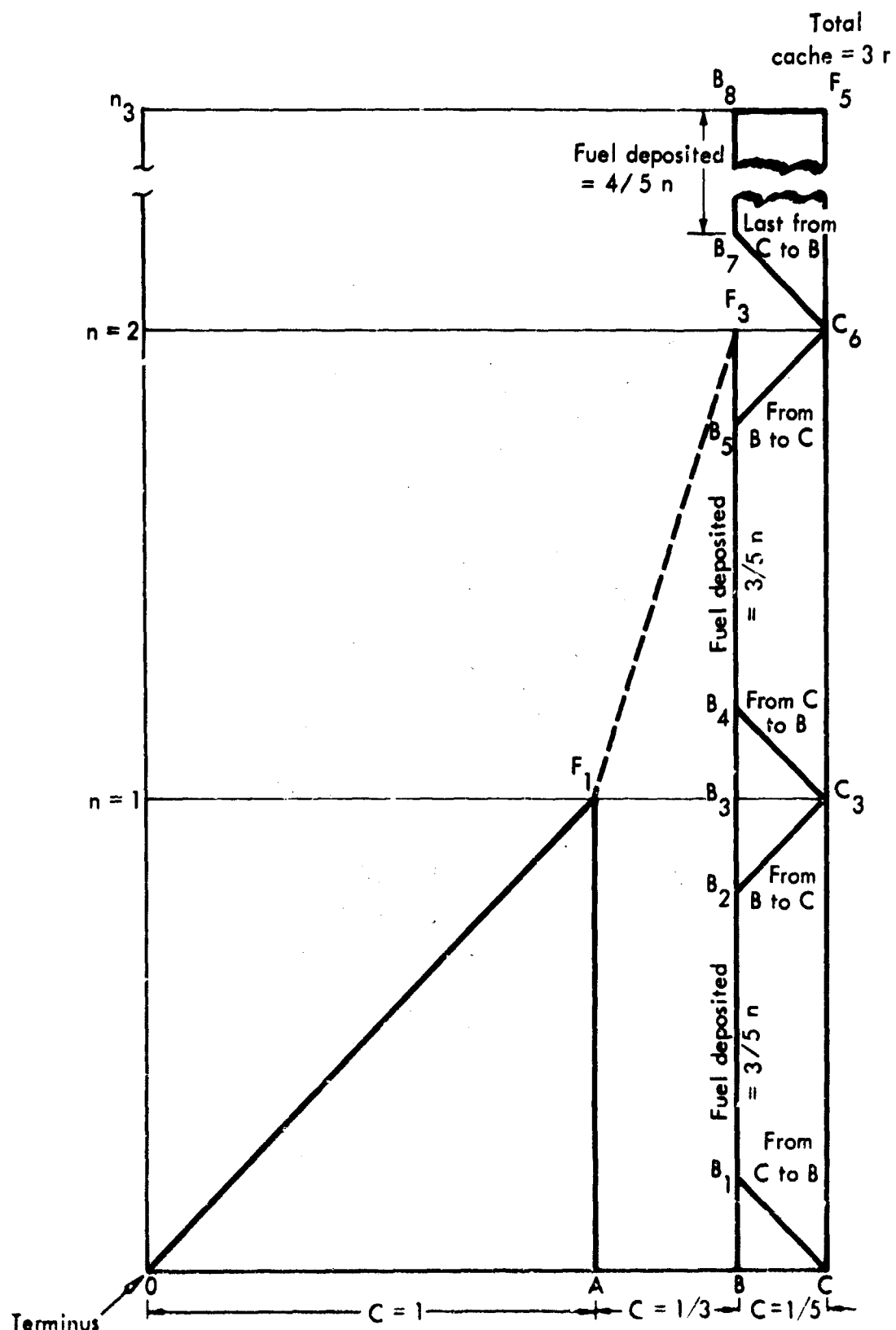
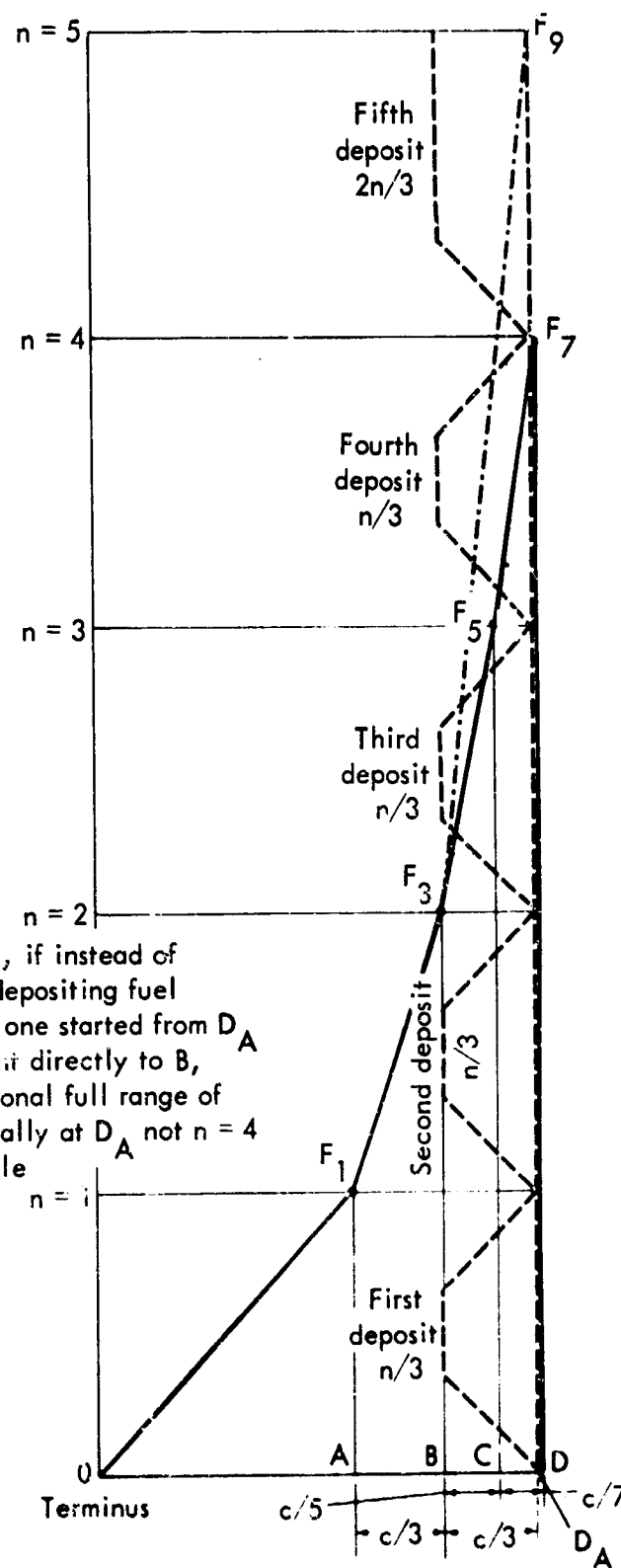


FIGURE 3.



This illustration shows that, if instead of starting from point D and depositing fuel at C and proceeding to B, one started from D_A distant $C/3$ from B and went directly to B, this would entail an additional full range of travel, thus requiring initially at D_A not $n = 4$ but $n = 5$; $BD = 12/35$ while $BD_A = 1/3$.

FIGURE 4.

Similar tests (Fig. 5) will readily prove that fuel dump locations closer than those originally chosen in conformance with the stated postulates will not affect the fuel requirements but will increase the number of trips, while locations greater than the original ones will result in severe penalty of the required fuel.

This illustration proves that there is no need to have an intermediate cache of fuel between A and B because it saves no fuel, but merely increases the number of trips.

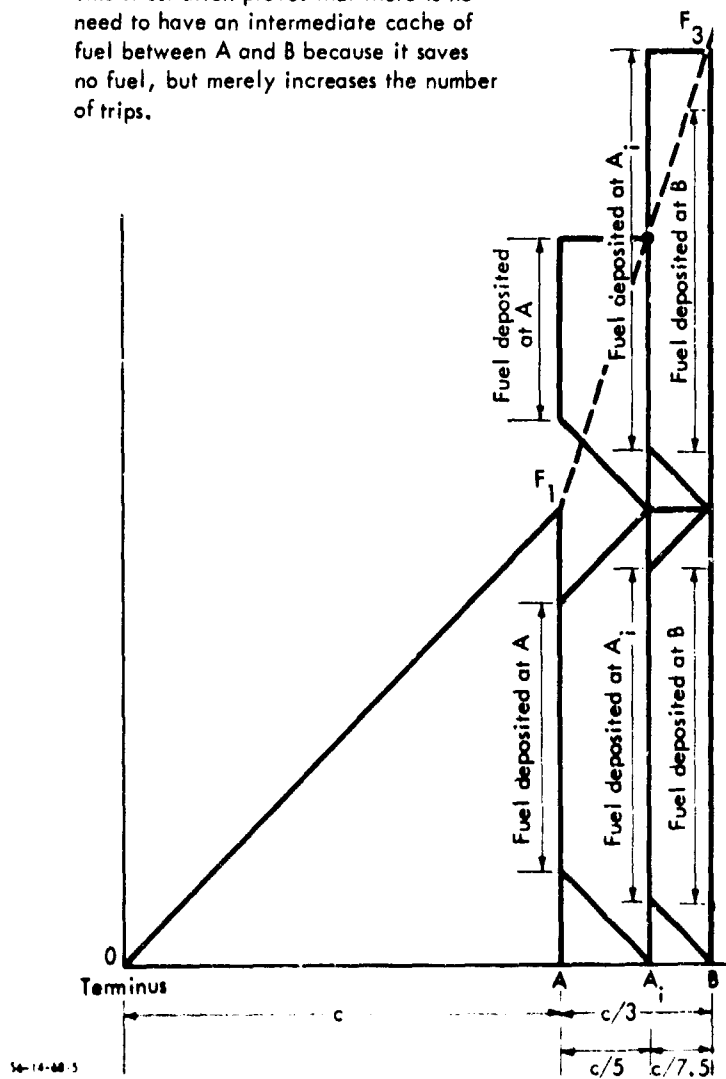


FIGURE 5.

Thus, we conclude that fuel dump locations $1, 1/3, 1/5, 1/7, 1/9, 1/11$, etc. result in the optimum, i.e., a minimum amount of fuel, but not a minimum number of trips. This fact is summarized in Fig. 6.

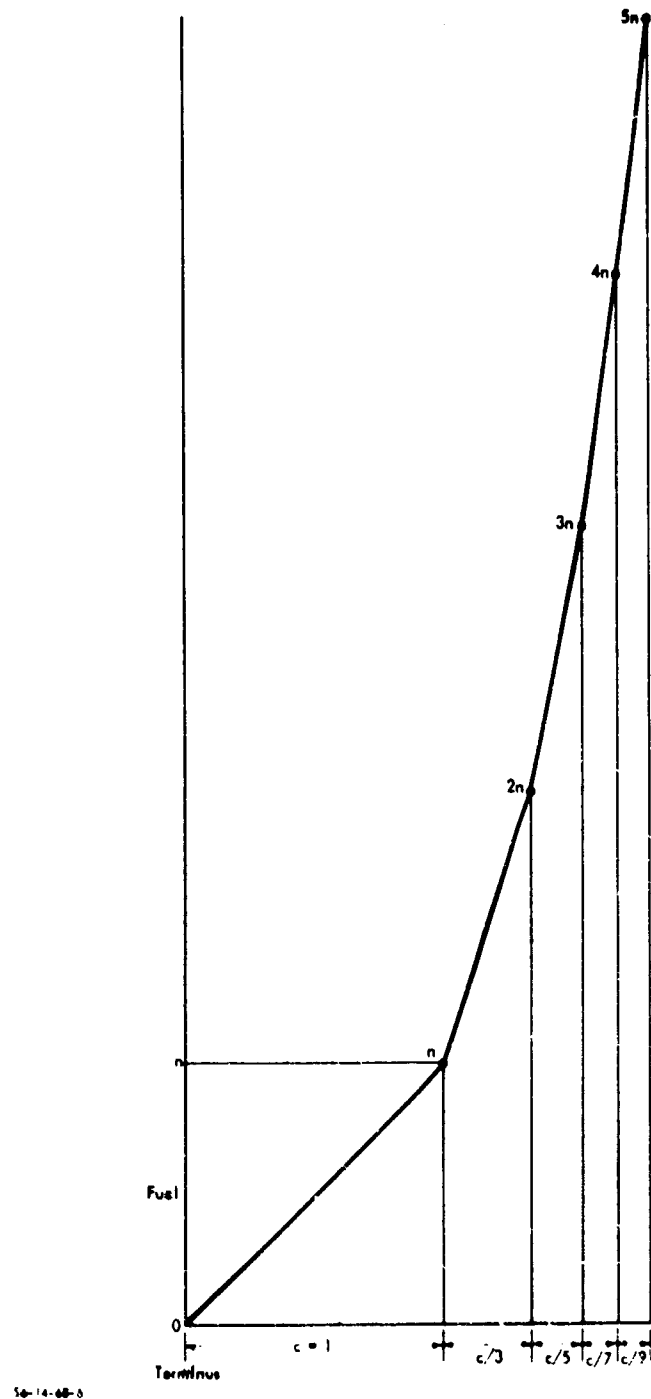


FIGURE 6.

IV. THE RANGE OF A FLEET OF AIRCRAFT*#

J. N. FRANKLIN†

1. Introduction. The problem discussed in this paper is to determine the range of a fleet of n aircraft with fuel capacities g_i gallons and fuel efficiencies r_i gallons per mile ($i = 1, \dots, n$). It is assumed that the aircraft may share fuel in flight and that any of the aircraft may be abandoned at any stage. The range is defined to be the greatest distance which can be attained in this way. Initially the fleet is supposed to have g gallons of fuel.

A theoretical solution is obtained by the method which Richard Bellman [1] calls dynamic programming. Explicit solutions are obtained in the case of two aircraft with different fuel capacities and fuel efficiencies and in the case of any number of aircraft with identical fuel capacities and identical fuel efficiencies.

The problem is similar to the so-called jeep problem. The jeep problem was solved rigorously by N. J. Fine [2]. A solution was also obtained by O. Helmer [3, 4]. Fine cited an unpublished solution by L. Alaoglu. The problem was generalized by C. G. Phipps [5]. Phipps informally developed the special result which is deduced in § 4 of this paper.

2. A recurrence formula. Let C_m be any subset of m of the given n aircraft. Mathematically C_m may be represented by a subset of m of the first n positive integers. Let $M(g, C_m)$ be defined as the range of the fleet of m aircraft C_m starting with g gallons of fuel. Then the required range of the n given aircraft is $M(g, C_n)$, where $C_n = \{1, 2, \dots, n\}$. When there is only one aircraft,

$$(1) \quad M(g, C_1) = \min(g/r_1, g/r_1),$$

where C_1 consists of just the i th aircraft.

When there are $m > 1$ aircraft, a distance x is flown by all m aircraft. Then one aircraft is abandoned, leaving a subset $C_{m-1} \subset C_m$. It is unnecessary to consider abandoning more than one aircraft at a time. For example, the effect of abandoning two aircraft from C_m may be obtained by abandoning one of the aircraft from C_m and then immediately abandoning the second aircraft from C_{m-1} . After the distance x the amount of fuel remaining is

$$(2) \quad h = g - x \sum_{i \in C_m} r_i.$$

The greatest distance which can be attained by the remaining aircraft

* Received by the editors August 20, 1960 and in revised form March 17, 1960.

† California Institute of Technology, Pasadena, California.

Reproduced by permission of the publisher.

C_{m-1} starting with h gallons of fuel is $M(h, C_{m-1})$. If g , C_m , and x are prescribed, the subset C_{m-1} should be chosen so as to maximize the remaining distance $M(h, C_{m-1})$. The total distance traveled will then be

$$(3) \quad x + \max_{C_{m-1} \subset C_m} M(g - x \sum_{c_m} r_i, C_{m-1}).$$

The maximum distance $M(g, C_m)$ is obtained by maximizing the last expression with respect to x . In other words, if g is \leq the total capacity $\sum g_i$ for i in C_m ,

$$(4) \quad \begin{aligned} M(g, C_m) \\ = \max_{x \leq g / \sum_{c_m} r_i} [x + \max_{C_{m-1} \subset C_m} M(g - x \sum_{c_m} r_i, C_{m-1})]. \end{aligned}$$

In this maximization it is required that x be $\leq g / \sum r_i$, since this is the greatest distance which all m aircraft can fly with g gallons of fuel before one aircraft is abandoned. If g is given in excess of the total fuel capacity $\sum g_i$ of the aircraft in C_m , then some fuel must be thrown away and

$$(5) \quad M(g, C_m) = M(\sum_{c_m} g_i, C_m) \quad (g > \sum_{c_m} g_i).$$

The recurrence formulas (4) and (5) uniquely determine $M(g, C_m)$ for all subsets C_m with $m = 2, 3, \dots, n$. It is easy to see that each function $M(g, C_m)$ is polygonal in g , i.e., continuous and piecewise linear. In fact, (4) may be rewritten, by the identity (2), as

$$(6) \quad M(g, C_m) = \max_{h \leq g} [a(g - h) + \max_{C_{m-1} \subset C_m} M(h, C_{m-1})],$$

where $a = 1 / \sum_{c_m} r_i$. We know from (1) that every function $M(g, C_1)$ is polygonal. Let us suppose that every function $M(h, C_{m-1})$ is polygonal. Then

$$(7) \quad P(h) = \max_{C_{m-1} \subset C_m} M(h, C_{m-1})$$

is polygonal, since it is the largest of a finite number of polygonal functions. Now (6) takes the form

$$(8) \quad M(g, C_m) = ag + \max_{h \leq g} [-ah + P(h)].$$

Since $-ah + P(h)$ is polygonal, its maximum value for $h \leq g$ is a polygonal function of g , say $P^*(g)$, and therefore $M = ag + P^*(g)$ is also polygonal. This completes an inductive proof that $M(g, C_m)$ is polygonal for $g \leq \sum g_i$, within which range (8) holds. It now follows from (5) that $M(g, C_m)$ is polygonal for all g . Incidentally, the identity (8) shows that $M(g, C_m)$ is steadily increasing with rate $\geq a = 1 / \sum_{c_m} r_i$ when $g \leq \sum g_i$. For larger values of g , (5) shows that M is constant.

3. The case of two aircraft. Let

$$(9) \quad M(g) = M(g, C_2), M_i(g) = M(g, C_1) \quad (C_1 = i = 1, 2).$$

For $g \leq g_1 + g_2$, (8) takes the form

$$(10) \quad M(g) = ag + \max_{h \leq g} [-ah + P(h)],$$

where

$$(11) \quad P(h) = \max_{i=1,2} M_i(h), \quad a = 1/(r_1 + r_2).$$

By the identity (1),

$$(12) \quad M_i(h) = \min (h/r_i, g_i/r_i) \quad (i = 1, 2).$$

Without loss of generality it will be assumed that $r_1 \leq r_2$.

Case 1. Suppose that $g_1/r_1 \geq g_2/r_2$. In this case

$$(13) \quad P(h) = M_1(h) \quad (\text{for all } h).$$

Then

$$(14) \quad -ah + P(h) = \begin{cases} -ah + h/r_1 & (h \leq g_1) \\ -ah + g_1/r_1 & (h \geq g_1). \end{cases}$$

Since $a < 1/r_1$, it follows that

$$(15) \quad P^*(g) = \begin{cases} -ag + g/r_1 & (g \leq g_1) \\ -ag_1 + g_1/r_1 & (g \geq g_1), \end{cases}$$

where $P^*(g) = \max [-ah + P(h)]$ for $h \leq g$. From (8) it follows that

$$(16) \quad M(g) = \begin{cases} g/r_1 & (g \leq g_1) \\ a(g - g_1) + g_1/r_1 & (g_1 \leq g \leq g_1 + g_2). \end{cases}$$

For $g > g_1 + g_2$, equation (5) gives

$$(17) \quad M(g) = ag_2 + g_1/r_1 \quad (g > g_1 + g_2).$$

From the definition (2) of the remaining fuel h as a function of the distance x to be traveled by both aircraft, it is clear that the optimal procedure in Case I is to use just aircraft 1 if $g \leq g_1$, or if $g > g_1$ to use both aircraft until only g_1 gallons of fuel remain and then to complete the trip with just aircraft 1.

Case 2. Suppose that $g_1/r_1 < g_2/r_2$. In this case

$$(18) \quad P(h) = \begin{cases} h/r_1 & (h \leq g_1) \\ g_1/r_1 & (g_1 \leq h \leq g^*) \\ h/r_2 & (g^* \leq h \leq g_1) \\ g_2/r_2 & (h \geq g_1) \end{cases}$$

where $g^* = r_2 g_1 / r_1$ is the abscissa of the point of intersection of the graphs of $M_1(h)$ and $M_2(h)$. The function $-ah + P(h)$ is a polygonal function with peaks at $h = g_1$ and $h = g_2$. There are two subcases, depending upon whether the first peak is higher (A) or lower (B) than the second peak.

Case 2A. Suppose that $g_1/r_1 < g_2/r_2$ and $g_1/r_1^2 \geq g_2/r_2^2$. Then

$$(19) \quad P^*(g) = \begin{cases} -ag + g/r_1 & (g \leq g_1) \\ -ag_1 + g_1/r_1 & (g \geq g_1), \end{cases}$$

and, as in Case 1, $M(g)$ has the form (16), (17). The optimal procedure in this case is the same as that in Case 1.

Case 2B. Suppose that $g_1/r_1 < g_2/r_2$ and $g_1/r_1^2 < g_2/r_2^2$. Let $g' = g_1 r_2^2 / r_1^2$; this is the first value of $h > g_1$ at which $-ah + P(h) = -ag_1 + P(g_1)$. Then

$$(20) \quad P^*(g) = \begin{cases} -ag + g/r_1 & (g \leq g_1) \\ -ag_1 + g_1/r_1 & (g_1 \leq g \leq g') \\ -ag + g/r_2 & (g' \leq g \leq g_2) \\ -ag_2 + g_2/r_2 & (g \geq g_2). \end{cases}$$

Therefore,

$$(21) \quad M(g) = \begin{cases} g/r_1 & (g \leq g_1) \\ a(g - g_1) + g_1/r_1 & (g_1 \leq g \leq g') \\ g/r_2 & (g' \leq g \leq g_2) \\ a(g - g_2) + g_2/r_2 & (g_2 \leq g \leq g_1 + g_2), \end{cases}$$

and, according to equation (5),

$$(22) \quad M(g) = ag_1 + g_2/r_2 \quad (g > g_1 + g_2)$$

The optimal procedure is as follows. If $g \leq g_1$, use only aircraft 1. If $g_1 \leq g \leq g'$, use both aircraft until only g_1 gallons remain; then use just aircraft 1. If $g' \leq g \leq g_2$, use only aircraft 2. If $g_2 \leq g \leq g_1 + g_2$, use both aircraft until only g_1 gallons remain; then use just aircraft 2. If $g > g_1 + g_2$, some fuel must be thrown away, and the trip is made with $g = g_1 + g_2$ as described in the preceding sentence.

From these results it is apparent that in the general case of n aircraft the optimal policy will depend in a complicated way upon g as well as upon the g_i and r_i . For example, the value of g may determine which of the aircraft finishes the trip.

4. The case of identical aircraft. Let

$$(23) \quad g_i = G, \quad r_i = R \quad (i = 1, \dots, n),$$

and let $M_m(g) = M(g, C_m)$ ($m = 1, \dots, n$). In this case the recurrence formulas (4), (5) take the form

$$(24) \quad M_m(g) = \max_{x \leq g/mR} [x + M_{m-1}(g - mRx)] \quad (g \leq mG),$$

$$(25) \quad M_m(g) = M_m(mG) \quad (g > mG).$$

It will be shown that, if $k = \lfloor g/G \rfloor$, the greatest integer $\leq g/G$,

$$(26) \quad M_m(g) = \frac{G}{R} \left(1 + \frac{1}{2} + \dots + \frac{1}{k} \right) + \frac{g - kG}{(k+1)R} \quad (g \leq mG, k \geq 1),$$

$$(27) \quad M_m(g) = \frac{G}{R} \left(1 + \frac{1}{2} + \dots + \frac{1}{m} \right) \quad (g > mG).$$

The right-hand side of (26) is defined as g/R when $k = 0$. In the optimal policy, if $g = kG \leq mG$, the trip is begun with k aircraft. If $kG < g \leq (k+1)G \leq mG$, the trip is begun with $k+1$ aircraft. If $g > mG$, then $g - mG$ gallons of fuel must be thrown away, and the trip is begun with all m aircraft. In any case, if the trip is begun with K aircraft, the first aircraft is abandoned when only $(K-1)G$ gallons of fuel remain. Then $K-1$ aircraft are flown until only $(K-2)G$ gallons remain, and so on.

This result can be established by induction. If $m = 1$, formulas (26) and (27) become

$$(28) \quad M_1(g) = g/R \quad (g \leq G),$$

$$(29) \quad M_1(g) = G/R \quad (g > G),$$

which is correct according to (1). Assume that the result holds for $m-1$ aircraft. Then

$$(30) \quad \frac{d}{dh} M_{m-1}(h) \geq \frac{1}{(m-1)R} \quad (0 < h < (m-1)G)$$

at all points h at which the polygonal function $M_{m-1}(h)$ has a derivative. Therefore, $x + M_{m-1}(g - mRx)$ is a steadily decreasing function of x for $0 \leq x \leq g/mR$ if $x \leq (m-1)R$. Setting $x = 0$ in (24) gives the maximum value

$$(31) \quad M_m(g) = M_{m-1}(g) \quad (g \leq (m-1)G).$$

But $M_{m-1}(g)$ is given by the right-hand side of (26) for all $g \leq (m-1)G$. Therefore, (26) is established for $g \leq (m-1)G$.

Next suppose that $(m-1)G < g \leq mG$. Then $M_{m-1}(g - mRx)$ is constant for $g - mRx \geq (m-1)G$; for larger values of x the rate of in-

crease is $\leq -mR/(m-1)R < -1$. Therefore, the maximum (24) is attained when $g - mRx = (m-1)G$, and

$$(32) \quad \begin{aligned} M_m(g) &= \frac{g - (m-1)G}{mR} + M_{m-1}((m-1)G) \\ &= \frac{g - (m-1)G}{mR} + \frac{G}{R} \left(1 + \frac{1}{2} + \cdots + \frac{1}{m-1} \right). \end{aligned}$$

This establishes the result (26) for $(m-1)G < g \leq mG$. The result (27) for $g > mG$ follows from (5).

5. An asymptotic formula for g . The solution (26), (27) in the case of identical aircraft is similar to the solution of the jeep problem, although the solutions were established by different methods. In this section an asymptotic formula will be developed for the amount of fuel g which is necessary in order to transport identical aircraft a distance x . Let $g = f(x)$. It will be shown that

$$(33) \quad f(x) = A(x) + O(\exp(-Rx/G)),$$

where

$$(34) \quad A(x) = G \left(-\frac{1}{2} + \exp \left(\frac{Rx}{G} - C \right) \right).$$

In these identities G and R are the fuel capacity and the fuel efficiency of each of the aircraft, and C is Euler's constant, $.577\cdots$. This result is comparable to Fine's asymptotic formula for the solution of the jeep problem [2].

From the result of the last section it is clear that x is the range of $n+1$ aircraft with initial fuel supply g , where $nG < g \leq (n+1)G$. Setting $m = n+1$ in (26) gives

$$(35) \quad x = x^* + \frac{g - nG}{(n+1)R},$$

where

$$(36) \quad \begin{aligned} x^* &= \frac{G}{R} \left(1 + \frac{1}{2} + \cdots + \frac{1}{n} \right) \\ &= \frac{G}{R} \left(\log n + C + \frac{1}{2n} + O\left(\frac{1}{n^2}\right) \right). \end{aligned}$$

This well-known asymptotic formula is derived in [6, p. 529]. From (36) it follows that

$$(37) \quad \exp \left(\frac{Rx^*}{G} - C \right) = n \exp \left(\frac{1}{2n} + O\left(\frac{1}{n^2}\right) \right) = n + \frac{1}{2} + O\left(\frac{1}{n}\right).$$

This relation shows that

$$(38) \quad n \geq \text{constant} + \exp\left(\frac{Rx^*}{G} - C\right),$$

$$(39) \quad \frac{1}{n} = O(\exp(-Rx^*/G)),$$

$$(40) \quad n = -\frac{1}{2} + \exp\left(\frac{Rx^*}{G} - C\right) + O(\exp(-Rx^*/G)).$$

Since $nG = f(x^*)$, multiplication by G gives

$$(41) \quad f(x^*) = A(x^*) + O(\exp(-Rx^*/G)).$$

In order to justify replacement of x^* by x in the identity (41), it is convenient first to show that

$$(42) \quad f'(x) - A'(x) = O(1) \quad (0 < x - x^* < G/(n+1)R).$$

Differentiation of g as a function of x in (35) gives

$$(43) \quad f'(x) = (n+1)R.$$

But

$$(44) \quad \begin{aligned} A'(x^*) &< A'(x) = R \exp\left(\frac{Rx}{G} - C\right) \\ &\leq A'(x^* + G/(n+1)R) \leq A'(x^*) \exp(1/(n+1)). \end{aligned}$$

Since, by (39), $A'(x^*)/(n+1) = O(1)$, it follows that

$$(45) \quad A'(x) = A'(x^*) + O(1).$$

Subtraction of (45) from (43) gives

$$(46) \quad f'(x) - A'(x) = (n+1)R - R \exp\left(\frac{Rx^*}{G} - C\right) + O(1).$$

The required relation (42) now follows from (40). Integration of (42) gives

$$(47) \quad \begin{aligned} f(x) - A(x) &= f(x^*) - A(x^*) + O(x - x^*) \\ &= O(\exp(-Rx^*/G)) + O(1/n) = O(\exp(-Rx^*/G)). \end{aligned}$$

Since $x - x^*$ is bounded, x^* may be replaced by x in the last expression, and this gives the asymptotic formula (33).

REFERENCES

1. RICHARD BELLMAN, *Dynamic Programming*, Princeton University Press, Princeton, 1957.
2. N. J. FINE, *The jeep problem*, Amer. Math. Monthly, 54 (1947), pp. 24-31.
3. O. HELMER, *A problem in logistics: The jeep problem*, RAND Report RA-15015, 1946.
4. O. HELMER, *A problem in logistics: The jeep problem (Part 2)*, RAND Report RA-15019, 1947.
5. C. G. PHIPPS, *The jeep problem: A more general solution*, Amer. Math. Monthly, 54 (1947), pp. 458-462.
6. KONRAD KNOPP, *Theory and Application of Infinite Series*, Blackie and Son, London, 1949.

V. GRAPHICAL SOLUTION TO EXAMPLE NO. 2 (THE RANGE OF A FLEET OF AIRCRAFT)

I am indebted to my colleague Dr. H. Morris, who encouraged me to clarify the presentation and to provide a treatment of the case of aircraft of unequal speed. Two solutions are presented.

A. CASE OF AIRCRAFT WITH EQUAL SPEEDS

Initially, the problem will be solved using the two tacit assumptions contained in Franklin's solution, namely:

1. All aircraft are flying at the same speed.
2. Time lost in refueling is neglected.

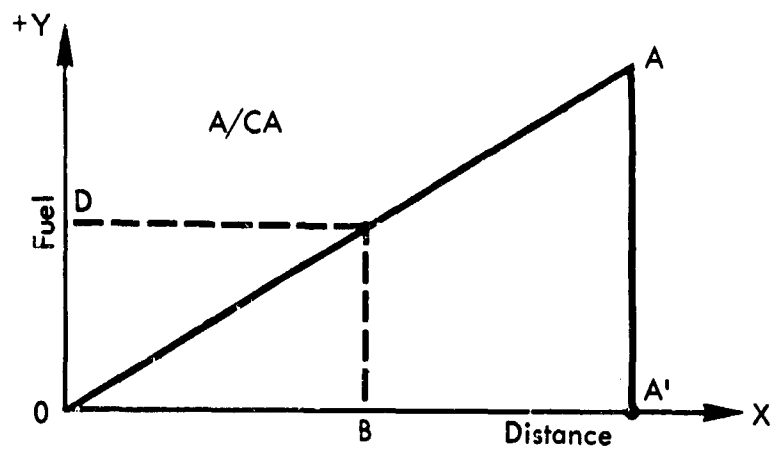


FIGURE 1.

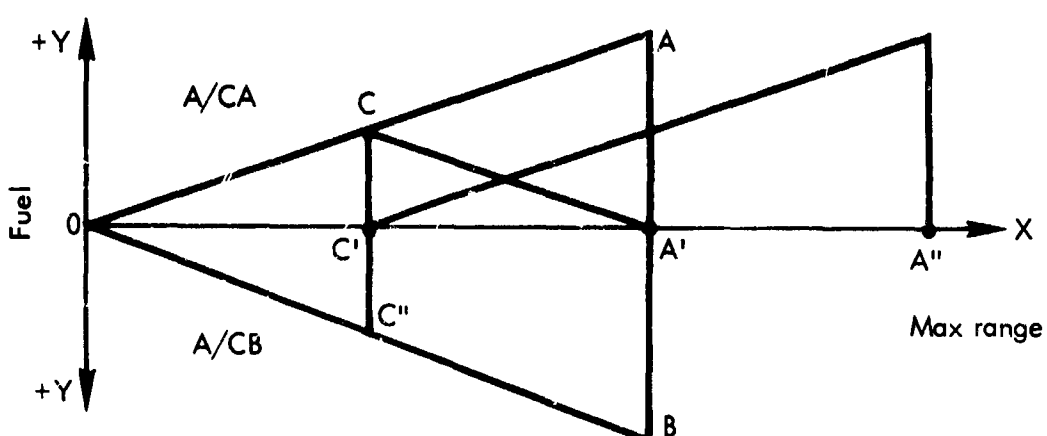


FIGURE 2.

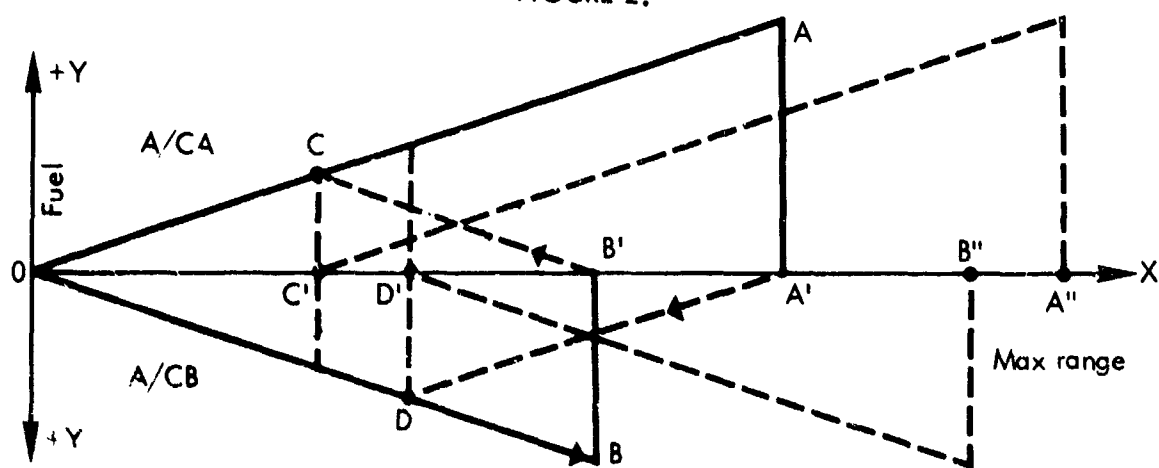


FIGURE 3.

Figure 1 shows the relationship between fuel consumed and distance flown; for example, the fuel required to travel distance OB is given by the ordinate OD. The relative efficiencies of aircraft are readily indicated by the slope of lines AO--the smaller the slope, the more efficient is the aircraft.

Figure 2 shows the solution for the case of two aircraft of equal efficiency and equal range. In this case it is immaterial which of the two aircraft gives up its fuel--the maximum range remains the same in either case. To determine the range and location for refueling, for convenience of graphical solution the fuel-distance relationship for these aircraft is drawn, one below and the other above the x-axis, OA applying to aircraft A and OB to aircraft B.

If we draw line A'C parallel to line OB, the ordinates CC' and C'C" give the amounts of fuel required by aircrafts A and B, respectively, to cover the distance OC'. It becomes evident that at point C, aircraft B, by giving up all its fuel, can replenish the fuel consumed by aircraft A. In fact, $CC'' = A'B$, and $CC' = A'B - C'C''$; therefore, at C', aircraft B has just enough fuel left to restore the fuel originally carried by aircraft A. Thus, aircraft A can now proceed to a new destination A" such that $C'A'' = OA'$.

Next, we consider the case of two aircraft of equal efficiency but unequal range. In this case it is not self-evident which of the two aircraft should give up its fuel. Examining both cases, as shown in Fig. 3, we see that aircraft B should refuel aircraft A. The graphical construction involved is the same as before but is repeated for each aircraft to establish two maximum range points: point B' if aircraft B is used to refuel aircraft A at a distance OC' from start of flight, and point A' if aircraft A refuels aircraft B at a distance OD' from the departure point.

Figures 4, 5, and 6 show the determination of maximum ranges for pairs of aircraft of differing efficiencies and ranges.

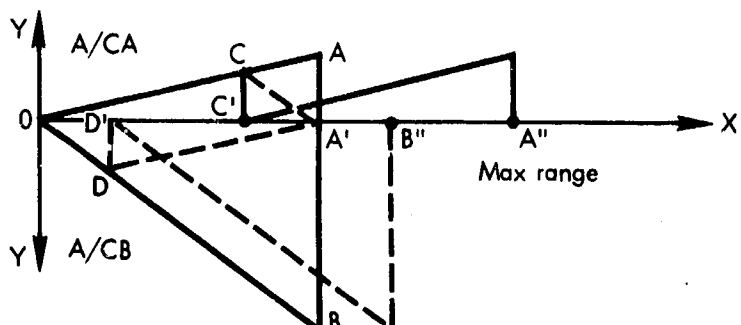


FIGURE 4.

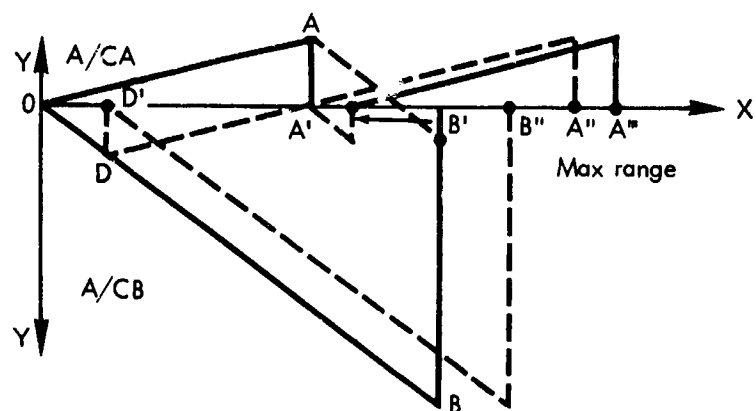


FIGURE 5.

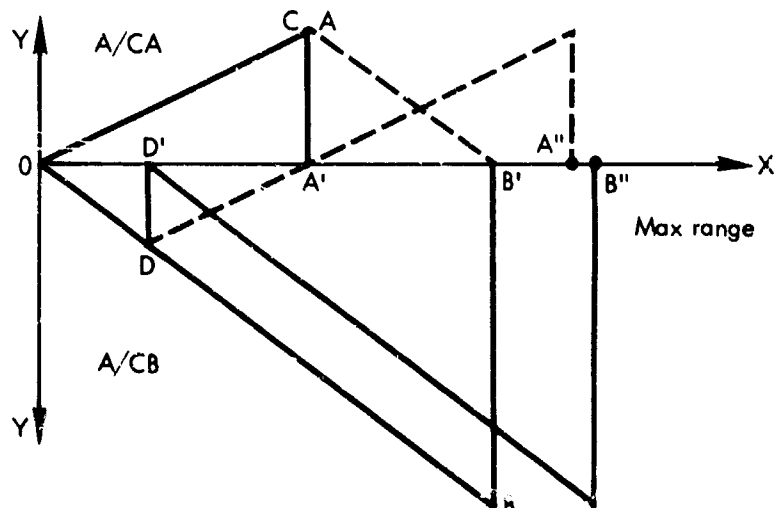


FIGURE 6.

We will assume now that fleet of aircraft examples shown in Figs. 4, 5, and 6 represented six aircraft flying together. Having established the preferred order for refueling for each pair, we are now left with three aircraft, A_4 , A_5 , and B_6 , the subscript designating the figure where we have determined the new range of the respective aircraft. We also established the locations where the refuelings took place. Figures 7 and 8 reproduce these locations at the time of refueling, also individual ranges which each aircraft could cover without further refueling. For clarity we redraw Figs. 4, 5, and 6, combining the fuel-distance relationship of the three aircraft in Fig. 7 to facilitate graphical solution of the problem. If aircraft B were to refuel aircraft A, the amount of available fuel is given by line $O'B_{64}$. Proceeding as before, we find point A'_4 and thus the range extension of aircraft A_4 to point A''_4 from the sequence of refueling A''_4 with aircraft B and finally with aircraft A_5 .

Figure 8 is merely a check to see whether a different refueling sequence would improve the range. In the illustration, A_4 refuels A_5 , and B_6 completes the refueling cycle by giving up its fuel to A_5 . The range, although close to that found in Fig. 7, is, however, smaller.

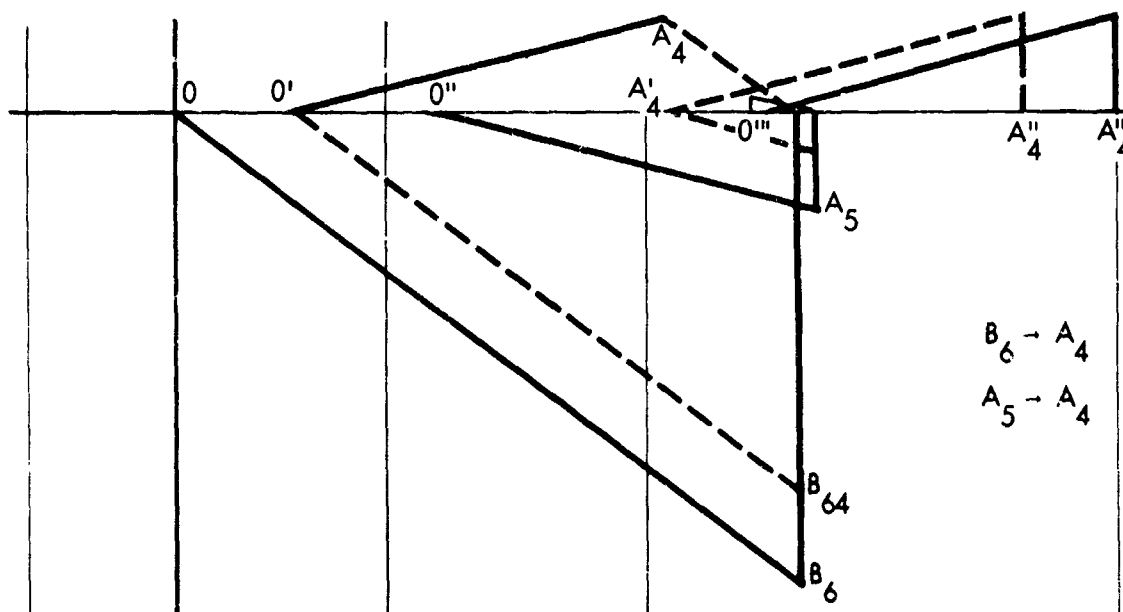


FIGURE 7.

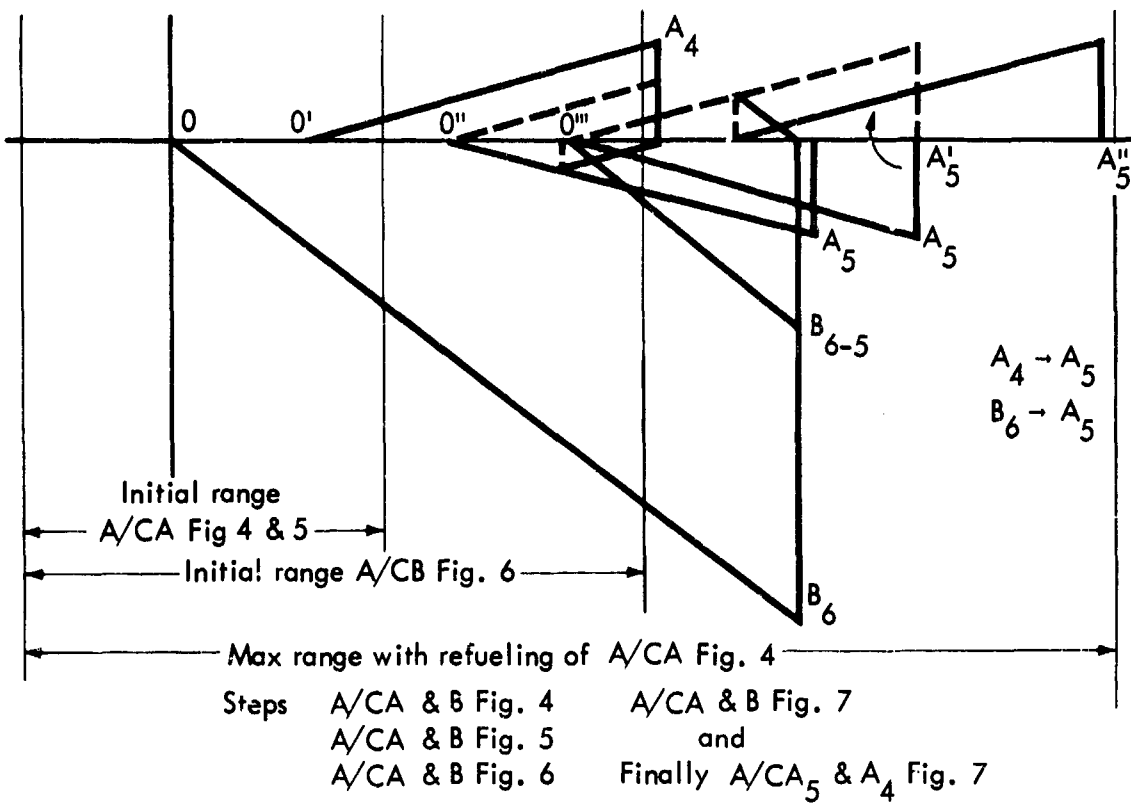


FIGURE 8.

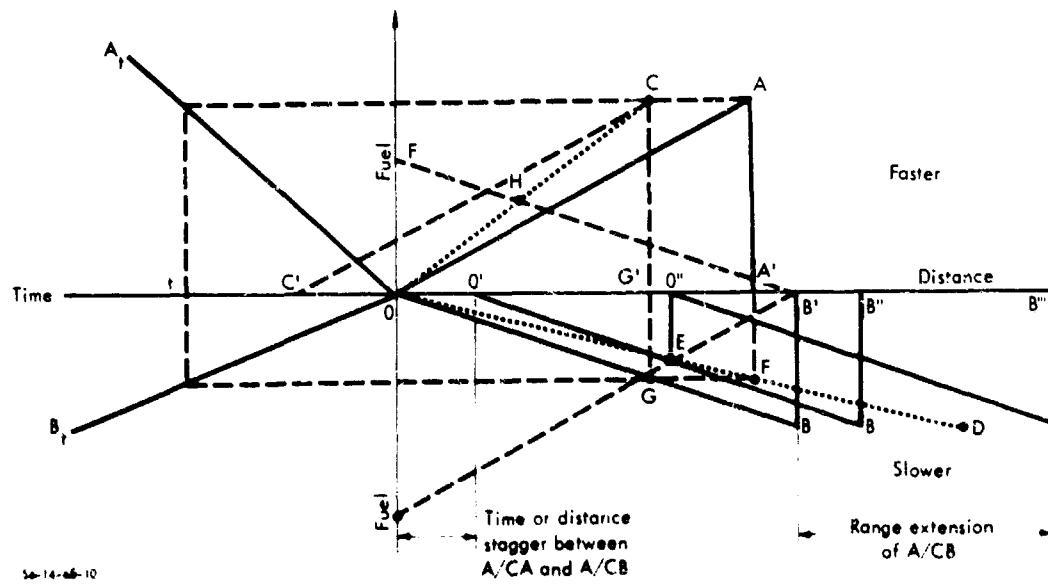


FIGURE 9.

B. CASE OF AIRCRAFT OF DIFFERENT SPEEDS AND EFFICIENCIES

This case is shown in Fig. 9. In addition to the abscissae of distance we show to the left of the origin an abscissa of time. Thus, lines OA_t and OB_t give the time-fuel relationship for aircraft A and B, respectively. Selecting time interval t from start--assuming in this case that both aircraft depart simultaneously--we find that aircraft A would have outdistanced aircraft B by $G'A'$. For aircraft A to arrive at G' , it would have been necessary to delay its departure by a segment AC , using the scale of time, or to move its departure point back a distance AC , using the scale of distances. On the other hand, if we wanted to have the two aircraft meet at a point A' , it would have been necessary for aircraft B to be stationed distance $G'A'$ ahead of aircraft A or to have delayed the departure of aircraft A by a time interval represented by a segment $G'A'$, using the scale of times.

Because of linear relationship of the variables involved it can be seen that lines OC and OD represent the locus of points through which pass lines OA and OB appropriate to selected distances of rendezvous of the two aircraft. Thus, line CC' would describe a condition in which aircraft A would arrive at point G' when aircraft B has consumed $G'G$ amount of fuel. This suggests that if we drew lines $B'F$ parallel to line OB, and $B'I$ parallel to line OA, we would establish points H and E, giving the earliest time for complete refueling of aircraft A by aircraft B, and aircraft B by aircraft A, respectively. By inspection it is evident that the latter choice results in better range. The new range is at point B'' .

It is believed that this method can be readily extended to the case of several aircraft. Although it requires a trial-and-error solution because it is not evident in what combinations refueling should proceed, the simplicity of the solution results in relatively small labor.

VI. GRAPHICAL SOLUTION TO EXAMPLE NO. 3 (A BEAM UNDER COMBINED COMPRESSION AND TRANSVERSE LOAD)

A. PRECISE BENDING MOMENT

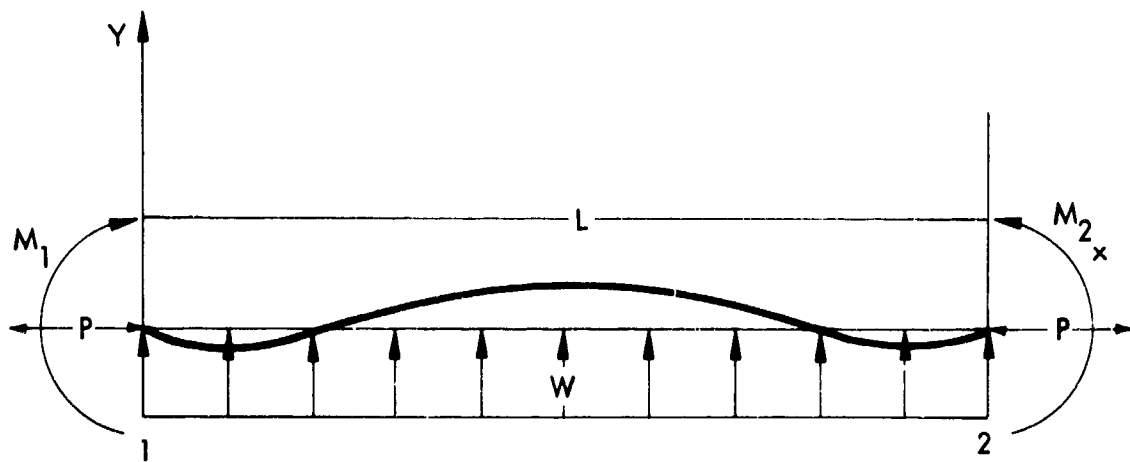
The general expression of the bending moment can be written as

$$M = C_1 \sin(x/j) + C_2 \cos(x/j) + wj^2 \quad (1)$$

where x is the distance from the left support and w is the uniformly distributed transverse load. In the expression of $j = \sqrt{\frac{EI}{P}}$, E is the modulus of elasticity, I the effective moment of inertia and P the axial compression. C_1 and C_2 are the constants of integration which can be determined from the conditions at the two supports; $C_1 = [D_2 - D_1 \cos(L/j)]/\sin(L/j)$; $C_2 = D_1$; D_1 and D_2 are introduced for brevity and designate as follows: $D_1 = M_1 - wj^2$; $D_2 = M_2 - wj^2$, L is the length of the bay, M_1 the bending moment at the left support, M_2 is the moment at the right support. See Fig. 1.

Attention is invited to the mathematical significance of the trigonometric functions appearing in the solution of differential equations involved in the problem of combined compression and bending.

These trigonometric functions must be thought of actually as representing the infinite series whose limiting magnitude can be considered as the sides of a right triangle usually employed to define the Sine x and Cosine x , when one angle of a right triangle is x radians in magnitude. This property makes possible the graphical construction described in this article, but the reader should not lose sight of the true significance of the functions.



56-14-68-11

FIGURE 1.

While the present solution can be extended to include the case of transverse loading other than uniform the present article deals with a uniformly distributed transverse loading only. Examining equation 1, we observe that by drawing two circles with radii equal respectively to C_1 and C_2 and distant wj^2 and by considering the signs of the products $C_1 \sin(x/j)$ and $C_2 \cos(x/j)$, it is possible easily to obtain their magnitude for any value of x from zero to L . It will be found in most practical cases that C_1 and C_2 will have a sign opposite to that of wj^2 and we will assume that they are negative. The construction, however, is simple and once it is understood it can be easily changed to take care of the actual signs of C_1 and C_2 . Noticing that $\sin(x/j)$ changes from zero to $\sin(L/j)$ while $\cos(x/j)$ from 1 to $\cos(L/j)$ it is obvious that the angle $57.3 \text{ deg } (L/j)$ must be drawn in such a way (if we want to measure the bending moment, along y axis) that for the value of $x = 0$ the products $C_1 \sin(x/j)$ and $C_2 \cos(x/j)$ become zero and C_2 , respectively. This can be obtained by measuring the angle $57.3 \text{ deg } (L/j)$ on the circle C_1 from the horizontal, while on the circle C_2 it must be measured from a vertical diameter.

Draw the beam 1-2 and on the continuation of the line choose a center from which the circle C_1 must be described. Measure downward along the continuation of the vertical diameter the distance wj^2 and from that point as a center describe the circle C_2 . Lay out the angle equal to 57.3 deg (L/j) from a horizontal diameter and construct this angle also on the circle C_2 , in which case it must be started from the vertical diameter. (The construction is illustrated in Fig. 2 and made clockwise.) Dividing the length of the bay and the arcs 1-2 of the circles C_1 and C_2 into any number of equal parts, we construct the bending moment diagram by simply projecting the points horizontally from the circles on the vertical lines passing through the corresponding points on the beam. In Fig. 2 the construction is illustrated for the point b . It can be easily proved that the ordinates enclosed by the lines $1b$, 2_1 and $1_2 b_2 2$ represent the bending moments at the corresponding points of the beam in the scale in which were drawn the circles C_1 and C_2 . In fact $b_1 b_2 = Ob_1 + Ob_2 = C_1 \sin(x/j) - wj^2 + C_2 \cos(x/j)$.

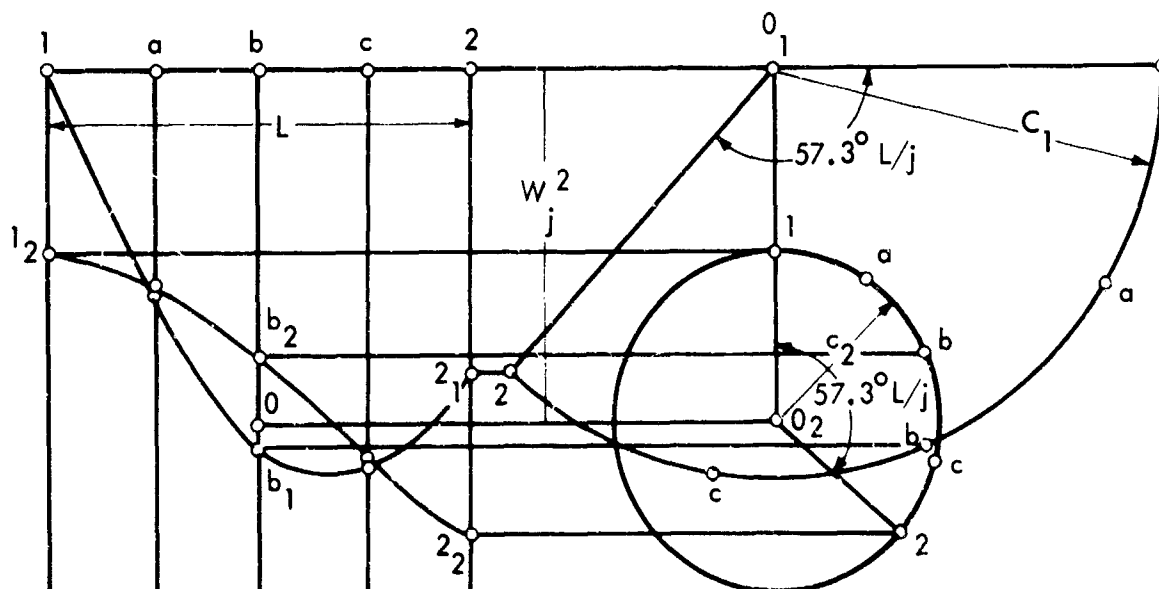


FIGURE 2. Construction of Precise Bending Moment Diagram

In order to obtain the circles C_1 and C_2 it is, however, not necessary to calculate the magnitude of C_1 and C_2 , since we can make the following observations: From Fig. 3, we see that since the distance $O_1 O_2$ is equal to wj^2 , if we lay out downward from O_1 the segment $O_1 2_2$ such that it is equal to M_1 we obtain immediately C_2 .
 $C_2 = D_1 = M_1 - wj^2 = - (wj^2 - M_1)$.

To obtain the $D_2 = M_2 - wj^2$ lay out upward $O_2 O_1^1$ equal to M_2 , obtaining $O_1 O_1^1$ which is equal to $-D_2$. To obtain C_1 , after having constructed the angles 57.3 deg (L/j) we observe from Fig. 3 that taking $O_2 2_V$ and adding it downward to D_2 along vertical diameter we obtain point 2_V^1 such that the intersection of a horizontal through that point with radius $O_1 2_1$ gives us C_1 .

$$O_2 2_V = D_1 \cos (L/j)$$

$$O_1 2_V^1 = D_2 + D_1 \cos (L/j)$$

$$O_1 2_1 = O_1 2_V^1 / \sin(L/j) = - [D_2 - D_1 \cos(L/j)] / \sin(L/j).$$

The attention is invited to the fact that angle 57.3 deg (L/j) must be drawn accurately since otherwise it may result in a large error in C_1 . As a check, the distance $2_V^1 2_V$, equal to M_2 , may be used before proceeding with further construction.

B. PRECISE SHEAR

By differentiating the expression of the bending moments (equation 1) we obtain the expression for shear as follows:

$$\frac{dM}{dx} = S = \frac{1}{j} (C_1 \cos \frac{x}{j} - C_2 \sin \frac{x}{j})$$

It can be seen that if we draw the beam, divided into the same number of parts as before, along the continuation of the vertical diameter and project from the circles C_1 and C_2 the points 1 b 2 on the horizontal lines drawn through the corresponding points on the beam,

the horizontal distances between the two curves thus obtained will give us the magnitude of shear in the scale of M/j where M is the scale of moments (Fig. 4).

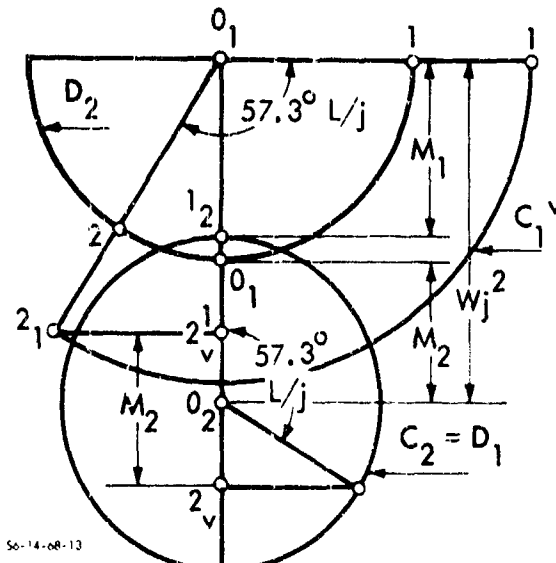


FIGURE 3. Circles C_1 and C_2

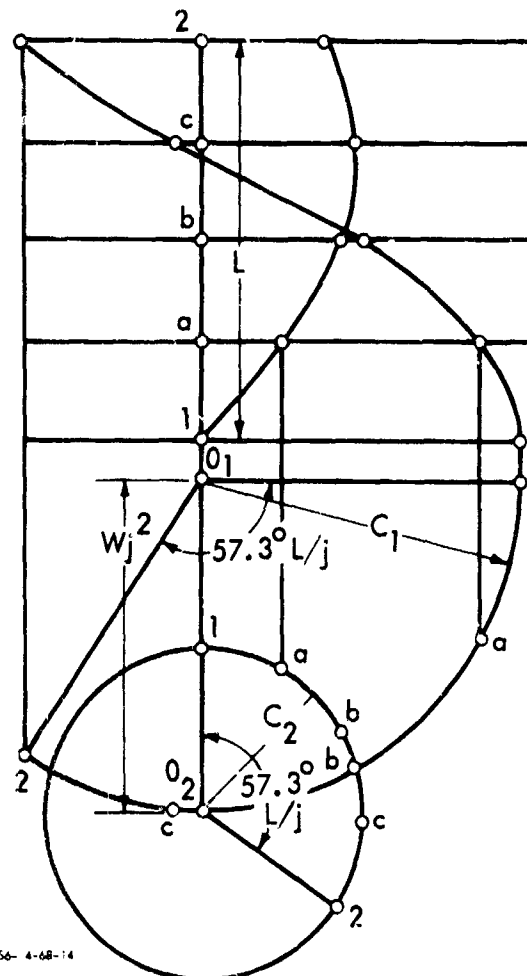


FIGURE 4. Construction of Precise Shear Diagram

C. MAXIMUM BENDING MOMENT

The location of the maximum bending moment is determined from the shear diagram at the point of zero shear.

D. DEFLECTIONS

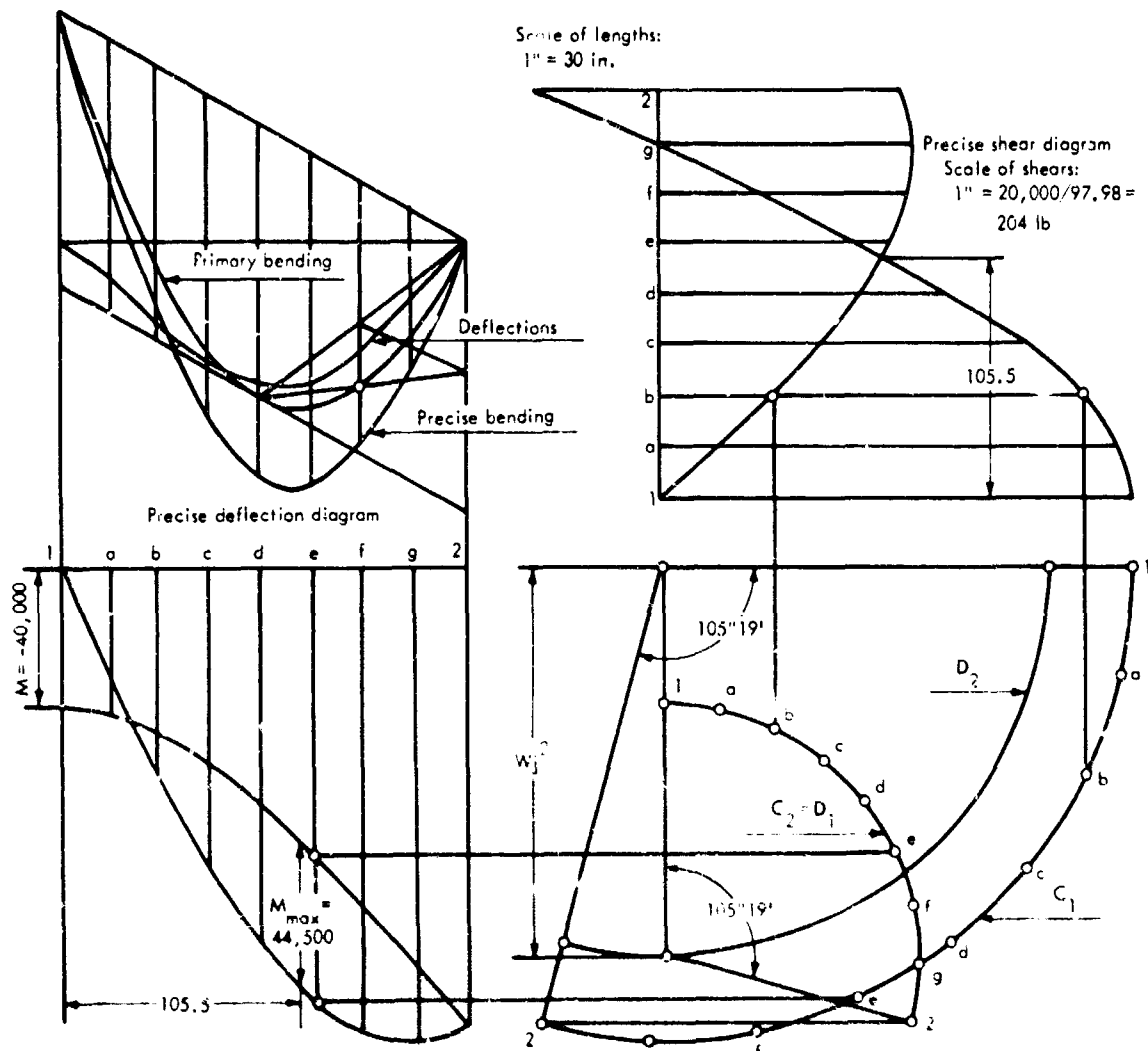
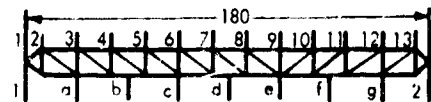
To obtain the deflection, we observe the fact that the expression for precise bending moment can be written

$$M = M_O - Py \quad (2)$$

Where M_O is the primary bending moment due to the transverse load alone.

Relationship of construction points to structure of the beam

Scale of moments: $1'' = 12,000$ in. lb
 Scale of deflections: $1'' = P/M$
 $-6000/12,000 = 1/2''$



Precise bending moment diagram: $1'' = 20,000$ in. lb

FIGURE 5. Graphical Solution of the Beam Analyzed in NACA Technical Note 383

From equation 2 we can express $y = (M_0 - M)/P$.

It is evident, therefore, that in order to obtain the deflection, we can simply superimpose the diagram of precise and primary moments and by dividing the difference between the two moments by axial load P , to determine the magnitude of the deflection at any point. If, however, we should replot the precise bending moment diagram on a horizontal base by using a new scale of moments $M = P$ (where M is the new scale of moments and P is the compression load) and construct the primary moment to the same scale, we will obtain directly the deflections to their actual magnitude. The replotting of the precise bending moment can be easily accomplished by using a proportional divider or by a method of similar triangles. The primary bending moment for a uniformly distributed load is simply constructed as a parabola and the example (Fig. 5) gives the constructional line involved.

E. EXAMPLE SHOWING APPLICATION OF THE METHOD

To illustrate the practical application of the method described in this article, a complete determination of precise bending moment, shear and deflection diagrams is given here for the metal truss beam whose properties and effective moment of inertia were determined by Mr. Andrew E. Swichard in NACA T.N. 393 (pages 24 to 31 inclusive).

Data:

$L = 180$ inches; $P = - 6000$ pounds; $I_{eff} = 5.76$ inches 4 ; $E = 10,000,000$ pounds/square inch; $M = - 40,000$ inch pounds; $M_0 = 0$; $w = - 12$ pounds/inches; $j = 97.98$; $j^2 = 9600$; $wj^2 = - 115,200$; $L/j = 1.838 = 105$ deg 19 1 ; $wL^2/8 = 48,600$ inch pounds.

VII. GRAPHICAL SOLUTION TO EXAMPLE NO. 4 (THE PROBLEM OF CAR REPLACEMENTS)

A given railroad owns N number of cars, purchased over a period of T years. It is assumed that the ages of the cars can be expressed as a linear function of time, thus giving $\frac{T}{2}$ as the average age of the cars. It is proposed to reduce the average age to a stipulated figure by purchasing new cars during the next ΔT period. Assuming that the replacements are being accomplished by yearly purchases and that car ages can be considered a linear function of time, determine the number of cars to be purchased and replaced in order to maintain the original number of cars but lower the average age of all the cars at the end of ΔT period to the desired figure.

In Fig. 1, at start, CD is the average age of the N cars. The average age is reduced to EF after the required number of cars was retired and replaced with new cars during the interval of time $\Delta T = \overline{AB} = 00_p$.

Assume - Linear variation of cars' ages.
Time and cars' ages are given by abscissa
while number of cars by the ordinate

CD is the average age of old cars

EF < CD average age of cars after
replacement of oldest cars with new
cars purchased during time period ΔT

EF is stipulated initially

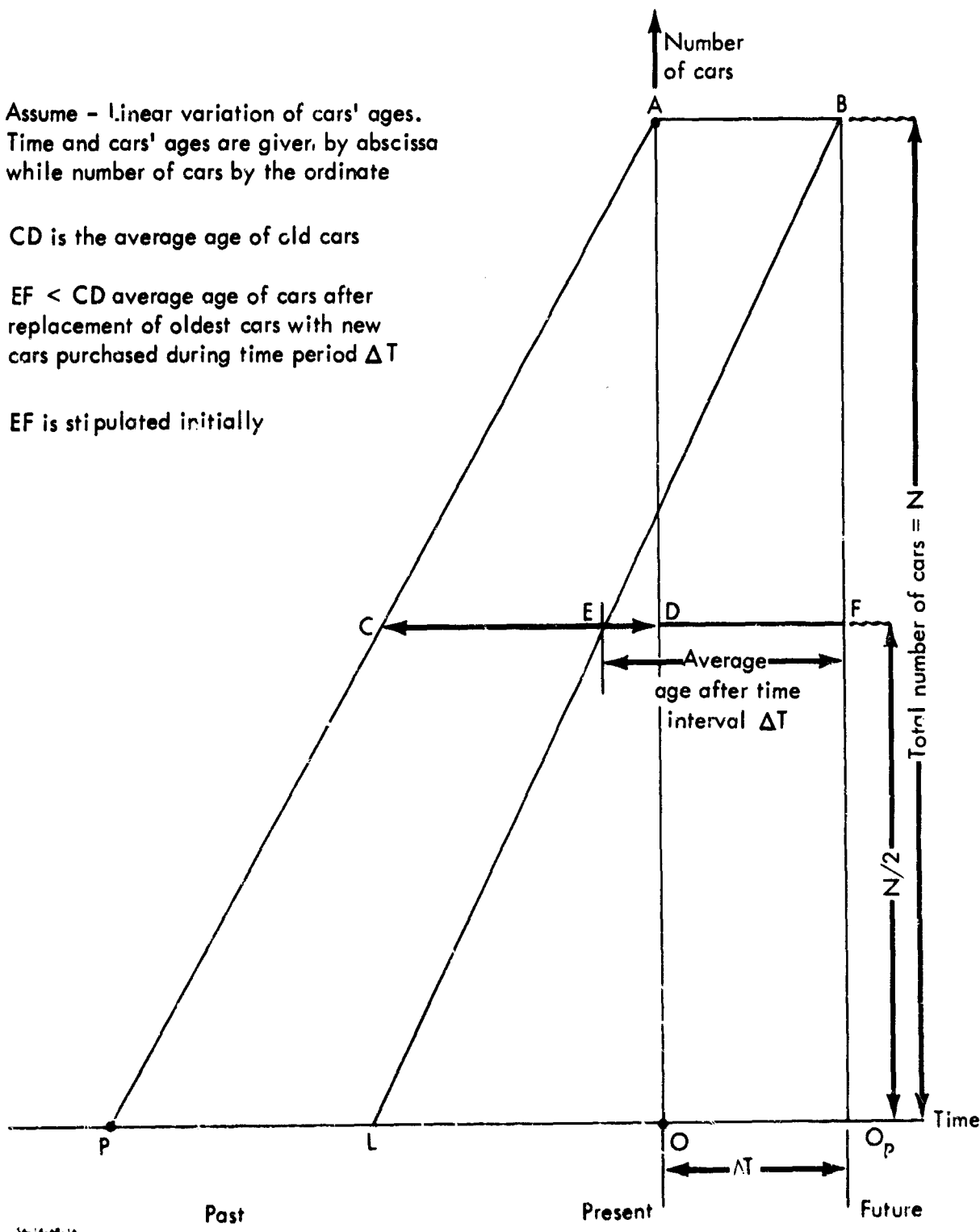


FIGURE 1.

Figure 2 shows the old and the new cars at the end of the ΔT replacement period.

Line OI gives the ages of M new cars purchased during the period of $\Delta T = \frac{O}{p}$ years (an equal number of old cars was retired); at the end of the $\frac{O}{p}$ period the ages of the remaining old cars are given by line AC. By averaging the ages of all cars at the end of the $\frac{O}{p}$ period, and drawing a straight line BEL passing through point E, such that EF is the specified new mean age of all the cars, we define an area LBO giving the total age of new and remaining old cars.

This implies by inspection that area AGHB must be equal to area LHIO or, which is the same, that area APLB is equal to GPOI.

Retire all cars between the ages OP and GI , i.e., O_p cars and replace them with new cars purchased during the same time period. To have reduced the average age from CD to EF means that at time O_p the area of triangle $BL O_p$ would represent the total age of all the cars. For that to be the case area $GABH$ must be equal to the area $LHIO$.

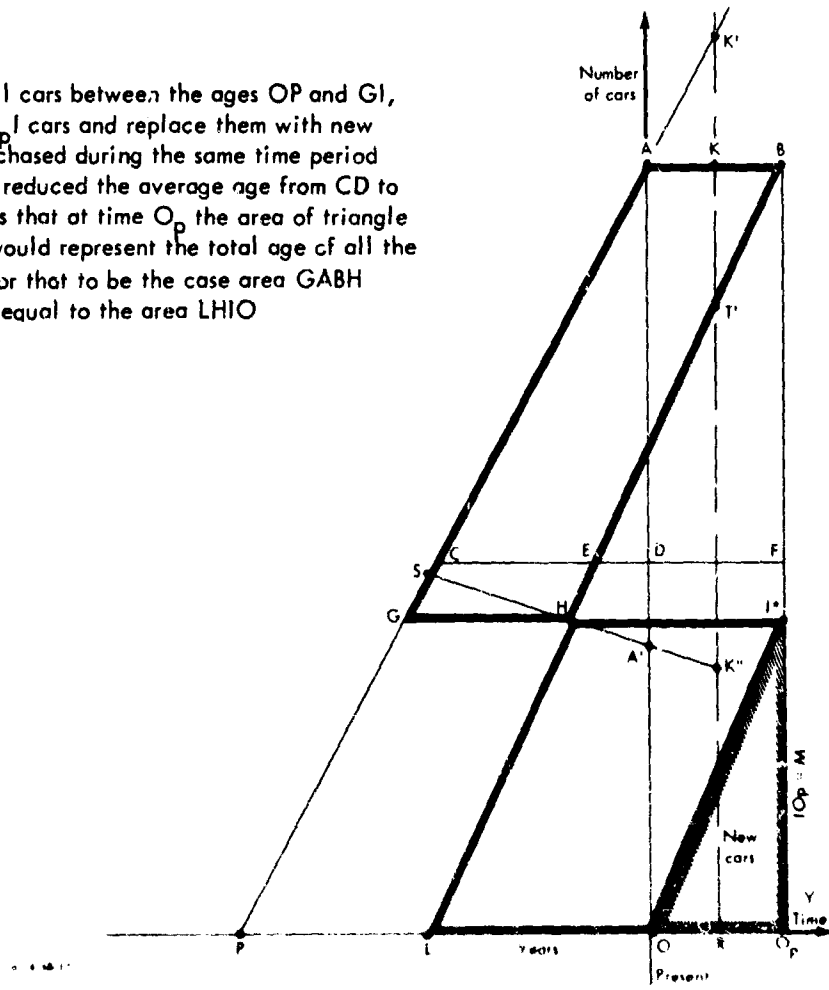


FIGURE 2.

One can resort to a graphical determination of M (Fig. 3) by proceeding as follows:

Draw line RK equidistant from lines AO and NO_p . Erect an ordinate at L intersecting lines PA at S . Continue PA until it intersects KR at K' . Mark off an ordinate K''_R equal to the segment $K'T'$ on the line KR . By inspection we state that with sufficient accuracy, area

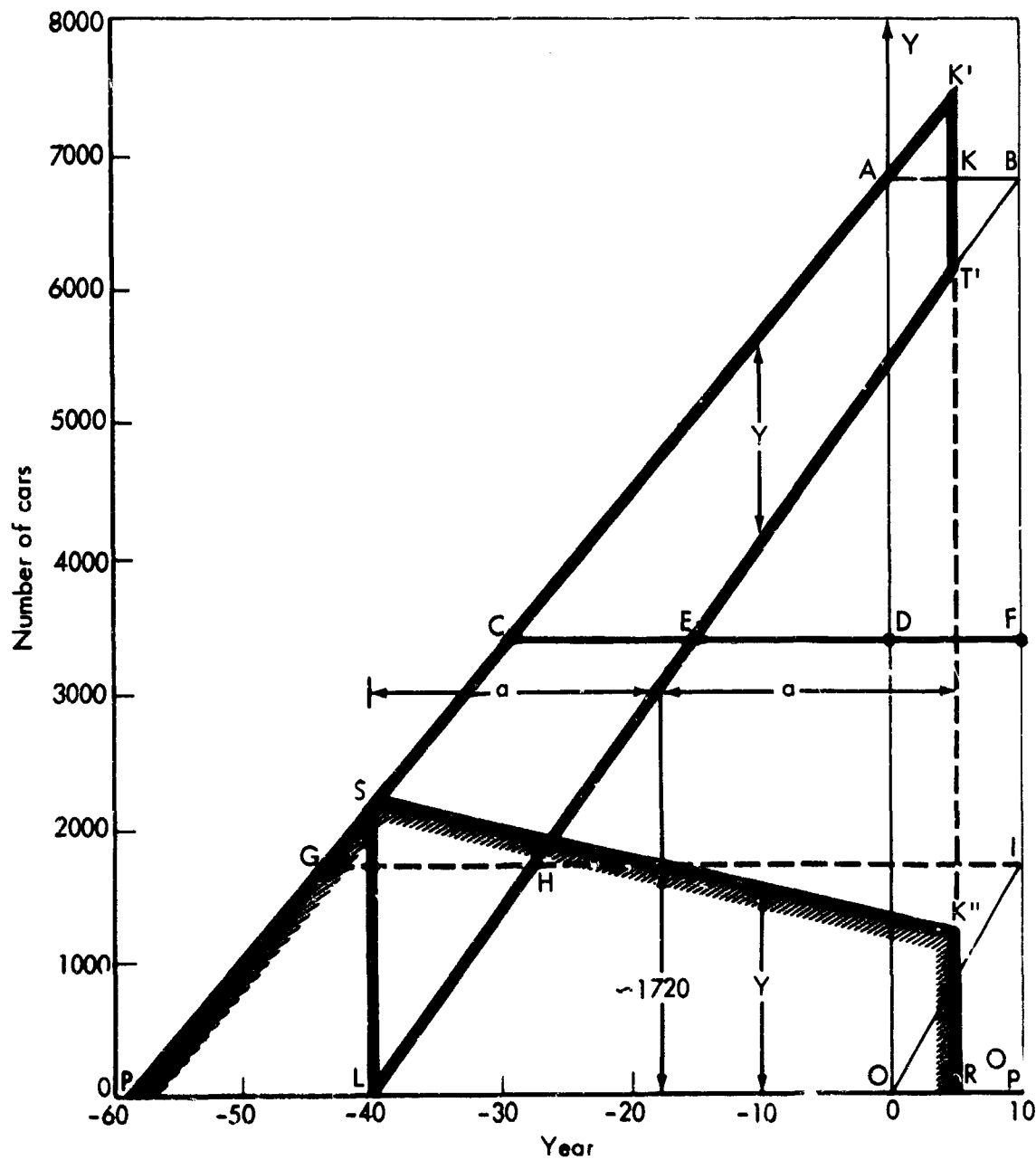


FIGURE 3.

LSK'T' is equal to the area LSK"R. If at midpoint of line SK" we draw line GI parallel to the abscissa axis, and a line joining I with O, the figure PGIO gives the required area, while its ordinate IO_p defines the number of cars, answering the problem.

Figure 4 gives an example of the application of the application of this method.

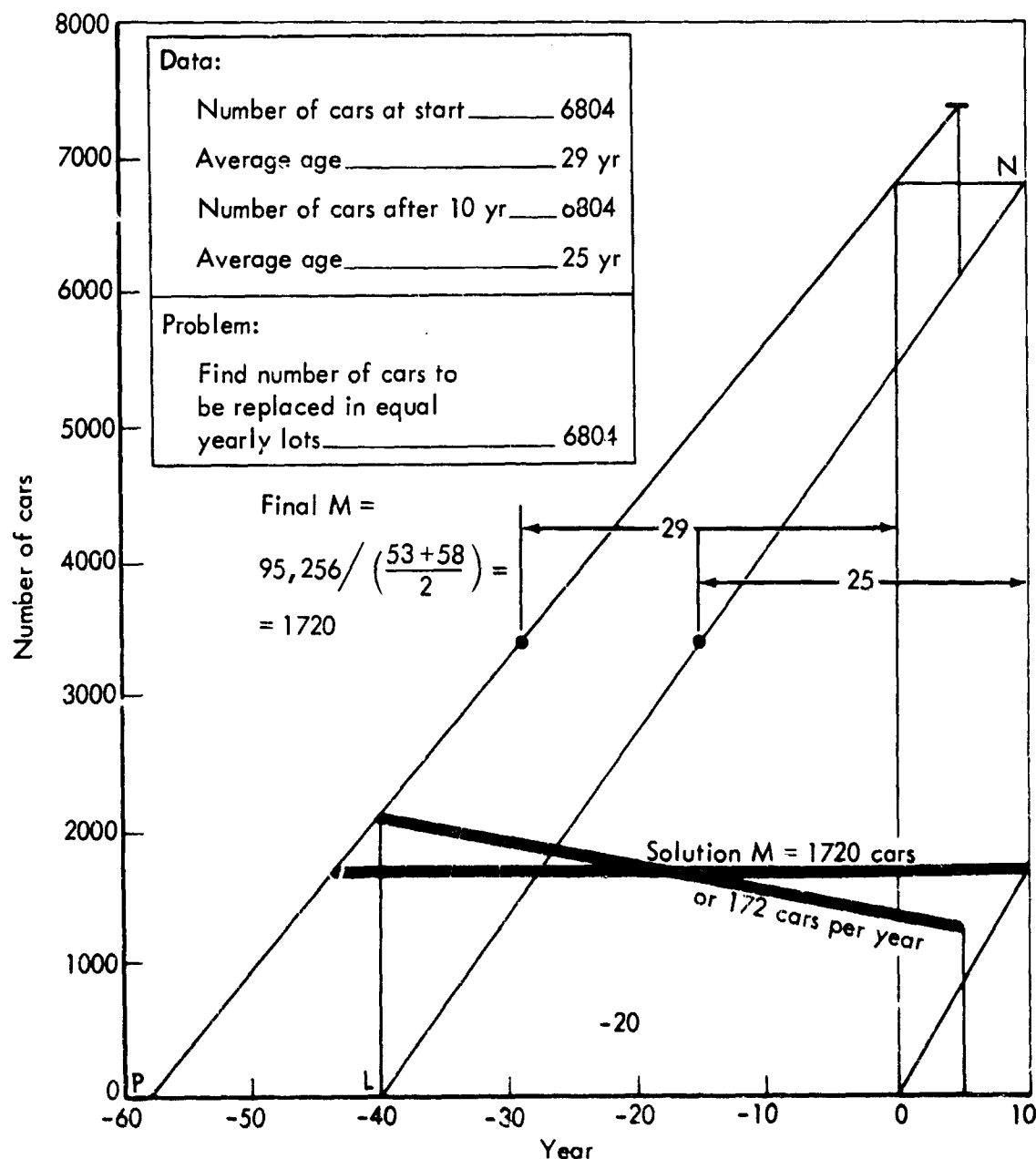


FIGURE 4.

VIII. GRAPHICAL SOLUTION TO EXAMPLE NO. 5 (DETERMINATION OF BALLISTIC TRAJECTORY PARAMETERS)

For much of the conceptual and analytical work dealing with ballistic missiles, computer precision is not required.

Given two of the three basic parameters (burnout angle, burnout speed, and range or range angle), the method described in this paper can be used to determine vacuum trajectory, velocity at any point, and time of flight, using only a slide rule, compass, and ruler. Figure 1, taken from "Free Flight of a Ballistic Missile," by Albert D. Whelan (American Rocket Society Journal, December 1959), gives the relationship of burnout speed, burnout angle (from vertical), and range angle. The method assumes a nonrotating earth and applies to the portion of the unpowered trajectory outside the atmosphere. For many problems the data are adequate for a complete trajectory from ground launch to reentry.

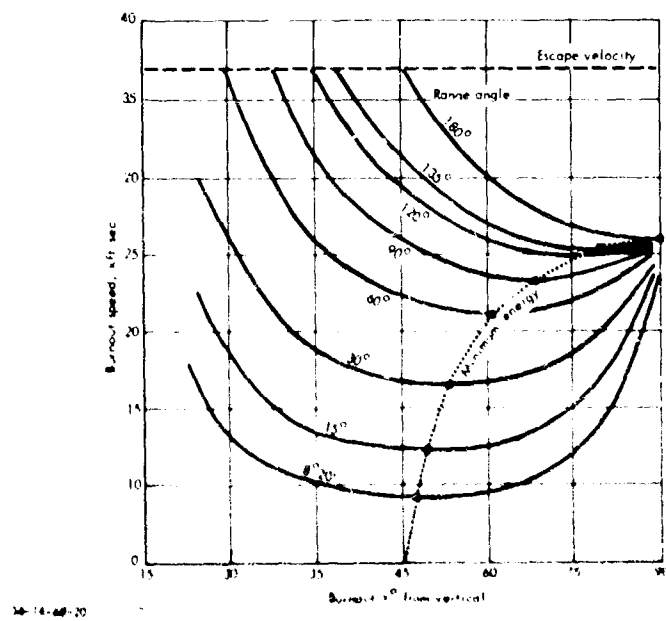


FIGURE 1. Relationship of Burnout Speed, Burnout Angle, and the Range Angle

A. BALLISTIC TRAJECTORY CONSTRUCTION

Graphical construction of the ballistic trajectory is made on the basis of the following laws of mechanics and properties of conics:

1. Ballistic trajectory is an ellipse whose one locus is the center of the earth.
2. Included angles between a tangent to the ellipse and lines joining the point of tangency with each focus are equal.
3. Sum of the length of the two lines joining any point on the ellipse and its two foci is constant.
4. Given its major and minor axis, an ellipse can be constructed by the use of the auxiliary circle.

Figure 2 shows the construction of ballistic trajectory ellipse.

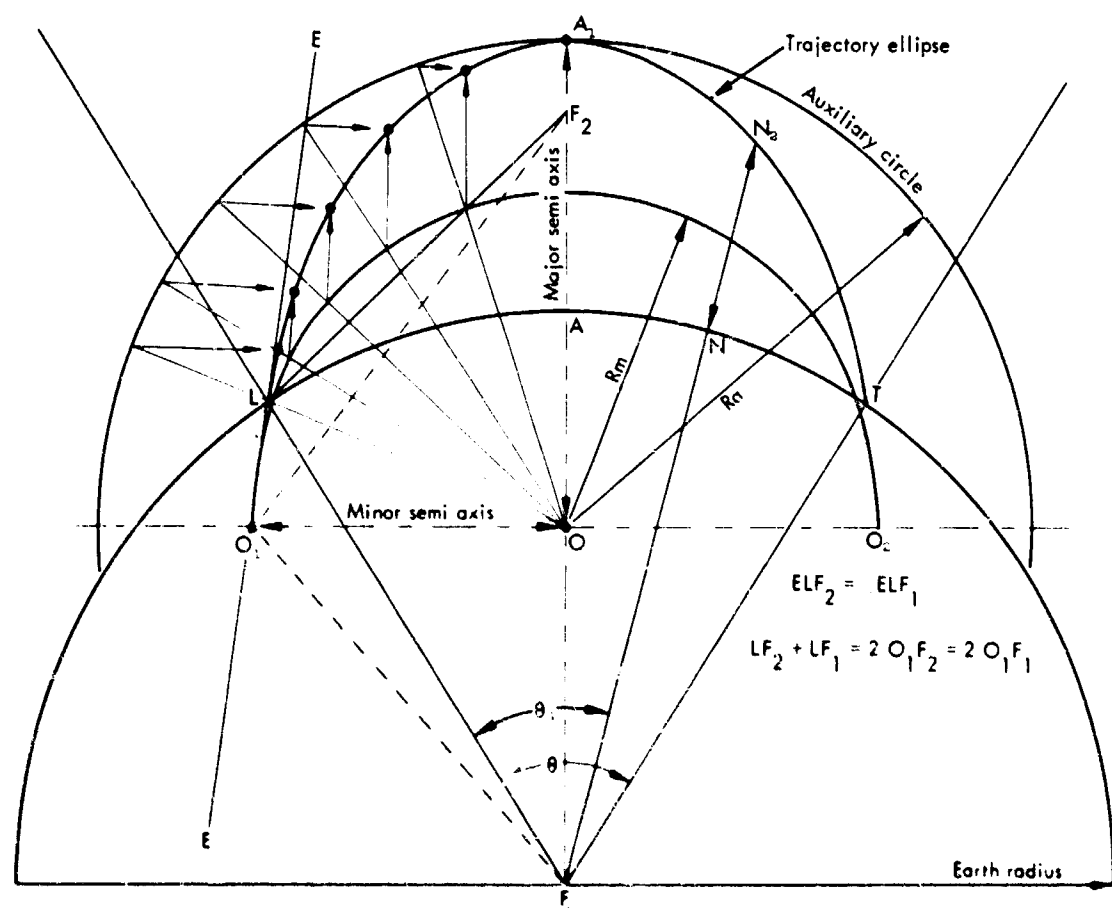


FIGURE 2. Construction of Ballistic Trajectory Ellipse

B. DETERMINATION OF SPEEDS AND TIMES ALONG THE TRAJECTORY

To determine missile speeds and times along the trajectory we make use of the energy relationship which gives the interplay between kinetic and potential energies:

$$\frac{1}{2}MV_0^2 = \frac{1}{2}MV^2 + \int_{R_0}^{H_N} \frac{Mg_0 R_0^2}{H_N^2} dH \dots \dots \dots \quad (1)$$

where V_0 is the burnout speed; V is missile speed at some point N ; g_0 is gravitational constant at sea level; H_N is a segment giving the height of the missile from the center of the earth.

After integration we obtain

$$V_0^2 = V^2 + 2g_0 R_0^2 \left(\frac{1}{H_N} - \frac{1}{R_0} \right) \text{ or} \\ \frac{V^2}{2g_0} = \frac{V_0^2}{2g_0} - \frac{R_0}{H_N} \quad . \quad (2)$$

Here H is the altitude of the missile, $H_N = R_0 + h$, and V is the speed at that point.

From Equation 2 it can be seen that previously obtained trajectory can be transformed into the curve of potential energy by correcting each altitude by a factor of $\frac{R_0}{H_N}$, as shown in Fig. 3.

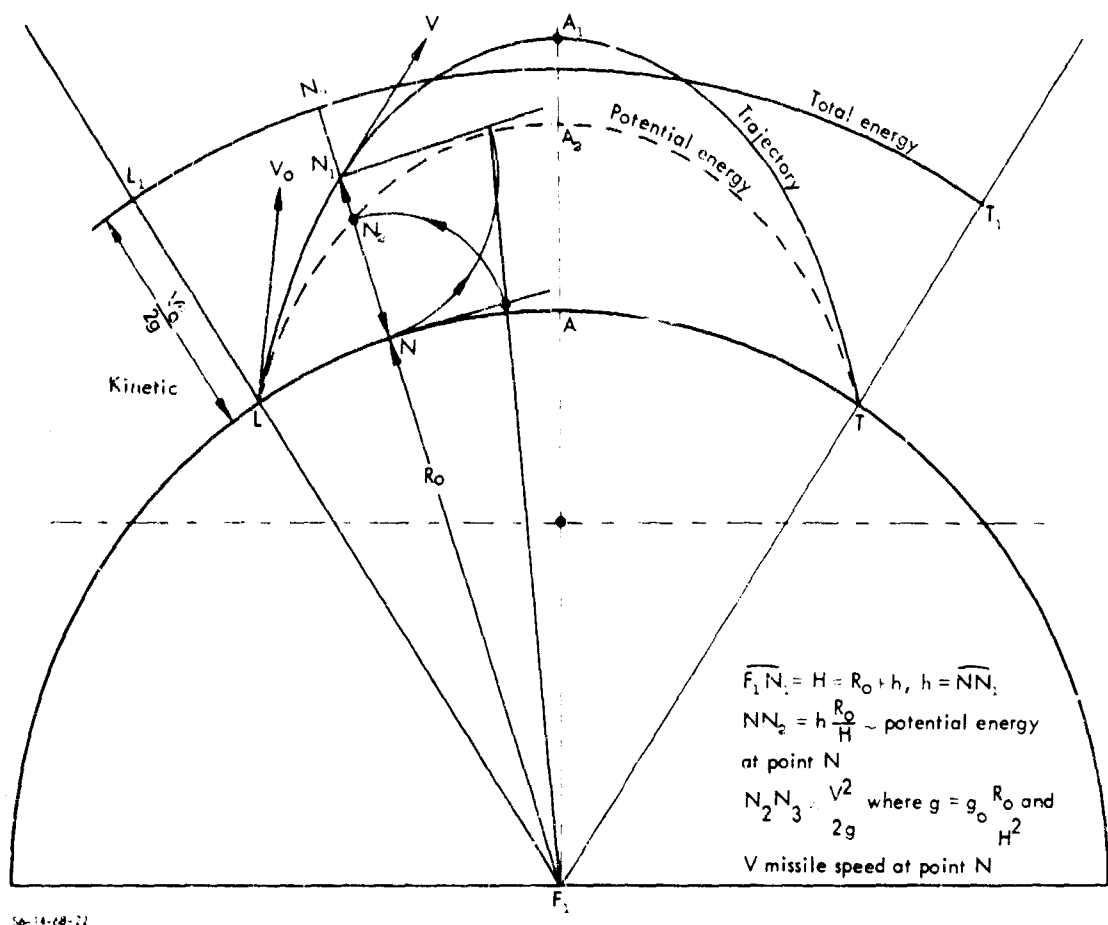


FIGURE 3. Determination of Kinetic and Potential Energy

It then becomes apparent that if $\overline{N N_1}$, the segment representing potential energy, is subtracted from the segment representing the initial kinetic energy, $\overline{L L_1} = \overline{N N_3}$, the difference thus obtained, $\overline{N_2 N_3}$ represents, to a proper scale, the velocity of the missile at that point on the trajectory. Assuming that we have obtained such a segment, then if speeds are taken in feet per second, accelerations in feet per second squared, and distances in nautical miles, the speeds would be obtained by measuring the length of the segment using the scale of distances and then taking a square root of the product:

(Segment length) $\times 2 g_0 \times 6080$, so that missile velocity at any point is

$$V = 625 \sqrt{\text{Segment length}} = 625 \sqrt{N_2 N_3}$$

If, now, we were to divide the trajectory into a number of equal segments and determine at midpoint of each such segment the average velocity V , then the ratio of the segment length divided by the average velocity would give us the time of flight along that segment of trajectory.

C. USE OF LOGARITHMIC SCALES FOR DETERMINATION OF SPEEDS AND TIMES

The graphical construction and calculation of speeds and times can be more conveniently accomplished by the use of logarithmic scales.

In Fig. 4, if we make $\lg V_0 = 0L$, we will have a convenient logarithmic scale ② of velocities and Δt .

Having previously divided the trajectory into a number of equal length segments $L-1$, $1-2$, $2-3$, etc., one measures lengths $\overline{N_2 N_3}$ with the linear scale of lengths l which in Fig. 4 we plotted to the left of 0. Next, using a logarithmic scale, these magnitudes of these lengths are plotted on corresponding rays as an extension of $\lg 625$ which was marked as an arc of a circle with 0 as its center. Because the magnitude required is $\frac{1}{2} \lg \overline{N_2 N_3}$, the logarithmic scale ③ of half the magnitude of that used for $\lg 625$ must be employed. A smooth curve LL_A plotted through these points gives at any point on the trajectory the speed at that point.

D. TIMES

Using logarithmic scale ②, we draw an arc of a circle with center at F_1 and radius equal to $\lg (400 \times 6080)$ because the length of the equal segments into which we divided the trajectory is 400 nmi. Thus,

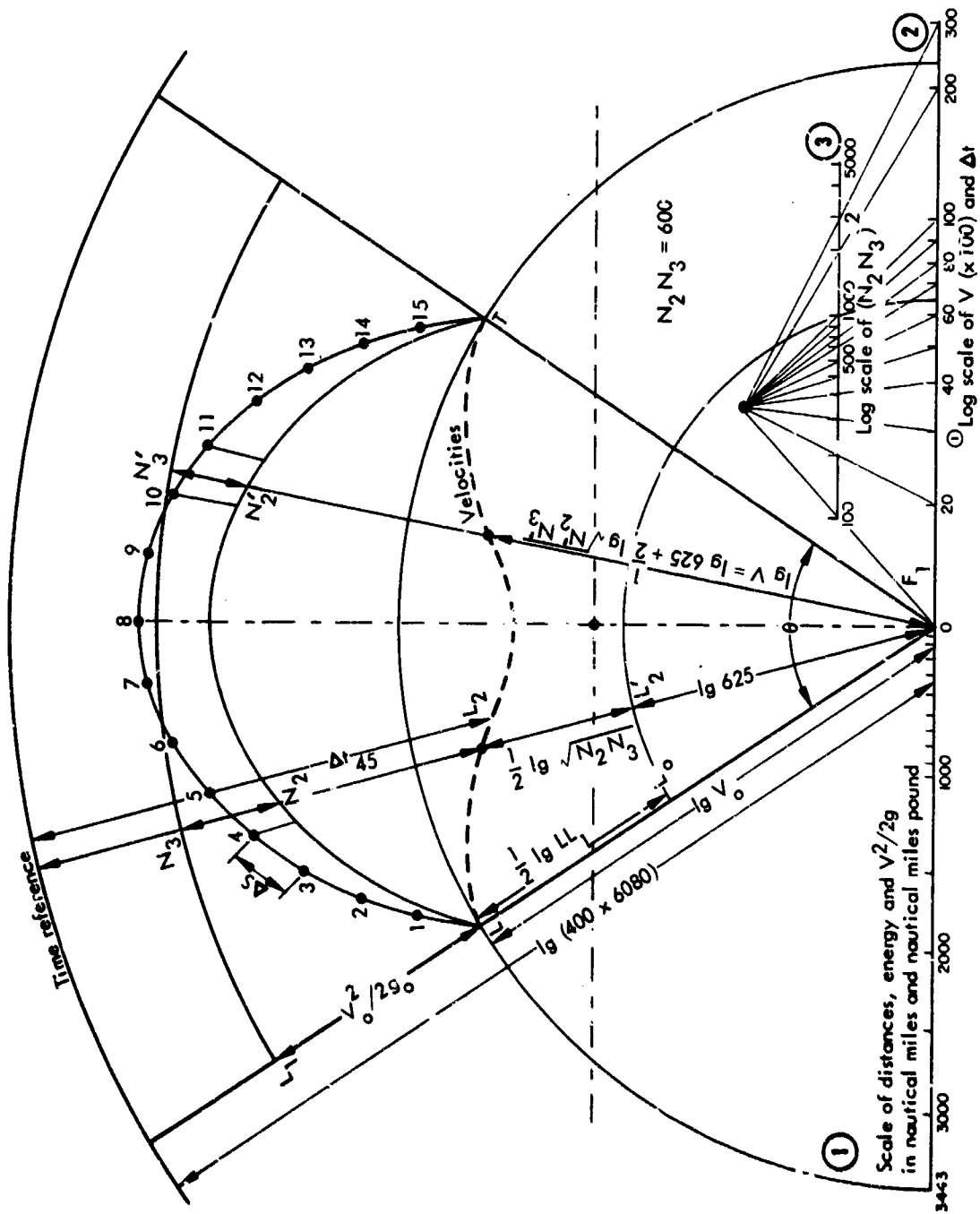


FIGURE 4. Determination of Speeds, Times and Plot of Complete Trajectory Data

$$\lg \Delta t = \lg \frac{\Delta S}{V} = \lg \frac{\Delta S}{625 \sqrt{\frac{N_2 N_3}{N_1}}} = L_{\text{time}} F_1 - (\lg 625 + \frac{1}{2} \lg \frac{N_2 N_3}{N_1}),$$

expressed in terms of logarithmic scale ②, gives logarithm of Δt at the appropriate points 1, 2, 3, etc. These lengths terminate on the arc L_{time} and the speed curve LL_A as shown in Fig. 4. By summation of the Δt 's, one obtains the elapsed times from launch to any point on the trajectory.

E. EXAMPLE

Figure 4 was drawn for a case in which the given initial conditions are

$$V_0 = 24,000 \text{ ft/sec}$$

$$\gamma_0 = 41 \text{ deg (from vertical)} .$$

From Fig. 1, one finds the angle $\theta = 67.8$ deg, equivalent to a range of 4070 nmi. Figure 4 gives the appropriate scales necessary to construct and to determine missile altitude, velocity, and time of flight at any point on the trajectory and summarizes the data graphically. The apogee is found to be 1870 nmi, the apogee speed 10,160 ft/sec, and the total time of flight 46.9 min. The total time of flight was obtained as the sum of Δt 's for each segment as shown in the following tabulation.

No.	Segment	Seconds	
		Δt	$\Sigma \Delta t$
1	L-1	118	118
2	1-2	130	248
3	2-3	146	394
4	3-4	163	557
5	4-5	184	741
6	5-6	205	946
7	6-7	221	1167
8	7-8	244	1411
9	8-7	244	1655
10	7-6	221	1876
11	6-5	205	2081
12	5-4	184	2265
13	4-3	163	2428
14	3-2	146	2574
15	2-1	130	2704
16	1-L	118	2822

I am indebted to Dr. R. Finke, who calculated principal trajectory parameters, using both a desk calculator and slide rule as well as the computer.

The following tabulation gives the three sets of figures and, thus, a relative precision of the graphical and analytical methods:

	Graphical	Analytical	Computer
Range, deg	68	67.74	67.74
Range, nmi	4,070	4,071.7	4,072.66
Apogee altitude, nmi	1,870	1,858.1	1,857.38
Apogee velocity, ft/sec	10,160	10,225.3	10,228.81
Flight time, min	47	46.78	46.78

IX. GRAPHICAL SOLUTION TO EXAMPLE NO. 6 (THE TWO-MAGNETIC REACTOR PROBLEM)

Given: Two magnetic circuits which are so constructed that they share some volume in which their respective magnetic fields and induction (also flux) are at right angles (Fig. 1). Each core may be of any reasonable material.

Problem: For a given $.4\pi NI$ in the control magnetic circuit, what is the flux through the power circuit for various $.4\pi NI$ of power.

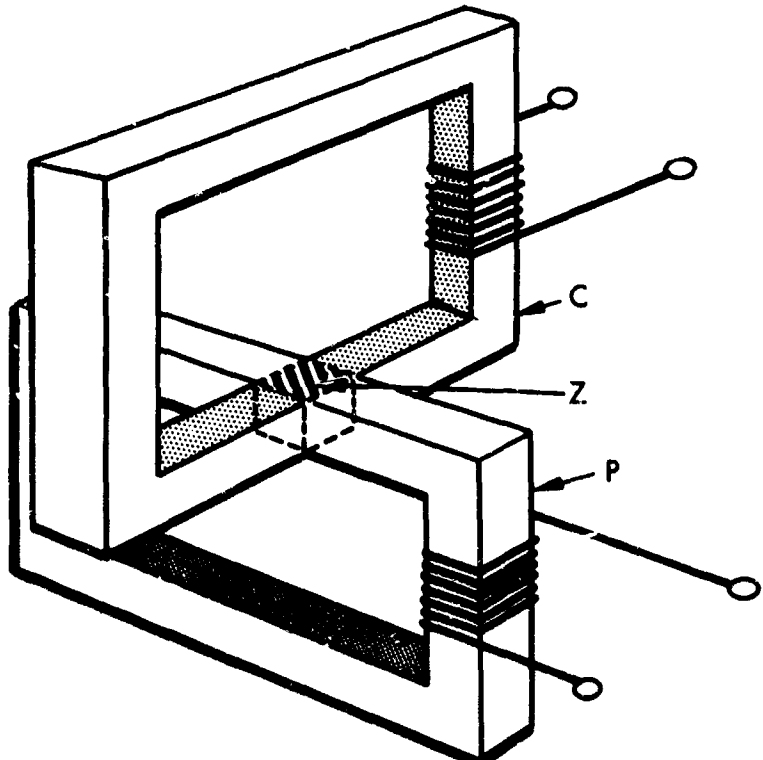


FIGURE 1.

A. METHOD A: GRAPHICAL SOLUTION

Legend

- I Current in amperes.
- N Number of turns.
- l Mean length of the magnetic path.
- B Flux density in gauss.
- H Magnetizing force in oersteds (gilberts/cm)
- F Magnetomotive force in gilberts.
- C,c Properties and characteristics of the control reactor circuit.
- P,p Properties and characteristics of the power reactor and circuits.
- Z,z Properties and characteristics of the common zone of C and P (Fig. 1).
- ZC&ZP Subscript denotes characteristics due to or induced by the the control and power reactor, respectively.

An examination of Fig. 1 suggests the following relationships:

$$B_{ZC} = B_C \quad (1)$$

$$B_{ZP} = B_P \quad (2)$$

$$H_{ZC}^2 + H_{ZP}^2 = H_Z^2 \quad (3)$$

$$B_{ZC}^2 + B_{ZP}^2 = B_Z^2 \quad (4)$$

In addition, since it is possible to orient the common zone material in such a way as to ensure identical magnetization properties at right angles along the direction of core C and core P, one can write

$$\frac{B_{ZC}}{H_{ZC}} = \frac{B_{ZP}}{H_{ZP}} \quad (5)$$

The magnetomotive forces in the control and the power circuit are:

$$F_C = \Phi H(l) dl = H_C l_C + H_Z C l_Z = 0.4\pi N_C I_C \dots \quad (6)$$

$$F_P = \Phi H(l) dl = H_P l_P + H_Z P l_Z = 0.4\pi N_P I_P \dots \quad (7)$$

The relationships B vs H are given in the form of usual magnetization curves, indicated schematically in Figs. 2, 3, and 4.

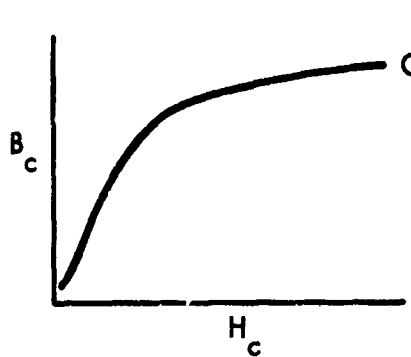


FIGURE 2.

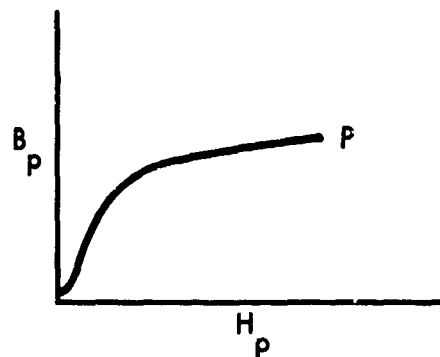


FIGURE 3.

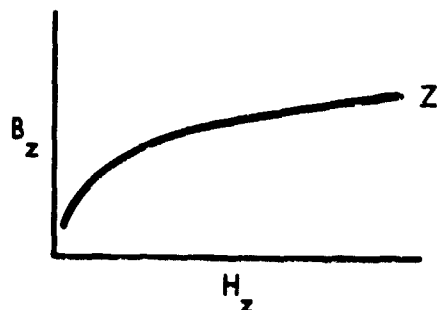


FIGURE 4.

Also known are the number of turns in the control and power reactor.

The solution of the problem requires the determination of the magnitudes of H_C , H_P , H_{ZC} , and H_{ZP} for any selected values of F_C and F_P .

We will proceed to develop a graphical solution based on the following observations:

Assume that for a specific value of F_C and a specific value of F_P we obtained the corresponding magnitudes of H_C , H_P , H_{ZC} , and H_{ZP} . Then, since $H_{ZC}^2 + H_{ZP}^2 = H_z^2$ we can spot the proper points on the three magnetization curves (as shown in Figs. 5, 6, and 7):

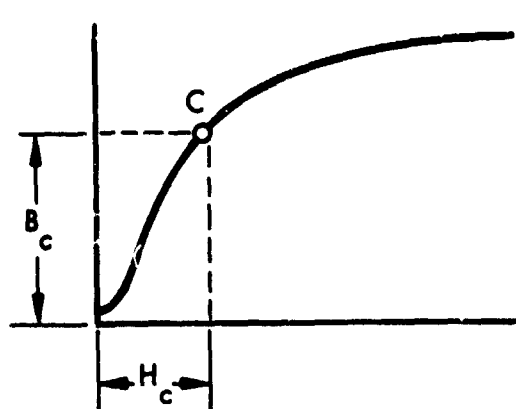


FIGURE 5.

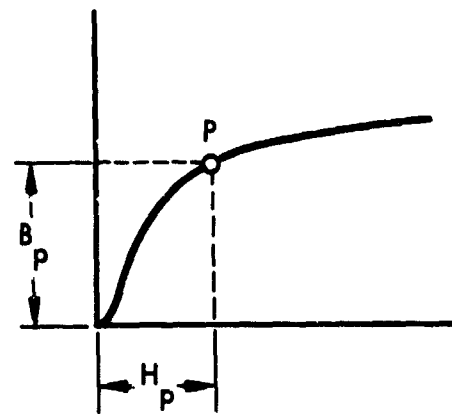


FIGURE 6.

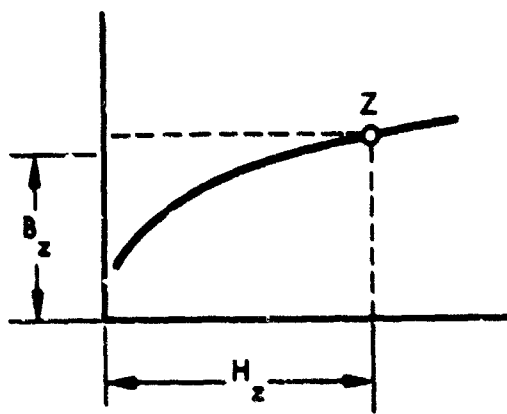


FIGURE 7.

We redraw curves of B_C vs H_C and B_P vs H_P by modifying their abscissae by a factor $\frac{l_C}{l_Z}$ and $\frac{l_P}{l_Z}$, respectively.

This is shown schematically in Figs. 8 and 9.

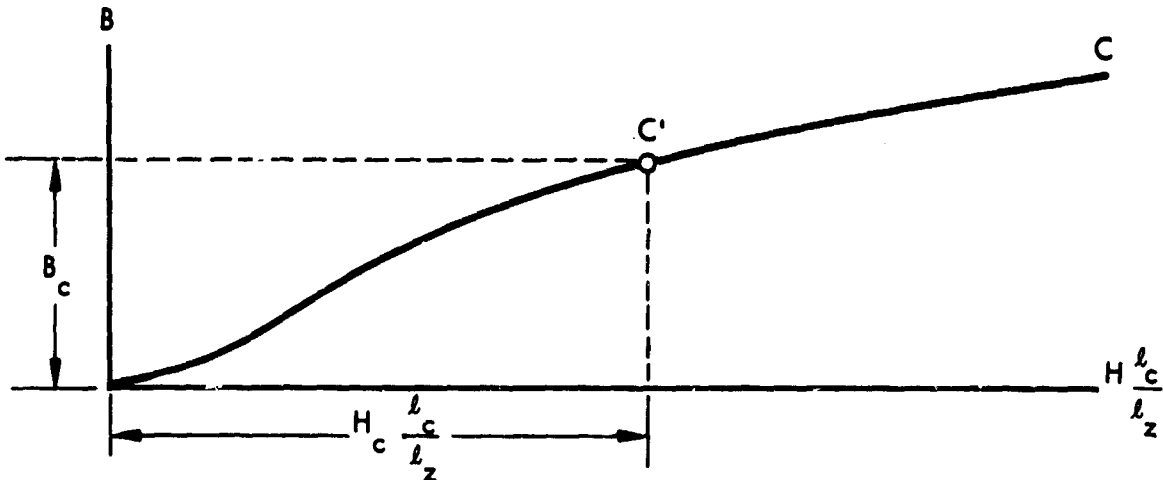


FIGURE 8.

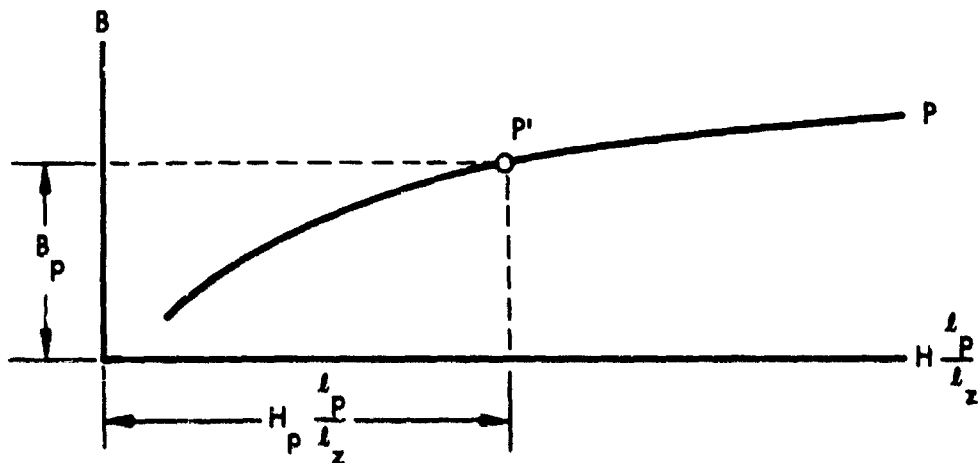


FIGURE 9.

Assuming that the scales selected remain the same, then B_C and B_p of Figs. 8 and 9 are equal, respectively, to B_C and B_p of Figs. 5 and 6.

We will now add to these curves a vertical line on each, such that its distance from the origin of coordinates is equal to $\frac{F_C}{l_Z}$ and $\frac{F_P}{l_Z}$ for control and power curve, respectively (Figs. 10 and 11).

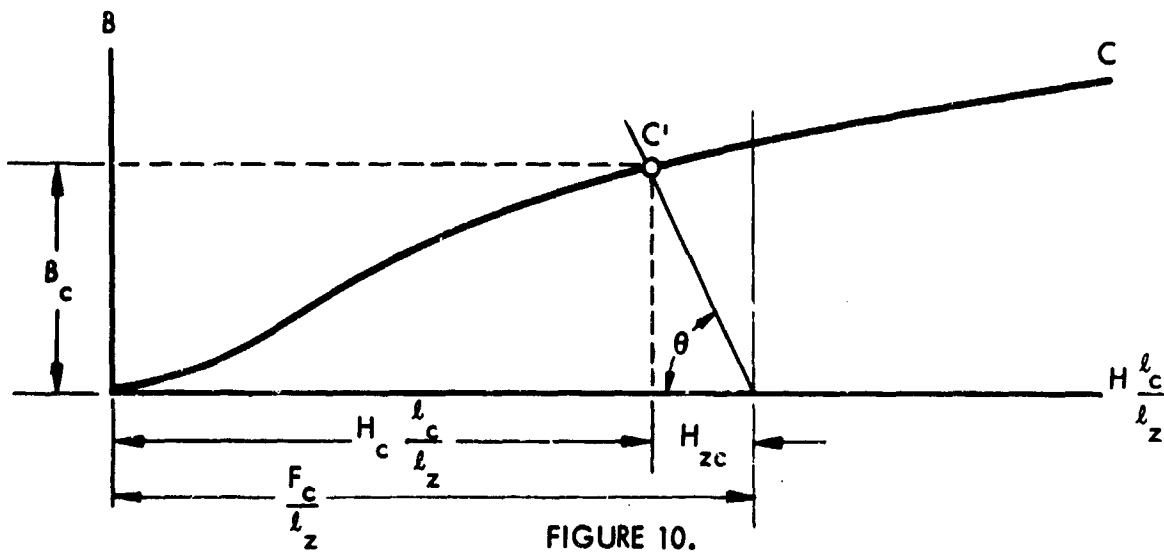


FIGURE 10.

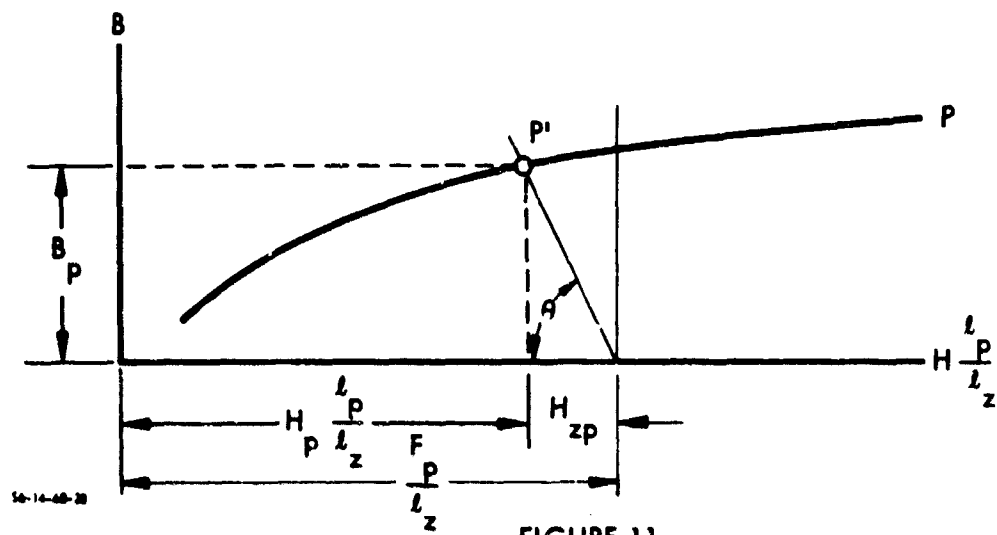


FIGURE 11.

Note that the difference of abscissae in these curves, namely $\frac{F_C}{l_z} - H_{CZ} \frac{l_c}{l_z}$ and $\frac{F_p}{l_z} - H_{ZP} \frac{l_p}{l_z}$ are equal to H_{ZC} and H_{ZP} , respectively.

Since we assumed that points C and P, and hence points C' and P' , represent the solution of our specific problem then angles θ in Figs. 10 and 11 are equal because, in that case,

$$\frac{B_C}{H_{ZC}} = \frac{B_p}{H_{ZP}} \quad \text{which fulfills the relationships (5) and (1) and (2).}$$

which fulfills the relationships (5) and (1) and (2).

A check of the correctness of our solution would be to construct right angle triangle shown in Fig. 12 below and compare the magnitude of H_z thus obtained with the H_z of Fig. 7.

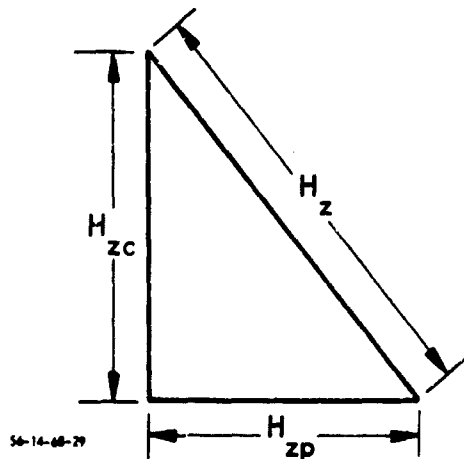


FIGURE 12.

The examination of Figs 10 and 11 suggests a graphical solution of the problem. We plot B_C vs $H_C \frac{\ell_C}{\ell_Z}$ and B_P vs $H_P \frac{\ell_P}{\ell_Z}$ having selected suitable scales for the coordinates.

On this diagram we draw vertical lines spaced $\frac{F_C}{\ell_Z}$ and $\frac{F_P}{\ell_Z}$ from the origin of coordinates as it was initially shown in Figs. 10 and 11. On curves C and P we mark several pairs of points corresponding to the number of equal θ^1 angles randomly picked by us. For each point we obtain a pair of magnitudes of B_C^1 and H_{ZC}^1 and a corresponding B_P^1 and H_{ZP}^1 among which accidentally there may be a point representing the solution of the problem.

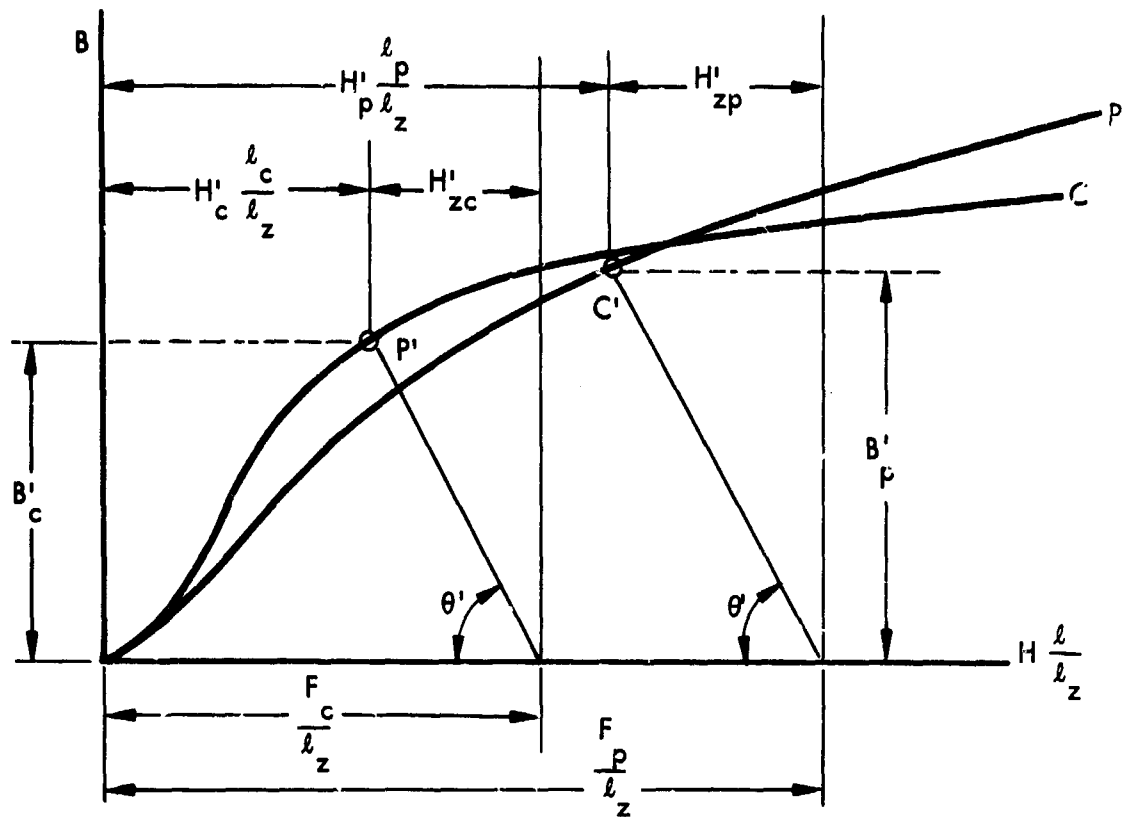


FIGURE 13

Since, however, this is improbable we must proceed differently.

Using values of B_C^1 and B_P^1 , and values of H_{ZC}^1 and H_{ZP}^1 from points corresponding to the same angles θ^1 we obtain graphically

$$B_Z^1 = \sqrt{(B_C^1)^2 + (B_P^1)^2}$$

because

$$B_{ZC} = B_C \quad \text{and} \quad B_{ZP} = B_P .$$

Similarly,

$$H_Z^1 = \sqrt{(H_{ZC}^1)^2 + (H_{ZP}^1)^2} .$$

The resulting curve contains one correct point, namely the point common with the magnetization curve B_Z vs H_Z (curve Z as shown in Fig. 14).

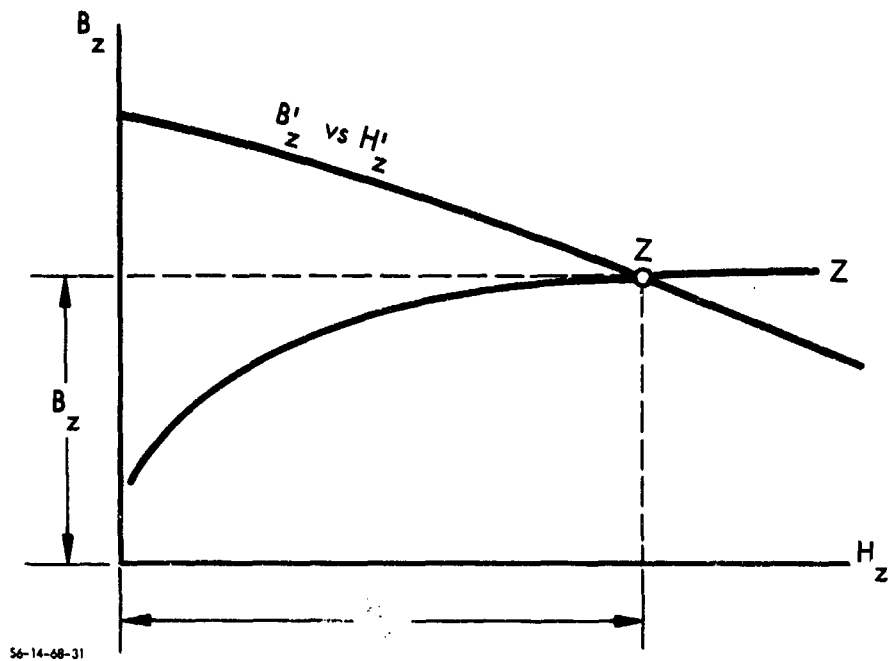


FIGURE 14.

Having determined H_z we obtain B_C and B_P as well as H_{ZC} and H_{ZP} , as it will be shown later.

The solution must be repeated for various values of F_C and F_P and cross-plotted to show the interdependence of the selected variables.

B. APPLICATION OF THE METHOD

Curves $B_C \frac{t_C}{t_Z}$ and $B_P \frac{t_P}{t_Z}$ are superimposed on the same graph using cross-section paper.

This graph is used as a template, the actual construction being performed for each pair of F_C and F_P on a separate piece of tracing paper which thus will contain all details of construction permitting an easy check of individual solutions.

For one group of solutions either F_C or F_P is kept constant. The curve corresponding to the variable factor is traced on the

individual vellum and placed so as to superimpose vertical lines $F \frac{\ell}{\ell_z}$ described on page 64. With this arrangement, a group of radial lines emanating from point O^1 provides a group of points 1_c and 1_p , 2_c and 2_p , 3_c and 3_p , etc. corresponding to points P^1 and C^1 of Fig. 13.

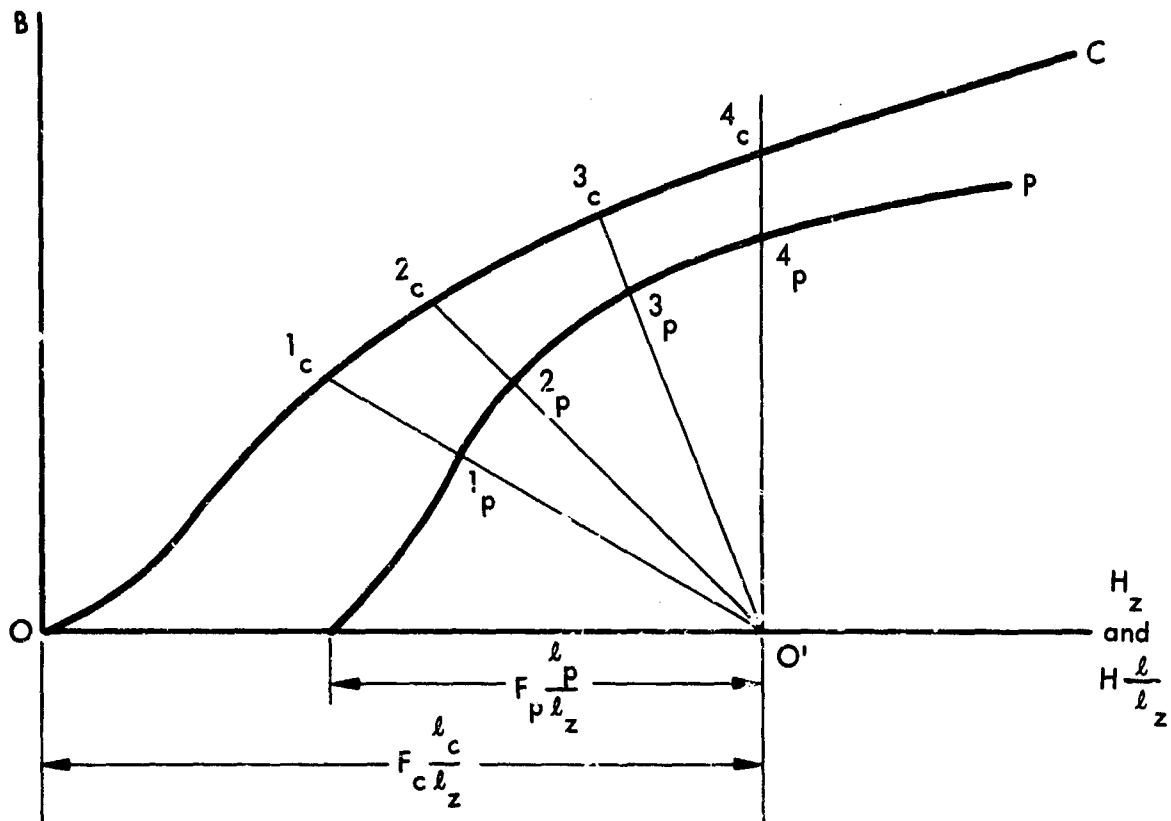


FIGURE 15.

To ensure uniformity of all solutions we will agree to retain the orientation of coordinates of curve C, for example, and rotate 90 deg the coordinates of curve P.

Having marked off a series of points 1, 2, 3, 4, etc., forming the same angle with the coordinate axes, we proceed to construct curve B_z^1 vs H_z^1 .

For clarity the construction is shown in Fig. 16 for point 2. Construction of B_z^1 vs H_z^1 curve illustrated for point 2. B_C^1 and H_{ZC}^1 ordinates remain oriented as drawn while B_p^1 and H_{ZP}^1 ordinate rotated 90 deg. Points "Z" define B_z^1 vs H_z^1 curve.

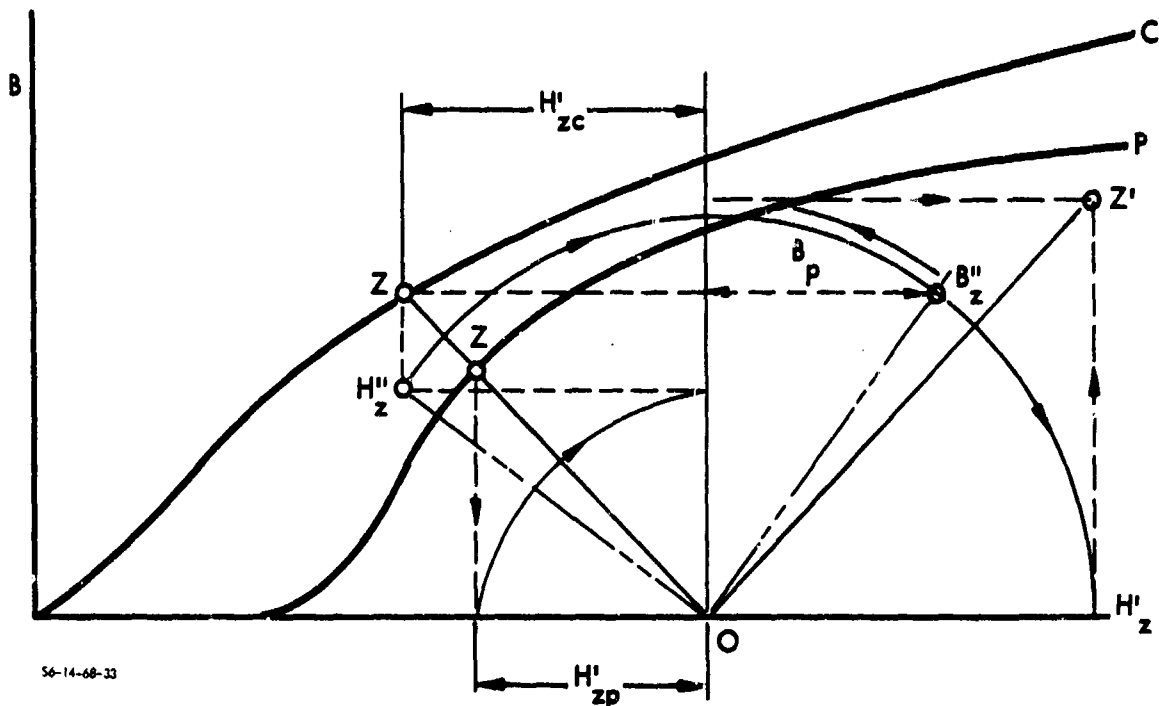


FIGURE 16.

After repeating this construction for all the points (normally 4 to 5 points suffice) curve B_Z^1 vs H_Z^1 is drawn (Fig. 17) and superimposed on the selected B_Z vs H_Z curve which thus determines point Z establishing the values of H_Z and B_Z forming the solution of the problem. The determination of point Z on B_Z vs H_Z magnetization curve is shown in Fig. 18.

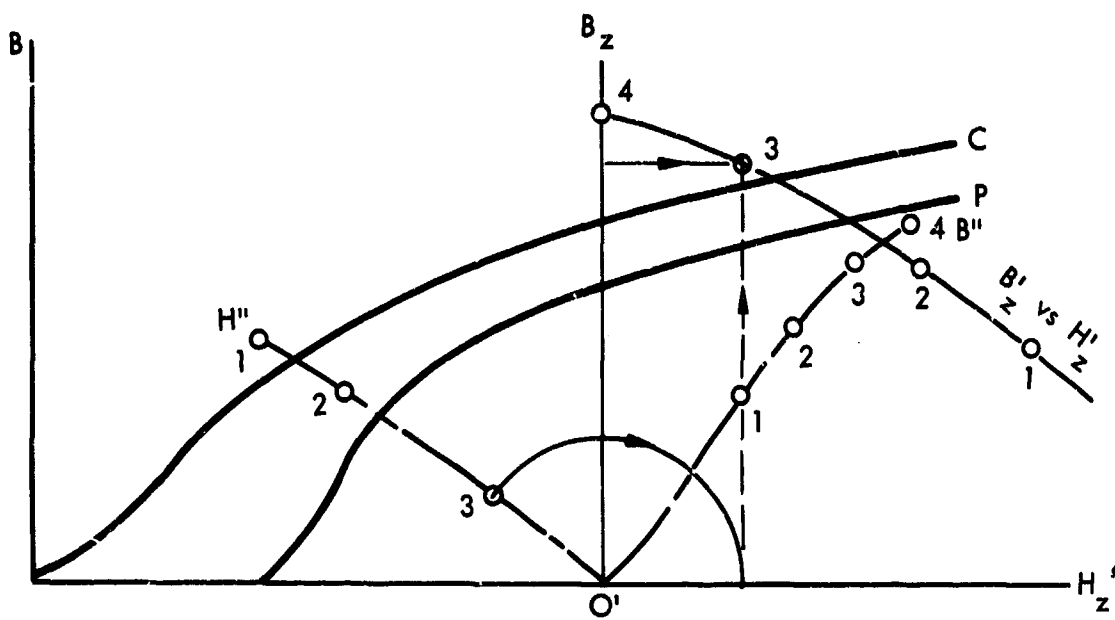


FIGURE 17. Construction of B'_z vs H'_z curve using curves $O'B''$ and $O'H''$

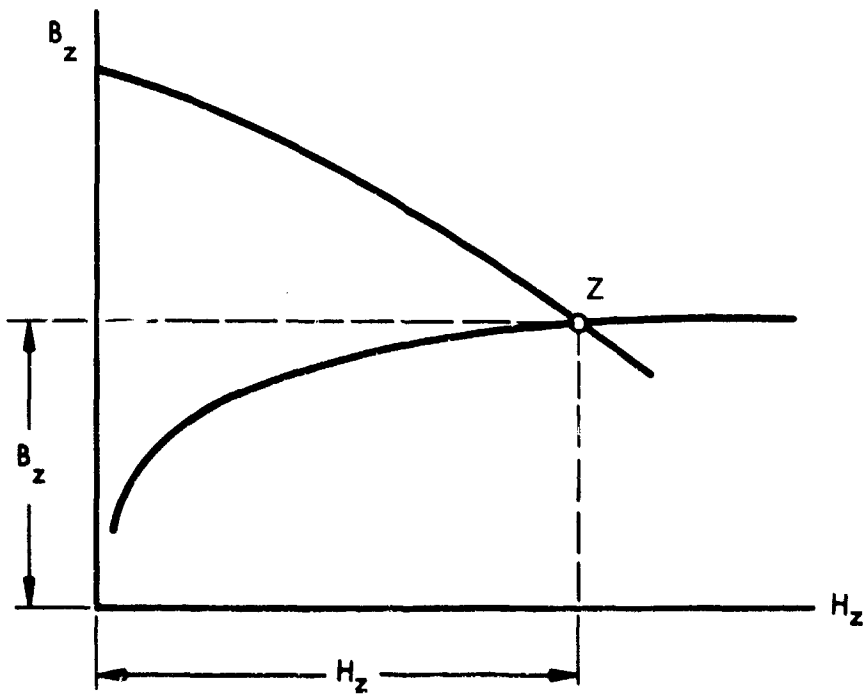


FIGURE 18. Determination of point Z on B_z vs H_z magnetization curve

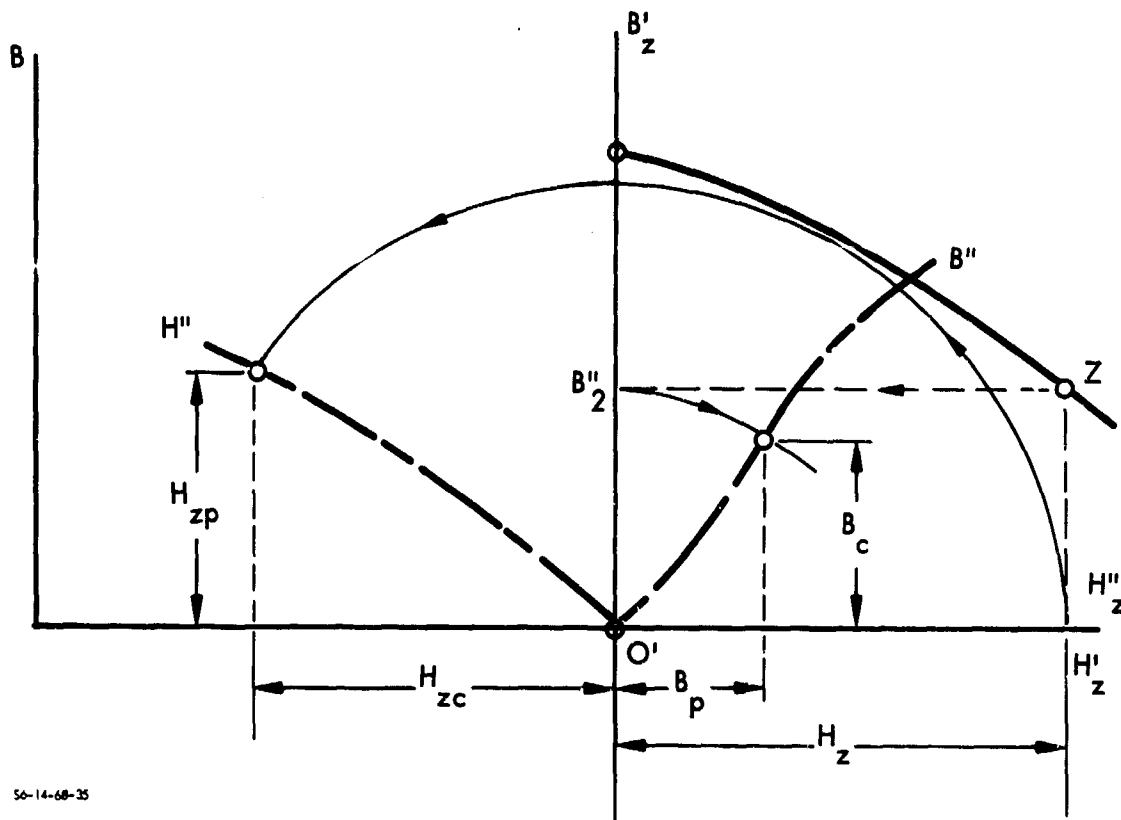


FIGURE 19.

Final determination of all the unknowns of the original problem is given in Fig. 19. Having obtained point Z we project it on $O'B'_Z$ and $O'H'_Z$ axes indicated here as points B''_Z and H''_Z . The magnitudes $O'B''_Z$ and $O'H''_Z$ are measured off on $O'B''$ and $O'H''$ curves and B_c , B_p , H_{zp} determined directly as shown.

The practical application of the method permits a number of shortcuts:

The curves need not be redrawn for separate constructions and many of the construction lines need not be drawn because of the reference offered by the graph paper on which are drawn the magnetization curves.

C. METHOD B: GRAPHO-ANALYTICAL SOLUTION

In describing the alternate method, reference will be made to the previous explanation of the graphical solution of the two-magnetic-reactor problem.

In this case the magnetization curves are drawn on log log paper having introduced on this paper two additional scales equal to one half of the original scales. The new scales thus permit direct reading of the magnitude of the square of any ordinate plotted using the original scale (Fig. 20).

Instead of obtaining graphically the curves of H_{ZC} vs B_C and H_{ZP} vs B_P as it was shown in Figs. 10 and 11, a table shown below is prepared.

TABLE 1

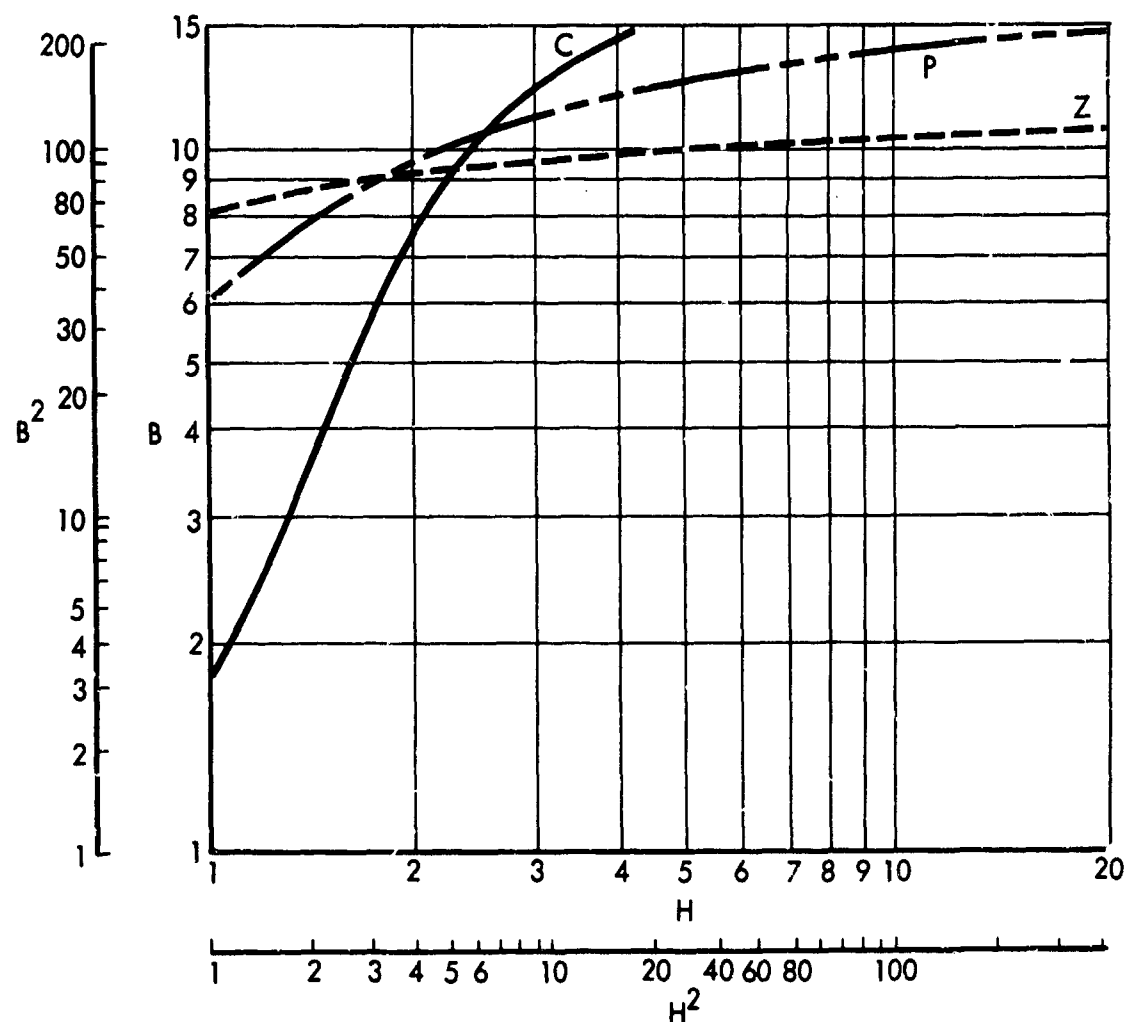
B_C	H_C	$H_C \frac{\ell_C}{\ell_Z}$	$H_{ZC} = \frac{F_C}{\ell_Z} - H_C \frac{\ell_C}{\ell_Z}$	B_P	H_P	$H_P \frac{\ell_P}{\ell_Z}$	$H_{ZP} = \frac{F_P}{\ell_Z} - H_P \frac{\ell_P}{\ell_Z}$
•	•	•	•	•	•	•	•
•	•	•	•	•	•	•	•

Curves of H_{ZC} vs B_C and H_{ZP} vs B_P are plotted on a sheet of vellum, using the previous log log plot as a template as shown in Fig. 21. Note now that randomly drawn set of 45 deg lines accomplishes the same purpose as the radial lines of Fig. 15. In fact, because the abscissae and ordinate scales are equal, we can write

$$\log B_C - \log B_P = \log H_{ZC} - \log H_{ZP} \quad \text{or}$$

$$\frac{B_C}{B_P} = \frac{H_{ZC}}{H_{ZP}} \dots$$

which fulfills condition (5).



54-14-68-36

FIGURE 20.

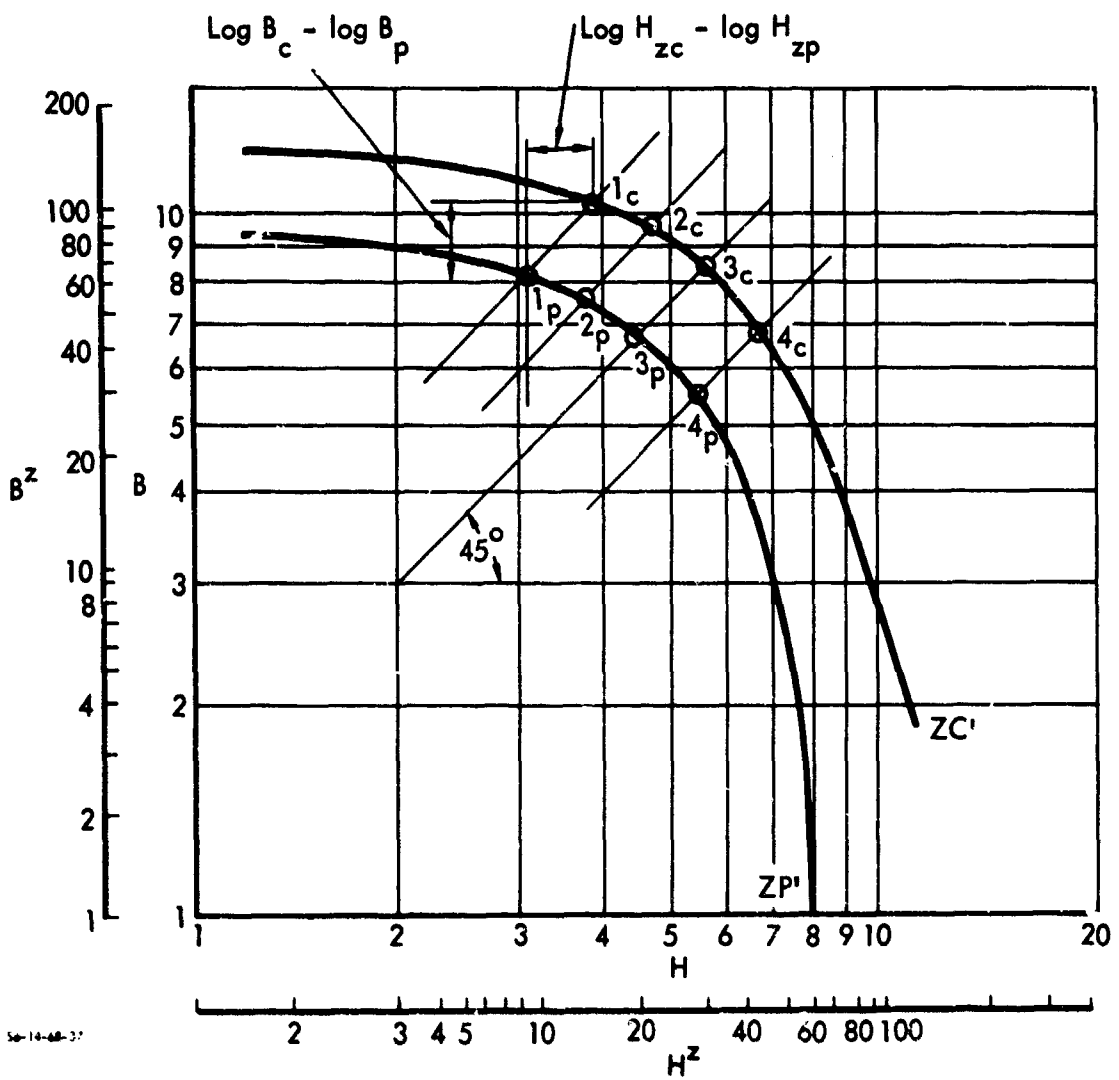


FIGURE 21.

Having thus obtained a series of 1c and 1p, 2c and 2p, 3c and 3p, etc., points we read the square of the corresponding ordinates, enter them into Table 2, add the respective magnitudes, and plot the curve of B_Z^1 vs H_Z^1 whose graphical determination was given in Fig. 17. In this instance the operation of extracting the square root in expressions

$B_Z^1 = \sqrt{B_{ZC}^2 + B_{ZP}^2}$ and $H_Z^1 = \sqrt{H_{ZC}^2 + H_{ZP}^2}$ is taken care of by using the proper scale.

TABLE 2

$B_C^2 = B_{ZC}^2$	$B_P^2 = B_{ZP}^2$	$B_{ZC}^2 + B_{ZP}^2$	H_{ZC}^2	H_{ZP}^2	$H_{ZC}^2 + H_{ZP}^2$
•	•	•	•	•	•
•	•	•	•	•	•

Figure 22 shows the plot of B_Z^1 vs H_Z^1 whose intersect with the selected B_Z vs H_Z magnetization curve determines the point Z.

The determination of points C and P and corresponding magnitudes of B_C , B_P , H_C , H_{ZC} , and H_{ZP} is given in the illustration and is self-explanatory.

Example:

Assumed magnitudes

$$\frac{\ell_C}{\ell_Z} = \frac{\ell_P}{\ell_Z} = 5; \frac{F_C}{\ell_Z} = 16.25; \frac{F_P}{\ell_Z} = 10$$

Curve C is Cobalt Iron (50% Co, 50% Fe)

Curve P is Medium Silicon Steel

Curve Z is Permalloy.

Table 3 is a completed version of Table 1, and Table 4 is a completed version of Table 2. Figure 22 which was used as an illustration of the method also represents a graphical solution to the values contained in Tables 3 and 4.

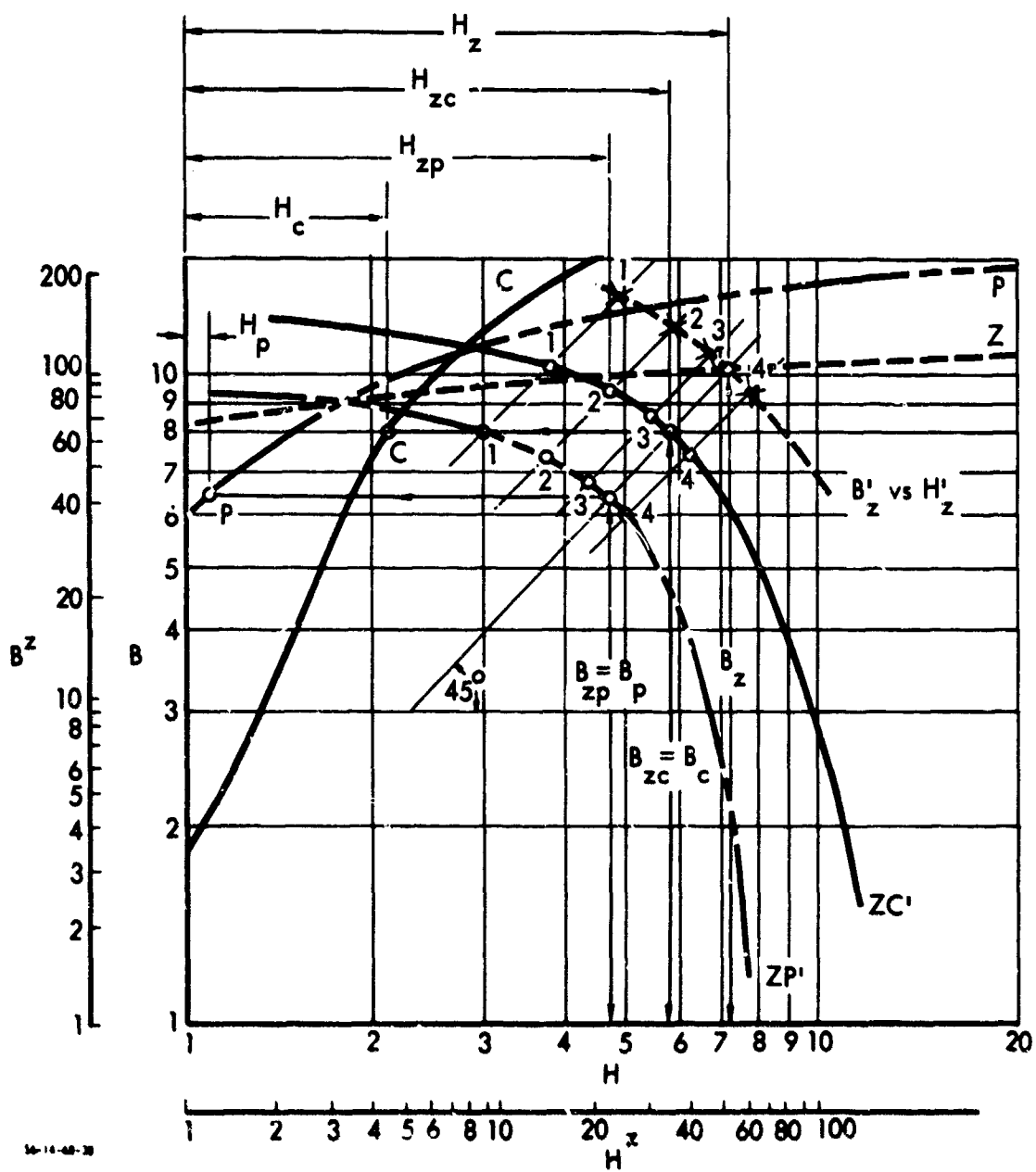


FIGURE 22.

TABLE 3

B_C	H_C	$H_C \frac{\iota_C}{\iota_Z}$	H'_{ZC}	B_P	H_P	$H_P \frac{\iota_P}{\iota_Z}$	H'_{ZP}
1.77	1.0	5.0	11.25	1.3	0.5	2.5	7.5
4.	1.5	7.5	8.75	3.5	0.75	3.75	6.5
7.6	2.0	10.0	6.25	6.0	1.0	5.0	5.0
10.2	2.5	12.5	3.75	7.3	1.25	6.25	3.75
12.1	3.0	15.0	1.25	8.4	1.5	7.5	2.5
13.3	3.5	17.5		9.1	1.75	8.75	1.25
14.3	4.0	20.0		9.8	2.0	10.0	0
15.5	5.0	25.0		10.6	2.5	12.5	
16.5	6.0	30.0		11.3	3.0	15.0	
17.2	7.0	35.0		11.8	3.5	17.5	
17.7	8.0	40.0		12.2	4.0	20.0	
18.2	9.0	45.0		12.7	5.0	25.0	
18.7	10.0	50.0		13.0	6.0	30.0	
20.0	15.0			13.3	7.0	35.0	
20.8	20.0			13.5	8.0	40.0	
21.4	25.0			13.7	9.0	45.0	
21.8	30.0			13.8	10.0	50.0	
				14.3	15.0		
				14.6	20.0		
				14.9	30.0		

TABLE 4

No.	B_C	B_P	B'_Z	H_{ZC}	H_{ZP}	H'_Z	B_C^2	B_P^2	$B_Z'^2$	H_{ZC}^2	H_{ZP}^2	$H_Z'^2$
5	6.78	5.42	8.7	6.75	5.42	8.7	45.8	29.4	75.2	45.6	30.0	75.6
4	8.4	6.4	10.5	5.6	4.42	7.1	70.6	40.9	111.5	31.4	19.6	51.0
3	9.4	7.4	11.9	4.68	3.68	5.9	88.4	54.8	143.2	21.4	13.6	35.0
2	10.2	8.0	12.8	3.82	3.0	4.9	100.4	64.0	164.4	14.6	9.0	23.6
1	11.2	8.7	14.1	2.76	2.15	3.5	124.0	75.6	199.6	7.6	4.6	12.2

X. CONCLUSIONS

The range of problems of the six examples presented here is broad enough to acquaint a reader not versed in the subject with the variety of approaches which could be used to solve a given problem. In all cases, however, graphical problem solving has one common ingredient--to prepare at the outset a diagrammatic presentation of the relationship of variables in several possible forms. In fact, very often the approach of classical Euclidean geometry will offer a hint of required construction. By the classical approach I mean the assumption that the problem has been solved, which thus permits the drawing of the solution figure. Inspection of this figure, with its juxtaposed variables, will often disclose their principal dependence or relationship pointing to a solution. A good illustration of this is given by Figs. 2 and 3 in the problem of Car Replacements (pp. 47,48).

The example problems contained in this paper could also form instructive exercises in training one in the use of graphical computer display and techniques of interaction between the computer and the operator.

If this paper will whet the graphical appetite of some of its readers it will amply justify its publication.

APPENDIX A. A NEW APPLICATION OF THE LOGARITHMIC POLAR DIAGRAM

The original adaption of the logarithmic polar diagram is credited to Mr. Rith of the Eiffel Laboratory and may be found in Eiffel's works "La Resistance de l'air et l'aviation" and "Nouvelles Recherches sur la Resistance de l'air et l'aviation." Disadvantages of the original Rith and later methods based on the use of the logarithmic polar diagram are in the approximate nature of the estimated performance obtained and the consequent inaccuracies and discrepancies as compared with other available methods.

THEORY OF THE LOGARITHMIC POLAR DIAGRAM

Rith points out that if the characteristic curves of the airplane are plotted as a polar in logarithmic coordinates, the plot represents a functional dependence of all the main factors entering into the two principal equations of the flight characteristics of an airplane:

$$W = LV^2 \quad \text{and}$$
$$HP = DV^3;$$

or expressed logarithmically:

$$\log W = \log L + 2 \log V \quad \text{and}$$
$$\log HP = \log D + 3 \log V;$$

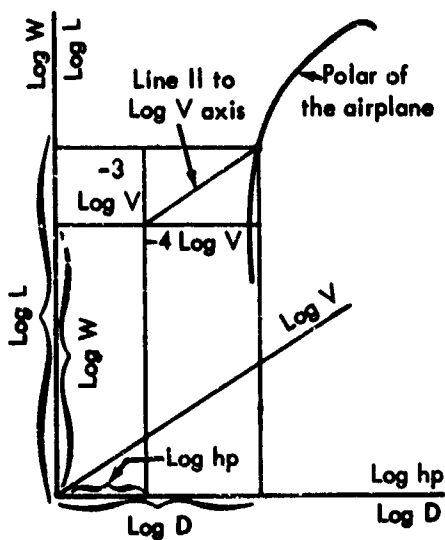
therefore:

$$\log L = \log W - 2 \log V \quad \text{and}$$
$$\log D = \log HP - 3 \log V.$$

From the last two equations it is apparent that we can consider $\log L$ as the sum of $\log W$ and $-2 \log V$, while $\log D$ can be considered as the sum of $\log HP$ and $-3 \log V$. The values of $\log W$ and $\log HP$ can be plotted on the direction of the ordinate and abscissae directly,

while $\log V$ can be plotted on a line inclined in such a way that the values projected on the direction of the ordinate will give $-2 \log V$ and the same point projected on the axis of abscissae will give a magnitude of $-3 \log V$. This new axis, called the speed axis, has the slope of $2/3$ and the graduations have a modulus of $\sqrt{3^2 + 2^2} = 3.605$ times that of the modulus used on the other axes.

The diagram (Fig. 1) thus constructed gives the necessary functional dependence of the factors entering into the two equations.



56-14-68-40

FIGURE 1.

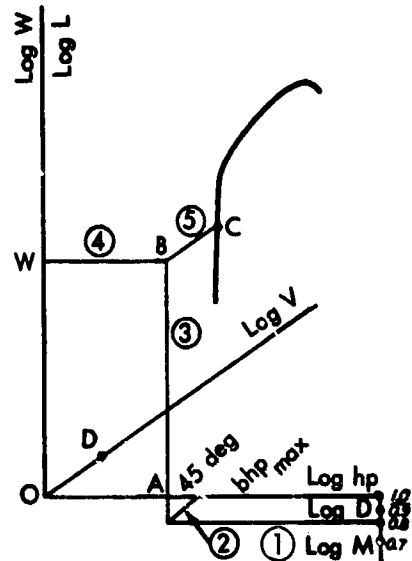


FIGURE 2. Determination of Maximum Speed at Sea Level

In order to take into account the effect of the density of the air and so to obtain the characteristics of flight at altitude, we observe that in the two equations mentioned above we must incorporate the value of relative density. The new equations are written as:

$$W = n L V^2 \quad \text{and}$$

$$HP = n D V^3$$

where n is the ratio of the density at altitude to that at sea level. The necessary transformation can be obtained by assuming the origin of coordinates moved along a 45-deg line so that the magnitudes of L and D assume a new value equal to $n L$ and $n D$. Consequently,

in order to obtain the relationship of the factors involved at altitude, it is sufficient to incorporate a new reference axis (the altitude axis) which has a slope of $1/1$, and to plot the logarithmic values of relative density with a modulus equal to $\sqrt{1+1} = 1.41$ of the modulus used for L and D axes.

Knowing the theory of the logarithmic polar chart, we can turn our attention to the practical application of it to performance estimate.

It is assumed that the characteristics of the airplane (that is, the lift and drag at one mph on a full-size machine) are determined either through calculations or from a wind tunnel test. Knowing the values of L and D and having a sheet of coordinates available, we plot the logarithmic polar curve.

DETERMINATION OF MAXIMUM SPEED AT SEA LEVEL

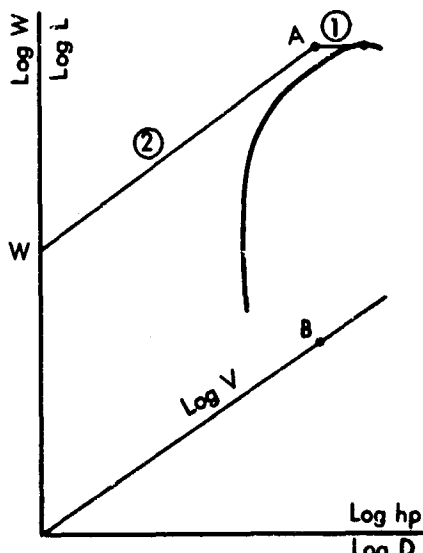
On the right hand side of the diagram (Fig. 2), a vertical logarithmic scale is marked scale μ . This scale facilitates the determination of the available thrust horsepower when the propeller efficiency is known. Draw a horizontal line through the known propeller efficiency (line 1) until it intersects a 45-deg line passing through the point of BHP maximum (line 2). Draw a vertical line (3) through the point thus obtained until it intersects a horizontal line (4) passing through the ordinate indicating the gross flying weight of the airplane. Point A is the thrust horsepower available at the maximum speed. Drawing through point B line (5) parallel to the speed axis, the segment BC obtained between the intersection of this line with the polar (point C) and point B gives the magnitude of the maximum speed of the airplane. To find its value lay out from the origin of coordinates an equal segment on the speed axis and the reading at the point D will give the desired magnitude.

DETERMINATION OF STALLING SPEED

Draw a horizontal line (1) tangent to the uppermost point of the polar (Fig. 3). Draw line (2) through given gross flying weight. Line (2) is parallel to the speed axis. Segment AW (where A is the point of intersection of the two lines) gives the stalling speed of the airplane, which must be measured on the speed axis.

SPEED FOR FLIGHT AT MINIMUM POWER

Draw line (1) tangent to the polar and parallel to the $\log V$ axis (Fig. 4). Draw line (2) through W corresponding to the given gross flying weight. The intersection of the two lines defines point A in such a way that AB is the speed corresponding to minimum power and AW is the minimum power.



56-14-68-41

FIGURE 3. Determination of Stalling Speed at Sea Level

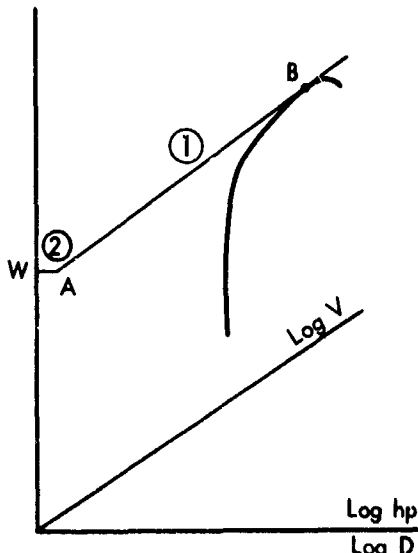


FIGURE 4. Determination of Speed for Flight at Minimum Power

MAXIMUM L/D

It can be easily proved that a vertical scale graduated logarithmically with the same modulus as used for the L and D axes, and located

arbitrarily on the drawing will give us the ratio of L/D at the point of intersection of this scale with a line passing through the chosen point and inclined at an angle of 45 deg. In graduating this scale, we must determine at least one reference point and graduate the scale in the same sense as the L axis. To obtain the value of maximum L/D , simply draw a line inclined at 45 deg and tangent to the polar (Fig. 5). Point A gives the maximum L/D of the design.

The brief explanation of the theory and a few illustrations of the possible uses of the logarithmic polar diagram given above will suffice to explain the practical use of the new grapho-analytical method which consists of incorporating the curves of horsepower available and required drawn in logarithmic coordinates. This involves an incorporation of a few more reference curves as explained and illustrated in the following paragraphs.

HORSEPOWER REQUIRED AT SEA LEVEL

Knowing V max., calculate values of 0.9, 0.8, 0.7, 0.6, 0.5, 0.4, 0.3 of V max., and mark them on the speed axis as shown in Fig. 3. This is not absolutely necessary for the purpose of obtaining the horsepower required, but later we will see that it will aid us in obtaining the horsepower available. The drawing of the curve of horsepower required will be illustrated by following the procedure for one point; for instance, point $V = 0.5 V$ max. (Fig. 6).

Draw line (1) through W and parallel to the speed axis. Project point $0.5 V$ max. on it. This gives point A . Draw a horizontal line through this point. Through the point B draw a line parallel to speed axis until it intersects the horizontal line passing through W . Through the point C thus obtained draw a vertical line until it intersects line AB . Since WC is the horsepower required to fly at a speed equal to $0.5 V$ max., point D represents a plot of it drawn at the proper point of the polar curve. Repeating this construction for several points and joining all these points by a smooth line we obtain the horsepower required plotted against the corresponding lift and, by virtue of construction, also the known speed.

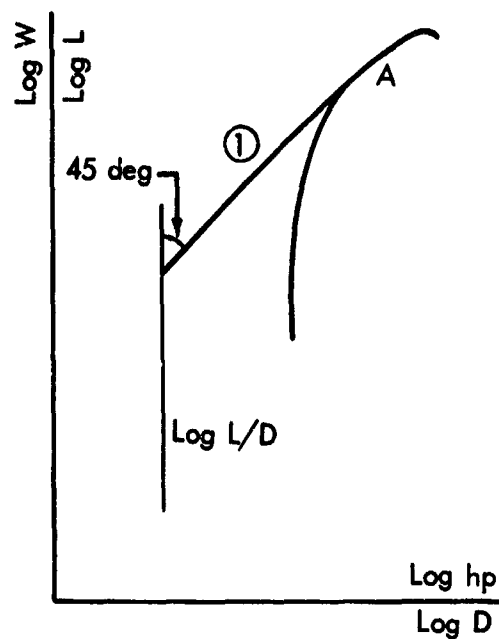


FIGURE 5. Determination of the L/D Ratio

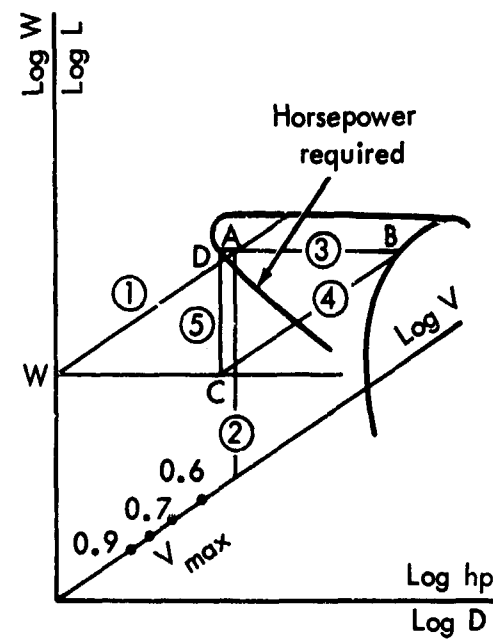


FIGURE 6. Determination of Horsepower Required at Sea Level

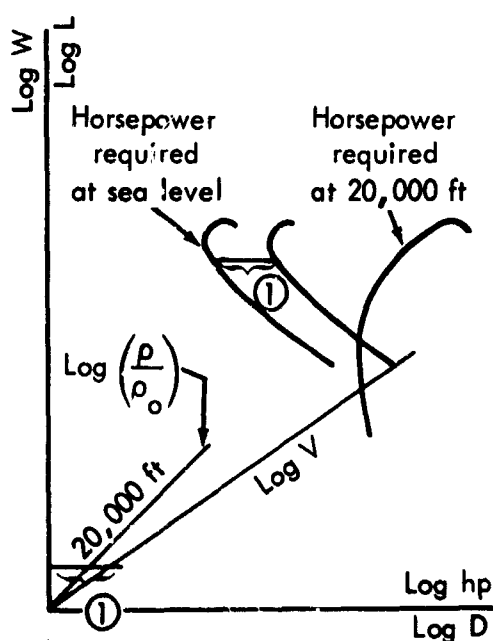


FIGURE 7. Determination of Horsepower Required at Altitude

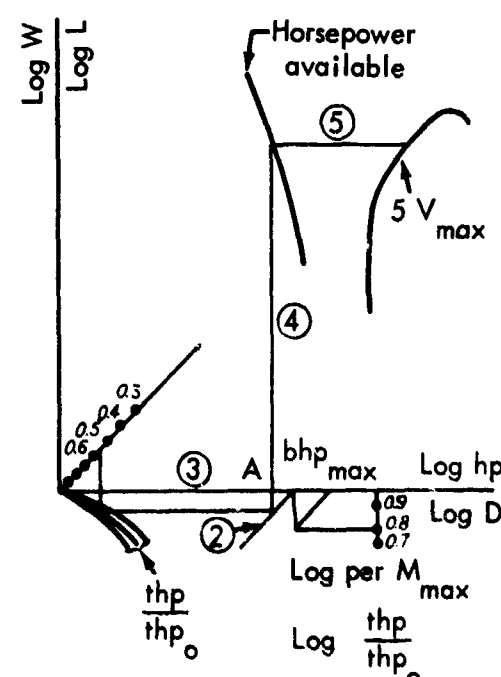


FIGURE 8. Determination of Horsepower Available at Sea Level

HORSEPOWER REQUIRED AT ALTITUDE

To obtain the curve of horsepower required at any altitude, it is sufficient to shift the sea level curve to the right by the amount equal to the distance (l) which is measured between the speed axis and the ordinate axis at the height corresponding to the chosen altitude. Figure 7 shows this construction for an altitude of 20,000 ft.

HORSEPOWER AVAILABLE AT SEA LEVEL

To construct the curves for horsepower available at sea level, we introduce three new constructional curves giving the variation of thrust horsepower against the ratio of V/V_{max} .

On page 144, Fig. 96, of Diehl's "Engineering Aerodynamics," we find the three general curves giving the necessary relationship. In the lower left part of the diagram we incorporate these three curves.

The scale of propeller efficiencies is used now as the scale of THP/THP_0 , while the scale of V/V_{max} , is assumed to be plotted on the axis of altitudes (Fig. 8). In this construction we make use of the line (2) from Fig. 1. The power plant used determines which of the three curves shall be used. The construction will be illustrated for one point and must be similarly repeated for the rest of the points corresponding to fractions of V/V_{max} . Figure 5 shows the construction for point of V equal to 0.5 V_{max} . See also Table 1.

Having chosen one of the THP/THP_0 curves we project the corresponding point on the line (2). The point at intersection projected on the HP scale gives the horsepower available at this particular speed. Drawing line (4) until it intersects the horizontal through the point on the polar corresponding to the speed chosen, we obtain point B of the horsepower available curve at sea level. Repeating this construction for several more points and joining them with a smooth curve, we obtain the curve of horsepower available. The curves of horsepower available and horsepower required will intersect at point B of Fig. 2, corresponding to the maximum speed when the horsepower available is equal to the horsepower required.

TABLE 1. VARIATION OF THP WITH V/V MAX RATIO

V/V max.	Ratio of THP/THP Max.		
	R.P.M. Max.		
	1800	2100	2400
1.2	1.035	1.015	0.995
1.1	1.025	1.015	1.005
1.0	1.00	1.00	1.00
0.9	0.96	0.97	0.975
0.8	0.908	0.925	0.94
0.7	0.85	0.865	0.885
0.6	0.78	0.80	0.82
0.5	0.70	0.72	0.74
0.4	0.60	0.617	0.635
0.3	0.488	0.495	0.515

HORSEPOWER AVAILABLE AT ALTITUDE, UNSUPERCHARGED

To obtain the horsepower at altitude, we will incorporate a curve giving the variation of the horsepower with altitude. Since our construction will be made assuming that the speed of the airplane remains constant, we can make use of the data given in Table 10, page 139, of Diehl's "Engineering Aerodynamics". See also Table 2.

TABLE 2. VARIATION OF THP WITH ALTITUDE

Altitude	THP/THP ₀
Sea level	1.000
5,000 ft	0.820
10,000 ft	0.667
15,000 ft	0.532
20,000 ft	0.425
30,000 ft	0.261
32,000 ft	0.234

Figure 9 illustrates the construction of the point corresponding to an altitude of 10,000 ft. Inasmuch as the transformation of the polar for any altitude is made by an imaginary shift of the origin of the coordinates along a 45-deg line it is sufficient to locate the point B on the horizontal passing through the 10,000-ft point on the axis of altitude so that a line drawn through it and inclined 45 deg will cross the axis of horsepower giving the magnitude CO equal to 0.667 CA; that is, if the point A corresponds to 1000 HP, the value read at C must be 567 HP. Having the curve of variation of horsepower with altitude it is sufficient to slide the curve of horsepower available at sea level parallel to itself by the amount and along the direction (1) corresponding to the desired altitude as shown in Fig. 9.

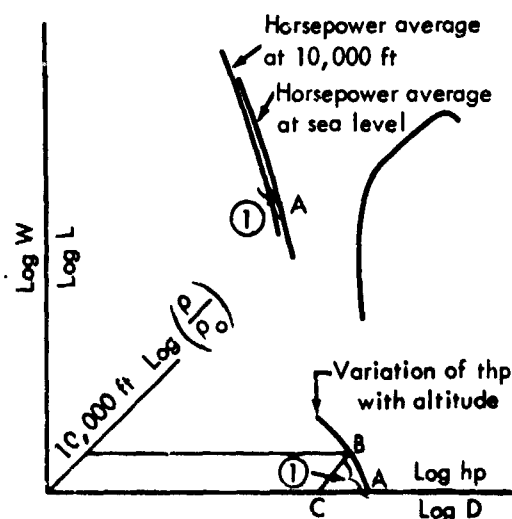
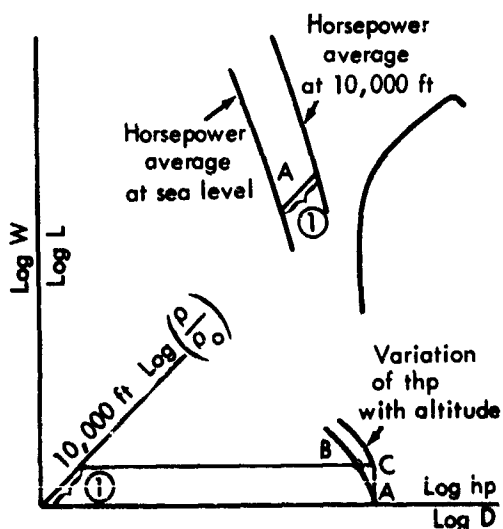


FIGURE 9. Determination of Horsepower Available at Altitude, Unsupercharged

HORSEPOWER AVAILABLE AT ALTITUDE WITH SUPERCHARGED ENGINE

Most of the present supercharged power plant installations are made so that the original sea level power is retained up to a certain fixed altitude, above which the power decreases at the normal rate. On our diagram this can be expressed by drawing instead of the previously

drawn horsepower variation curve a new curve consisting of two branches: a vertical straight line from point A up to the horizontal passing through the altitude up to which the sea level power is preserved and a curve from point C which is obtained by shifting horizontally the old curve until points B and C coincide. In Fig. 10 the power was assumed to be retained up to an altitude of 10,000 ft. As the altitude performance on the polar diagram is obtained by an imaginary shift of the origin of coordinates along a 45-deg line, to obtain the horsepower available at 10,000 ft, we must shift the curve of horsepower available at sea level to the right along a 45-deg line by the amount equal to the segment (1).



50-14-08-44

FIGURE 10. Determination of Horsepower Available at Altitude, Supercharged

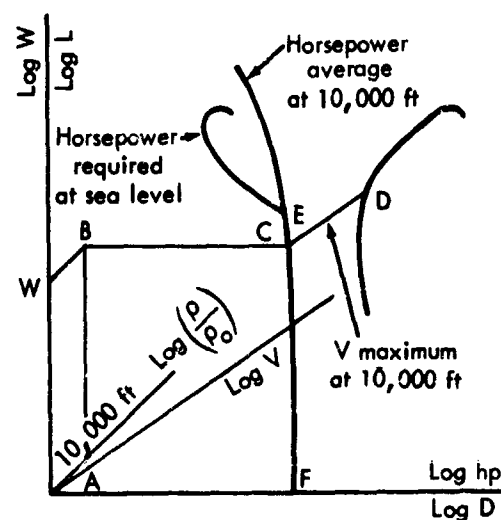


FIGURE 11. Determination of Performance at Altitude

PERFORMANCE AT ALTITUDE

To obtain the speed and corresponding horsepower required and available at altitude, we must bear in mind that by virtue of construction that instead of a horizontal line passing through W (as it was done in Fig. 6) it is necessary to use another horizontal line such that if WB is parallel to the altitude axis, the segment WB must be equal to the segment OA where A is the desired altitude.

Figure 11 illustrates this for an angle of attack corresponding to the maximum speed at 10,000 ft. Since the point of intersection of horsepower required and available curves corresponds to the maximum speed, project point E on line BC and OF. Segment OF gives the magnitudes of horsepower required and available, since in this case they are equal. Drawing line CD parallel to speed axis, we obtain the magnitude of the maximum speed given by the segment CD and point D permits us to interpolate the angle of attack corresponding to the maximum speed at 10,000 ft.

COMPLETE PERFORMANCE PREDICTION WITH THE AID OF LOGARITHMIC POLAR DIAGRAM

From the foregoing we are now able to obtain the complete data on theoretical performance of a new design. We can ascertain the maximum and stalling speeds for any altitude at which the plane is capable of flying. By joining the points of maximum speeds plotted on the corresponding horizontal lines and noting the intersection of this new curve with the line tangent to the polar and parallel to the speed axis (line used to obtain the minimum power required for flight), we can determine the absolute ceiling.

To obtain the best speeds for climbing and to determine the excess horsepower, we can make use of the following observation. From the analyses of a number of airplanes it can be found that the best speed at which to climb at sea level is usually equal to 0.58 V_{max} . At the ceiling, the planes would fly at a speed corresponding to the minimum power necessary to maintain flight. If we join by a straight line the point corresponding to the speed equal to 0.58 V_{max} ., on the horsepower-required curve at sea level with the point of minimum power necessary to fly at the ceiling, the points of intersection of this line with horsepower-required curves will define, within the accuracy of practical requirements, the best speeds for climb. Knowing these speeds, we can obtain the excess horsepower available for climb.

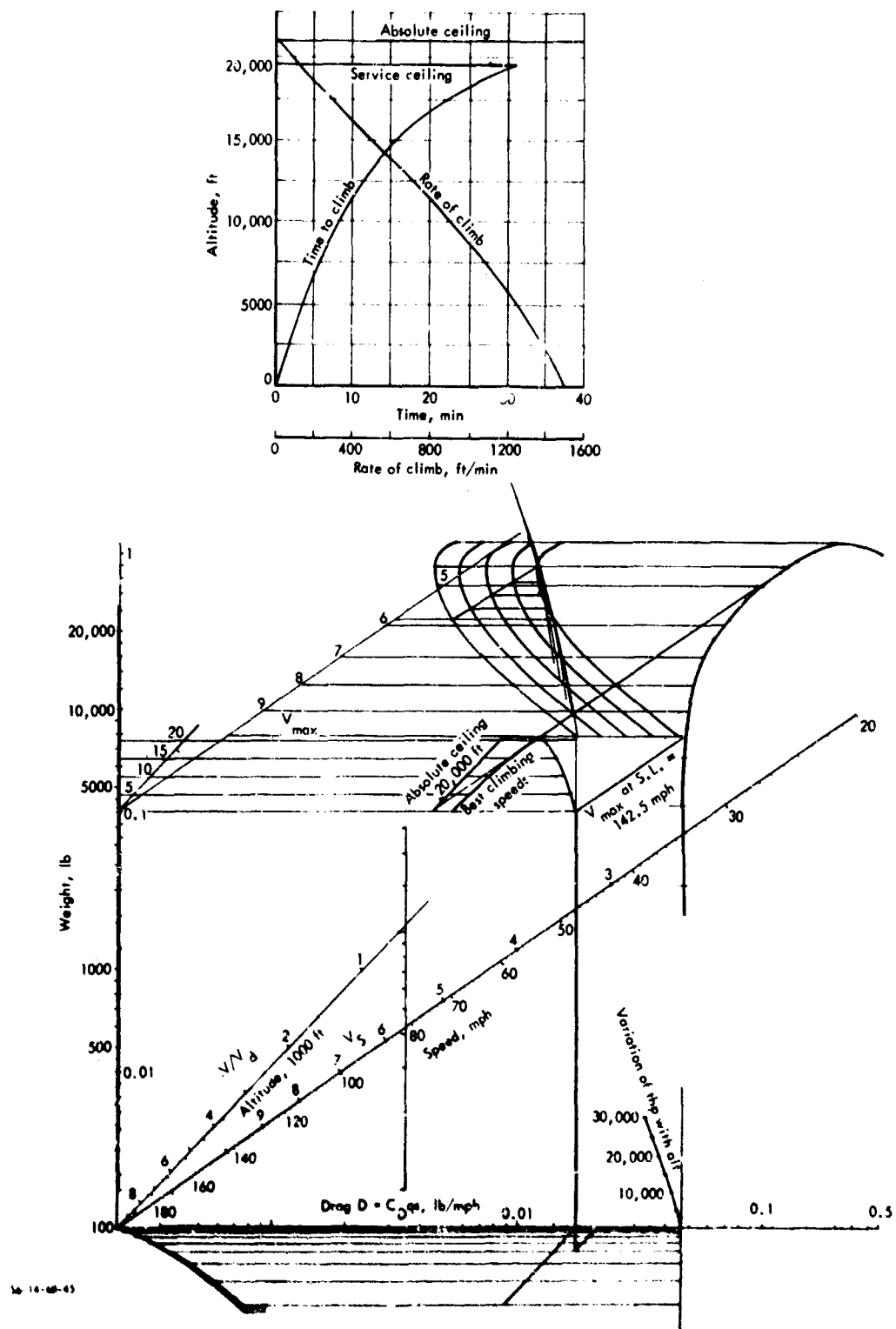


FIGURE 12. An Example of the Use of the Logarithmic Polar as Employed in Routine Practice

We can resort now to standard analytical methods and obtain the curve of rate of climb and time to climb to different altitudes. Figure 12 shows an example of the use of logarithmic polar as it is employed in routine practice.

CONCLUSIONS

The particular advantages afforded by the method described in the article, in addition to those already mentioned, consist of compactness of the record and a ready means of estimating slight changes of design. In many instances lack of time does not allow an elaborate revision of a performance estimate and in such a case the logarithmic polar diagram furnishes an easy and rapid estimate of the effect of changes in weight, parasite resistance, etc. To the trained eye the graphical picture of the polar gives other valuable information such as the general efficiency of the design, the approach to inefficient gross flying weight condition, and such.

UNCLASSIFIED

Security Classification

DOCUMENT CONTROL DATA - R & D*(Security classification of title, body of abstract and indexing annotation must be entered when the overall report is classified)*

1. ORIGINATING ACTIVITY (Corporate author)		2a. REPORT SECURITY CLASSIFICATION	
Institute for Defense Analyses		Unclassified	
2b. GROUP		-	
3. REPORT TITLE			
Examples of Graphical Solution of Six Problems in Engineering, Mechanics, and Operational Analysis			
4. DESCRIPTIVE NOTES (Type of report and inclusive dates) Research Paper P-405, July 1968			
5. AUTHOR(S) (First name, middle initial, last name) Michael Watter			
6. REPORT DATE July 1968		7a. TOTAL NO. OF PAGES 93	7b. NO. OF REFS 0
8a. CONTRACT OR GRANT NO. DAHC15-67-C-0011		9a. ORIGINATOR'S REPORT NUMBER(S) P-405	
b. PROJECT NO. ARPA Assignment 19		9b. OTHER REPORT NO(S) (Any other numbers that may be assigned this report) N/A	
10. DISTRIBUTION STATEMENT This document has been approved for public release and sale; its distribution is unlimited.			
11. SUPPLEMENTARY NOTES N/A		12. SPONSORING MILITARY ACTIVITY N/A	
13. ABSTRACT This paper illustrates the use of graphical analyses by presenting the solution of six problems in the fields of operational analyses, mechanics, and engineering: The Jeep Problem, the Range of a Fleet of Aircraft, a Beam under Combined Compression and Transverse Load, the Problem of Cars Replacement, Determination of Ballistic Trajectory Parameters, and the Two-Magnetic-Reactor Problem. The purpose of this paper is to arouse an interest in a methodology which is further enhanced by the graphical display capability available in today's Computers with all its potential problem solving flexibility. The examples treated in this paper are not the stereotyped problems forming the usual subject of textbooks on graphical methods and, in that sense, should prove of greater interest to the reader.			

DD FORM NOV. 1473

UNCLASSIFIED

Security Classification

Security Classification

14 KEY WORDS	LINK A		LINK B		LINK C	
	ROLE	WT	ROLE	WT	ROLE	WT

Security Classification